CONDUCTIVE POLYMER NANOCOMPOSITES OF POLYPROPYLENE AND ORGANIC FIELD EFFECT TRANSISTORS WITH POLYETHYLENE GATE DIELECTRIC

A THESIS SUBMITTED TO
THE GRADUATE SCHOOL OF NATURAL AND APPLIED SCIENCES
OF
MIDDLE EAST TECHNICAL UNIVERSITY

BY

YASİN KANBUR

IN PARTIAL FULFILLMENT OF THE REQUIREMENTS
FOR
THE DEGREE OF DOCTOR OF PHILOSOPHY
IN
POLYMER SCIENCE AND TECHNOLOGY

JUNE 2011

Approval of the thesis:

CONDUCTIVE POLYMER NANOCOMPOSITES OF POLYPROPYLENE AND ORGANIC FIELD EFFECT TRANSISTORS WITH POLYETHYLENE GATE DIELECTRIC

Submitted by **YASİN KANBUR** in partial fulfillment of the requirements for the degree of **Doctor of Philosophy in Polymer Science and Technology, Middle East Technical University** by,

Prof. Dr. Canan Özgen _____
Dean, Graduate School of **Natural and Applied Sciences**

Prof. Dr. Necati Özkan _____
Head of Department, **Polymer Science and Technology**

Prof. Dr. Zuhal Küçükyavuz
Supervisor, **Chemistry Dept., METU** _____

Examining Committee Members:

Prof. Dr. Erdal Bayramlı
Chemistry Dept., METU _____

Prof. Dr. Zuhal Küçükyavuz
Chemistry Dept., METU _____

Prof. Dr. Göknur Bayram
Chemical Engineering Dept., METU _____

Assist. Prof. Dr. Nurdan Sankır
Micro and Nanotechnology Dept., TOBB-ETU _____

Assist. Prof. Dr. Ali Çırpan
Chemistry Dept., METU _____

Date: June 15, 2011

I hereby declare that all information in this document has been obtained and presented in accordance with academic rules and ethical conduct. I also declare that, as required by these rules and conduct, I have fully cited and referenced all material and results that are not original to this work.

Name, Last name: YASİN KANBUR

Signature :

ABSTRACT

CONDUCTIVE POLYMER NANOCOMPOSITES OF POLYPROPYLENE AND ORGANIC FIELD EFFECT TRANSISTORS WITH POLYETHYLENE GATE DIELECTRIC

KANBUR, Yasin

Ph. D., Department of Polymer Science and Technology

Supervisor: Prof. Dr. Zuhal KÜÇÜKYAVUZ

June 2011, 124 pages

One of the aim of this study is to prepare conductive polymer nanocomposites of polypropylene to obtain better mechanical and electrical properties. Composite materials based on conductive fillers dispersed within insulating thermoplastic matrices have wide range of application. For this purpose, conductive polymer nanocomposites of polypropylene with nano dimentional conductive fillers like carbon black, carbon nanotube and fullerene were prepared. Their mechanical, electrical and thermal properties were investigated.

Polypropylene (PP)/carbon black (CB) composites at different compositions were prepared via melt blending of PP with CB. The effect of CB content on mechanical and electrical properties was studied. Test samples were prepared by injection molding and compression molding techniques. Also, the effect of processing type on mechanical and electrical properties was investigated. Composites become semiconductive with the addition of 2 wt% CB.

Polypropylene (PP) / Carbon Nanotube (CNT) and Polypropylene / Fullerene composites were prepared by melt mixing. CNT's and fullerenes were surface functionalized with HNO_3 : H_2SO_4 before composite preparation. The CNT and fullerene content in the composites were varied as 0.5, 1.0, 2.0 and 3.0 % by weight. For the composites which contain surface modified CNT and fullerene four different compatibilizers were used. These were selected as TritonX-100, Poly(ethylene-block-polyethylene glycol), Maleic anhydride grafted Polypropylene and Cetramium Bromide. The effect of surface functionalization and different compatibilizer on mechanical, thermal and electrical properties were investigated. Best value of these properties were observed for the composites which were prepared with maleic anhydride grafted polypropylene and cetramium bromide.

Another aim of this study is to built and characterize transistors which have polyethylene as dielectric layers. While doing this, polyethylene layer was deposited on gate electrode using vacuum evaporation system. Fullerene , Pentacene ve Indigo were used as semiconductor layer. Transistors work with low voltage and high on/off ratio were built with Aluminum oxide - PE and PE dielectrics.

Keywords: Conductive Polymer Composites, Nanocomposites, Mechanical Properties, Electrical Properties, Organic Field Effect Transistors

ÖZ

POLİPROPİLEN İLETKEN NANOKOMPOZİTLERİ VE POLİETİLEN KAPI DİLEKTRİKLİ ORGANİK ALAN ETKİLİ TRANSİSTÖRLER

KANBUR, Yasin
Doktora, Polimer Bilim ve Teknolojisi
Tez Yöneticisi: Prof. Dr. Zuhal KÜÇÜKYAVUZ

Mayıs 2011, 124 sayfa

Bu çalışmanın amaçlarından biri daha iyi mekanik ve elektiriksel özellikler elde etmek için iletken polipropilen nanokompozitleri hazırlamaktır. Termoplastik yalıtkan matrisler içerisinde iletken dolgu malzemelerinin dağılımına dayalı kompozit malzemeler geniş bir kullanım alanına sahiptir. Bu amaçla, polipropilenin karbon siyahı, karbon nanotüp ve fulleren gibi nano boyutlu iletken dolgu malzemeleri içeren nanokompozitleri hazırlandı. Kompozitlerin mekanik, elektiriksel ve termal özellikleri incelendi.

Polipropilen/Karbon Siyahı kompozitleri farklı bileşimlerde eriyik karıştırma yöntemiyle hazırlandı. Karbon siyahı miktarının mekanik ve elektiriksel özellikler üzerindeki etkisi araştırıldı. Test örnekleri enjeksiyonlu kalıplama ve basınçlı kalıplama teknikleri ile hazırlandı. Ayrıca proses tipinin mekanik ve elektiriksel özelliklere olan etkisi incelendi. Kompoziler 2 % karbon siyahı eklenmesi ile yarı iletken hale geldiler.

Polipropilen / Karbon Nanotüp ve Polipropilen / Fulleren kompozitleri eriyik karıştırma yöntemiyle hazırlandı. Kompozitlerin hazırlanmasından önce karbon

nanotüp ve fullerenin yüzeyi HNO_3 : H_2SO_4 ile fonksiyonlandırıldı. Kompozitlerdeki karbon nanotüp ve fulleren kompozisyonu ağırlık yüzdesi olarak 0.5, 1.0, 2.0 ve 3.0 % olarak değiştirildi. Yüzeyi modifiye edilmiş karbon nanotüp ve fulleren içeren kompozitlerde dört farklı uyumlaştırıcı kullanıldı. Bunlar, TritonX-100, Poli(etilen-blok-polietilen glikol), Maleik anhidrit graft edilmiş Polipropilen ve Setramiyum Bromür olarak seçildi. Yüzey modifikasyonu ve farklı uyumlaştırıcıların mekanik, termal ve elektiriksel özellikler üzerine olan etkisi incelendi. Bu özelliklerin en iyi değerleri maleik anhidrit graft edilmiş polipropilen ve setramiyum bromür ile hazırlanan kompozitlerde gözlemlendi.

Bu çalışmanın başka bir amacı polietilen dielektrik tabakası içeren transistörler yapmak ve karakterize etmektir. Bunu yaparken polietilen tabakasının oluşturulmasında vakumla buharlaştırma sistemi kullanıldı. Fulleren, Pentasen ve Indigo yarı iletken tabaka olarak kullanıldı. Aluminyum oksit -PE veya PE dielektrik tabakalarına sahip düşük voltajda çalışan ve yüksek açma kapama oranına sahip transistörler elde edildi.

Anahtar Sözcükler: İletken Polimer Kompozitleri, Nanokompozitler, Mekanik Özellikler, Elektriksel Özellikler, Organik Alan Etkili Transitörler

To My wife Seyhan and my son Eren

ACKNOWLEDGMENTS

I express my gratitude to my supervisor Prof. Dr. Zuhal Küçükyavuz for her guidance and excellent helps during this work. I also would like to thank her for not only her support throughout my PhD but also treated me like a son.

I would like to thank to Prof. Dr. Erdal Bayramlı and Göknur Bayram for their excellent help, guidance and support.

I am much indebted to Prof. Dr. N. Serdar Sarıçiftçi for his excellent help, guidance and support during my study in Linz, Austria. During 6 months in Linz, he always gave inspiration and encouragement to me.

Special thanks to Dr. Mihai Irimia Vladu who taught me a lot about organic field effect transistors.

I wish to thank to Dr. Mamatimin Abbas, Dr. Philip Stadler, Dr. Martin Egginger, Dr. Anita Fuchsbauer, Melanie Reisinger, Erik Glowacki, Sandra Kogler, Stefan Schauer, Serpil Tekoğlu, Ercan Avcı, for their help, hospitality and friendship during my stay in Linz.

My deepest thanks are to my wife Seyhan Kanbur and all of the my family members for loving me.

I would like to express my endless thanks to all my labmates, Çetin Börüban, Sevil Baytekin, Feride Tezal, Faris Yılmaz, Tamer Tezel, Bahadır Doğan for their supports and being a part of my life.

I am indepted to Assoc.Prof.Dr. Murat Kanbur and Dr. Özlem Usluer, for their meaningfull advices.

I would like to extend special thanks to Osman Yaslıtaş for his technical supports.

I offer sincere thanks to my friends, Yasin Arslan, Mehmet Doğan, Ali Sinan Dike, Ümit Tayfun, Selahattin Erdoğan, Fuat Çankaya, Ufuk Abacı, Elif Vargün, Arzu Yavuz, Tugba Efe, Yusuf Nur, Selin Kozanoglu, Buket Çarbaş, Murat Güzel for everything they have done for me.

I also wish to thank to my colleagues in Chemistry Department of METU.

I would like to thank to my PhD exam committee members for spending their time and interesting in my PhD.

This work was financially supported by ÖYP (Faculty Development Program) from the Middle East Technical University.

I would like to extend my deepest thanks to Atatürk University for supporting me to complete my PhD in the chemistry department of METU.

TABLE OF CONTENTS

ABSTRACT…… iv

ÖZ…… vi

ACKNOWLEDGEMENTS…… ix

TABLE OF CONTENTS……..……... xi

LIST OF TABLES…….…….... xv

LIST OF FIGURES…….…… xvi

ABBREVATIONS…….. xxi

CHAPTERS…..……

1. INTRODUCTION.…….. 1

2. BACKROUND INFORMATION…….…….... 3

2.1 Polymer Matrice for Composite Preparation……..……...…… 3

2.1.2 Polypropylene……...……. …… 3

2.2 Polymer Dielectric for Organic Field Effect Transistor…..……..….. 5

2.2.1 Polyethylene…..……. 5

2.3 Conductive Fillers……..……... 6

2.3.1 Carbon Nanotubes……..…….... 6

2.3.2 Carbon Black……..…….…….... 10

2.3.3 Fullerene……..……..…… 12

2.4 Composites and Nanocomposites..…….... 13

2.5 Conductive Polymer Composites……..……..……..... 14

2.6 Band Theory…..……..……..... 15

2.7 Principles of Organic Field Effect Transistors……..…… 16

2.7.1 Device Structures for OFET Application.……..…...……. 18

2.7.2 Characterization of OFET's……..……. 19

2.7.3 Importance of Gate Dielectric for OFET's…...……..…. 20

2.7.4 Techniques for OFET Preparation…….…… 22

3. EXPERIMENTAL……..... 24
3.1. Surface Modification of Carbon nanotube with HNO_3/H_2SO_4…… 24
3.2. Surface Modification of Fullerene with HNO_3/H_2SO_4……..... 26
3.3 Composite Preparation……..……..... 27
3.3.1 Preparation of Polypropylene / CNT composites……... 27
3.3.2 Preparation of Polypropylene / Fullerene composites…… 28
3.3.3. Preparation of Polypropylene /Carbon Black Composites…… 28
3.4 Injection Molding……... …….. 29
3.5 Compression Molding…..……..……... 30
3.6 Conductivity Measurements…….……. 30
3.7 Thermal Gravimetric Analysis……..…… 31
3.8 Fourier Transform Infrared Spectrometer (FTIR)……. 31
3.9. Differential Scanning Calorimetry……..……. 32
3.10 Scanning Electron Microscopy (SEM)……...……. 32
3.11 X Ray Photoelectron Spectroscopy (XPS)……..…… 32
3.12 Zeta Potential…….…….. 32
3.13 Transmission Electron Microscopy ……...……. 33
3.14 Tensile Test……..……..……. 33
3.15 Impact Test……...……... 33
3.16 Melt Flow Index……..…..…….. 33
3.17 Organic Field Effect Transistor Preparation …….. 34
3.17.1 Preparation of Glass Substrate and Gate Electrode……..…… 34
3.17.2 Alox Preparation……..…… 35
3.17.3 Evaporation of Low Density Polyethylene……...……... 35
3.17.4 Evaporation of C_{60} and Pentacene …….. 36
3.17.5 Evaporation of Source and Drain electrode …….……... 36
3.17.6 OFET Characterization……..…….. 37
3.17.7 Dielectric Characterization…...…..…….…… 39
4. RESULTS AND DISCUSSION……..…… 41
4.1 Polypropylene / Carbon Black Composites…….…….. 41

4.1.1 Melt Flow Index ……..……. 41
4.1.2 Percent Crystallinity of PP/CB composites……..…… 42
4.1.3 Impact Test……..…….……. 43
4.1.4 Scanning Electron Microscopy (SEM)……..…..... 44
4.1.5 Mechanical Properties …...……..……..…… 47
4.1.6 Electrical Properties ……..……..…….. 49
4.1.7 Thermal Gravimetric Analysis (TGA)……... 52
4.2 Surface Modification of Carbon Nanotube.……. 53
4.2.1 Fourier Transform Infrared Spectroscopy (FTIR)..……... 53
4.2.2 Elemental Analysis……..…..... 54
4.2.3 Electrical Conductivity.……..…… 55
4.2.4 X Ray Photoelectron Spectroscopy (XPS).…….……...…… 55
4.2.5 Zeta Potential ……...…….. 57
4.2.6 Scanning Electron Microscopy.……..……... 58
4.2.7 Transmission Electron Microscopy (TEM).……...…… 60
4.3 Surface Modification of Fullerene ……...……..... 61
4.3.1 Fourier Transform Infrared Spectroscopy (FTIR) ……..... 61
4.3.2 X Ray Photoelectron Spectroscopy (XPS)…… 62
4.3.3 Elemental Analysis……..……... 63
4.3.4 Electrical Conductivity ……..…… 64
4.3.5 Transmission Electron Microscopy ……...…… 64
4.3.6 Zeta Potential ……..... 66
4.3.7 Scanning Electron Microscopy ……. 66
4.4 Polypropylene/ Carbon Nanotube Composites……. 68
4.4.1 Mechanical Properties ……..…….. 68
4.4.2 Electrical Conductivity ……..…… 72
4.4.3 Scanning Electron Microscopy (SEM)…….. 73
4.4.4 Thermal Gravimetric Analysis (TGA)……... 77
4.5 Polypropylene /Fullerene Composites …….. 78
4.5.1 Mechanical Properties ……..…….. 78

4.5.2 Electrical Conductivity……... 82
4.5.3 Scanning Electron Microscopy…….. 83
4.5.4 Thermal Gravimetric Analysis (TGA)……... 87
4.6 Organic Field Effect Transistors with Polyethylene Gate Dielectric…… 88
4.6.1 Fourier Transform Infrared Spectroscopy…..……..... 88
4.6.2 Atomic Force Microscopy…….. 90
4.6.3 Dielectric Properties…..……... 91
4.6.4 Characterization of OFET's……... 92
5. CONCLUSIONS…… 98
5.1 Polypropylene / Carbon Black Composites……... 98
5.2 Surface Modification of Carbon Nanotube ……..... 98
5.3 Surface Modification of Fullerene …… 99
5.4 Polypropylene/ Carbon Nanotube Composites…….. 99
5.5 Polypropylene / Fullerene Composites ……. 100
5.6 Organic Field Effect Transistors with Polyethylene Gate Dielectric …… 100
REFERENCES…… 101
APPENDICES……. 113
A. STRESS AT BREAK OF THE POLYPROPYLENE / CARBON NANOTUBE AND POLYPROPYLENE / FULLERENE COMPOSITES... 113
B. STRESS VS STRAIN CURVES FOR POLYPROPYLENE / CARBON NANOTUBE AND POLYPROPYLENE / FULLERENE COMPOSITES.. 115
CURRICULUM VITAE…….. 122

LIST OF TABLES

TABLES

Table 4. 1 Elemental analysis results of CN 1 and CN 2……...…….. 54
Table 4. 2 Electrical conductivity of Untreated CN, CN 1 and CN 2……. 55
Table 4. 3 Elemental analysis results of surface modified fullerenes …….. 63
Table 4. 4 Electrical Conductivity of the F1 and F2…….…… 64
Table 4. 5 Observed peaks and literature-reported peaks for polyethylene…. 89

LIST OF FIGURES

FIGURES

Figure 2. 1 Synthesis of Polypropylene……..…….. 3

Figure 2. 2 Structure of Isotactic, Syndiotactic and Atactic Polypropylene…. 4

Figure 2. 3 Structure of Polyethylene ……..…….…….. 5

Figure 2. 4 Structures of HDPE, LLDPE and LDPE …….. 5

Figure 2. 5 Structure of graphite sheet ……..…….. 7

Figure 2. 6 Structure of Multi walled carbon nanotube and Single walled carbon nanotube..... 7

Figure 2. 7 Structural isomers of Carbon Nanotubes, armchair (top) zig zag (middle), chiral(bottom)…..……. 8

Figure 2. 8 Agglomerate and Aggregate sizes of Carbon Black..……...…….. 10

Figure 2. 9 Structures of Diamond, Graphite and Carbon Black …… 11

Figure 2. 10 Structure of C_{60} ……..…...……... 12

Figure 2. 11 Structures of some conjugated polymers ……...…….. 15

Figure 2. 12 Energy Levels of Insulator, Semiconductor and Conductor…… 16

Figure 2. 13 Structure of an OFET ……...……... 16

Figure 2. 14 Working Principle of an OFET ……..……...…….. 18

Figure 2. 15 Different built structures for OFET's : a) bottom-gate bottom-contact, b) bottom gate top-contact, c) top-gate bottom-contact, d) top-gate top-contact ……..……..... 19

Figure 2. 16 Typical transfer curve for an OFET ……....…… 20

Figure 2. 17 Typical output curve for an OFET ……...…… 20

Figure 3. 1 Experimental set up for surface modification……. 25

Figure 3. 2 Chemical structure of the chemically modified carbon nanotube.. 25

Figure 3. 3 Reaction of Fullerene with $HHO_3/H2SO_4$……..... 26
Figure 3. 4 DSM Explore Microcompounder……... 27
Figure 3. 5 Brabender PLV-151 Plasticorder……..…. 28
Figure 3. 6 Daca Injection Molding Instrument…… 29
Figure 3. 7 Dimension of the injection molded test samples…… 29
Figure 3. 8 Dimension of the compression molded samples……... 30
Figure 3. 9 Four point probe technique ……..….. 31
Figure 3. 10 Structure of gate mask…….. 34
Figure 3. 11 Preparation of Al_2O_3 insulator layer…… 35
Figure 3. 12 Edwards organic evaporator……. 36
Figure 3. 13 Structure of source- drain mask…… 37
Figure 3. 14 Agilent 5273 A Transistor Measurement Device……. 38
Figure 3. 15 Transistor measurement set up……. 38
Figure 3. 16 Mbraun MB200B Glove box…… 39
Figure 3. 17 Novocontrol dielectric characterization equipment…….. 40
Figure 3. 18 MIM structure for dielectric measurements……. 40
Figure 4. 1 Melt flow properties of PP/CB composites ……... 42
Figure 4.2 Percent crystallinity of the PP/CB composites…… 43
Figure 4. 3 Impact test results for PP/CB composites ……..... 44
Figure 4. 4. a Fracture surface of Pure Polypropylene …… 45
Figure 4. 4.b Fracture surface of the PP/CB composites containing 5% CB… 45
Figure 4. 4.c Fracture surface of the PP/CB composites containing 15% CB. 46
Figure 4.4.d Fracture surface of the PP/CB composites containing 30% CB. 46
Figure 4. 5 Tensile Strength of PP/CB composites ……..... 47
Figure 4. 6 Young Modulus of PP/CB composites……... 48
Figure 4.7 Percent elongation at break of the PP/CB composites……. 49
Figure 4.8 Electrical conductivity of the PP/CB composites prepared by compression and injection molding …….…. 50
Figure 4.9 The relationship between electrical conductivity and percent elongation at break as a function of carbon black content for composites 51

prepared by compression molding ……...
Figure 4.10 The relationship between electrical conductivity and percent elongation at break as a function of carbon black content for composites prepared by injection molding……... 52
Figure 4. 11 TGA of the PP/CB composites.……..…….. 53
Figure 4. 12 FTIR spectrums of CN 1 and CN 2…… 54
Figure 4. 13 XPS spectra of the CN 1 ……. 56
Figure 4. 14 XPS spectra of the CN 2…….. 57
Figure 4. 15 SEM micrograph of untreated CN ……... 58
Figure 4. 16 SEM micrograph of untreated CN 1 …… 59
Figure 4. 17 SEM micrograph of untreated CN 2…….**.....** 59
Figure 4. 18 TEM micrograph of CN 1……. 60
Figure 4. 19 TEM micrograph of CN 2…… 60
Figure 4. 20 FTIR spectrum of F 1 and F 2…….. 61
Figure 4. 21 XPS spectrum of F1 ……. 62
Figure 4. 22 XPS spectrum of F 2……. 63
Figure 4. 23 TEM micrograph of neat fullerene ……**....** 65
Figure 4. 24 TEM micrograph of F1 …… 65
Figure 4. 25 TEM micrograph of F2……. 65
Figure 4. 26 SEM micrograph of neat fullerene ……... 67
Figure 4. 27 SEM micrograph of F1 ……... 67
Figure 4. 28 SEM micrograph of F2 …… 68
Figure 4. 29 Young's Modulus of PP/CNT composites …….. 70
Figure 4. 30 Percent elongation at break of PP/CNT composites ……**....** 71
Figure 4. 31 Electrical Conductivity of the PP/CNT composites …… 73
Figure 4. 32.a SEM micrograph of PP/m-CNT/ CTAB ……..… 74
Figure 4. 32.b SEM micrograph of PP/m-CNT/ MA-g-PP ……..… 75
Figure 4. 32.c SEM micrograph of PP / m-CNT ……. 75
Figure 4. 32.d SEM micrograph of PP / neat CNT……. 76
Figure 4. 32.e SEM micrograph of PP / m-CNT / Triton X-100.…… 76

Figure 4. 32.f SEM micrograph of PP / m-CNT/ PE-block- PEG …… 77
Figure 4. 33 TGA of the PP/CNT composites ……..….. 78
Figure 4. 34 Young's Modulus of PP/F composites …….…….…….. 80
Figure 4.35 Percent elongation at break of PP/F composites …….. 81
Figure 4. 36 Electrical Conductivity of the PP/F composites ……..... 83
Figure 4. 37.a SEM micrograph of PP / neat F…… 84
Figure 4. 37.b SEM micrograph of PP / m-F …….. 85
Figure 4. 37.c SEM micrograph of PP/m-F/ CTAB……. 85
Figure 4. 37.d SEM micrograph of PP/m-F/ MA-g-PP …….. 86
Figure 4. 37.e SEM micrograph of PP / m-F / Triton X-100 …….. 86
Figure 4. 37.f SEM micrograph of PP / m-F/ PE-block- PEG…… 87
Figure 4. 38. TGA of the PP/F composites…….…….. 88
Figure 4.39 FTIR Spectrum of vacuum evaporated polyethylene…….…... 89
Figure 4.40 Atomic force microscopy of vacuum-processed polyethylene on aluminum oxide gate dielectric showing island formation and growing of the film: a)10 nm thick film; b) 10 nm thick film annealed at 100°C for 15 min; c) 20 nm thick film; d) 20 nm thick film annealed at 100°C for 15 min. ……. 91
Figure 4.41 Relative permittivity of a 250 nm-thick film of evaporated polyethylene..... 92
Figure 4.42 Transfer characteristics of field effect transistors with polyethylene dielectric: Channel design: L = 75 μm, W = 2 mm. Dielectric capacitance per area C_{0d} = 8.5 nF /cm^2..... 93
Figure 4.43 Output characteristics of field effect transistors with polyethylene gate dielectric: Channel design: L = 75 μm, W = 2 mm. Dielectric capacitance per area C_{0d} = 8.5 nF /cm^2..... 94
Figure 4.44 Transfer characteristics of field effect transistors with polyethylene dielectric: Channel design: L = 35 μm, W = 7 mm. Dielectric capacitance per area C_{0d} = 60.4 nF /cm^2..... 94
Figure 4.45 Output characteristics of field effect transistors with polyethylene dielectric: Channel design: L = 35 μm, W = 7 mm. Dielectric 95

capacitance per area C_{0d} = 60.4 nF /cm^2.....
Figure 4.46 Transfer characteristics of field effect transistors with polyethylene dielectric: Channel design: L = 75 μm, W = 2 mm. Dielectric capacitance per area C_{0d} = 96 nF /cm^2..... 95
Figure 4.47 Output characteristics of field effect transistors with polyethylene dielectric: Channel design: L = 75 μm, W = 2 mm. Dielectric capacitance per area C_{0d} = 96 nF /cm^2..... 96
Figure 4.48 a) Transfer and b-c) output characteristics of indigo on evaporated polyethylene passivated aluminum oxide dielectric …….. 97
Figure A.1. Stress at Break of the Polypropylene/Carbon Nanotube Composites…… 113
Figure A.2. Stress at Break of the Polypropylene/Fullerene Composites…… 114
Figure B.1. Stress vs strain curves of PP/ neat CNT composites…….. 115
Figure B.2. Stress vs strain curves of PP/m-CNT composites…….. 116
Figure B.3. Stress vs strain curves of PP/ m-CNT/ PE-b-PEG composites….. 116
Figure B.4. Stress vs strain curves of PP/ m-CNT/ CTAB composites…… 117
Figure B.5. Stress vs strain curves of PP/ m-CNT/ MA-g-PP composites…... 117
Figure B.6. Stress vs strain curves of PP/m-CNT/Triton X-100 composites… 118
Figure B.7. Stress vs strain curves of PP/neat F composites……. 118
Figure B.8. Stress vs strain curves of PP/ m-F composites……... 119
Figure B.9. Stress vs strain curves of PP/ m-F/ PE-b-PEG composites…… 119
Figure B.10. Stress vs strain curves of PP/ m-F/ CTAB composites…… 120
Figure B.11. Stress vs strain curves of PP/ m-F/ MA-g-PP composites…….. 120
Figure B.12. Stress vs strain curves of PP/ m-F/ Triton X-100 composites….. 121

ABBREVATIONS

ALOX	Aluminum Oxide
ASTM	American Society for Testing and Materials
CB	Carbon Black
CNT	Carbon Nanotube
CTAB	Cetramium Bromide
DSC	Differential Scanning Calorimeter
F	Fullerene
FTIR	Fourier Transform Infrared Spectroscopy
HDPE	High Density Polyethylene
i-PP	Isotactic Polypropylene
LDPE	Low Density Polyethylene
LLDPE	Linear Low Density Polyethylene
MA-g-PP	Maleic anhydride grafted polylpropylene
m-CNT	Surface Modified Carbon Nanotube
m-F	Surface Modified Fullerene
MFI	Melt Flow Index
MIM	Metal-Insulator-Metal
OFET	Organic Field Effect Transistor
PE	Polyethylene
PE-b-PEG	Poly(ethylene- block- polyethylene glycol)
PP	Polypropylene
SEM	Scanning Electron Microscopy
TEM	Transmission Electron Microscopy
TGA	Thermal Gravimetric Analysis
XPS	X Ray Photoelectron Spectroscopy

CHAPTER 1

INTRODUCTION

Conductive polymer composites have become one of the most important research subject in recent years due to wide application area of them. Some of the polymers are inherently conductive because they have conjugated chain structure whereas some polymers like polyethylene and polypropylenes have no conjugated structures and they are good insulators. It is possible to make them conductive by addition of some conductive filler like carbon black, graphite, carbon nanotubes, etc. Different factors affect the properties of a composite material: type of the polymer matrix, filler type, filler size, filler dispersion, orientation of filler in the matrix, etc. The interaction between filler and polymer chains are the most important aspect to get improved properties of composite material. The interactions can occur by attractions between the polymer chain and filler or chemical bonding between polymer matrix and filler. Chemical bonding between filler and polymer matrix is more favourable especially for conductive polymer composites because it gives the ability of the charge carriers move along polymer chain [1].

One of the objection of this study is to produce mechanically and electrically good conductive polypropylene composites by using different filler types. Multi walled carbon nanotube, carbon black and fullerene were used as fillers. Functionalization of carbon nanotube and fullerene were done with HNO_3/H_2SO_4 before mixing with polypropylene. To increase the compability of the polyproplene and the fillers some compatibilizers, such as Poly (ethylene- block- polyethylene glycol), maleic anhydride grafted polypropylene, cetramium bromide and Triton-X-100 were selected in this study.

Energy is the main problem of the world in these days. The aim of the scientist is to produce devices working with low energy. Transistor is a part of electronic devices, used as amplifier or open-close the circuit. Because of this reason, manufacturing of transistors working with low operation voltage, low switching time, low threshold is the main goal of the transistor research. Dielectric layer is an important part of the transistor. It determines the operation voltage and threshold voltage of the transistor. Switching time depends on the mobility of the semiconductor and channel length. Low operation voltage devices can be produced by decreasing the thickness of the dielectric layer or usage of high dielectric constant materials as the gate insulator. Purity of the dielectric layer is another factor to obtain better device performances, low leakage and hysteresis free devices.

In this study, transistors with low operating voltage were also prepared by using Low Density Polyethylene (LDPE) as gate dielectric. Previously, Chua et al. studied the transistors with Polyethylene gate dielectric [2]. They used spin coating method to deposit dielectric layer on the gate. This technique is hard for polyethylene because hot xylene or mesitylene should be used to prepare polyethylene solution. Furthermore, all experimental apparatus should be hot otherwise polyethylene starts to crystallize. Another important point is the impurities coming from the production of polyethylene. This impurities cause hysteresis in transistor device. Chemical vapor deposition of polyethylene were tried long years ago by different groups [3,4] and thin films of polyethylene were prepared. The main advantage is that, it is solvent free because additional step is required to evaporate solvent after spin coating. During the evaporation of the solvent some pin hole structures are formed on film. In this study, two gate dielectric layer used as gate insulator. Low operation voltage transistors were produced with polyethylene alone or combination of polyethylene with anodized Aluminum Oxide. Pentacene and Fullerene (C_{60}) semiconductor layers were used during the preparation of device. High on-off ratio and hysteresis free transistors were prepared with PE dielectric layer.

CHAPTER 2

BACKROUND INFORMATION

2.1. Polymer Matrice for Composites Preparation

2.1.2 Polypropylene

Polypropylene (PP) is the third commonly used commercial polymer of the world. Synthesis of the polypropylene is carried out from propylene gas at temperatures between 50 and 80 ^{0}C (Figure 2.1). Polypropylene was firstly synthesized by Natta in 1957. During polymerization of Polypropylene Ziegler Natta catalysts like aluminum alkyls and titanium halides are used to prefer stereoregularity of the product [5]. Polypropylene is one of the widely used polymeric materials due to its desirable mechanic, physical and thermal properties. It has high melting point, low density and good impact resistance [6]. PP can be used in many areas like automotive industry [7,8], medical industry [9,10] and as electromagnetic interference (EMI) absorber materials [11]. For some applications, mechanical and electrical properties of PP should be improved. Different fillers can be used for this reason such as carbon black [12] , carbon nanotube [13] and glass fiber [14].

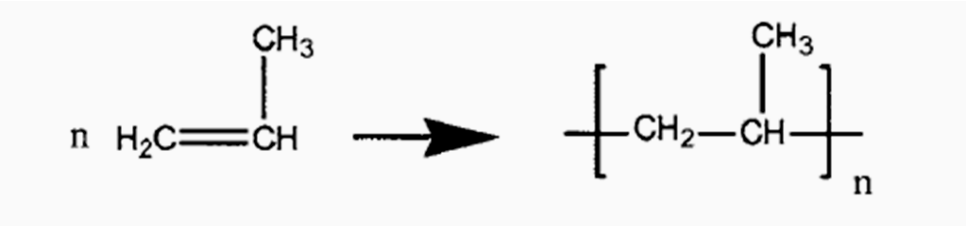

Figure 2.1 Synthesis of Polypropylene [15]

Polypropylene can be in the form of (*i* -PP), syndiotactic (*s* -PP), and atactic (*a* -PP) depending its stereoregularity (Figure 2.2). Depending on their structures, they have different properties. The mostly used polypropylene is the isotactic polypropylene [5] which has the ordered rearrangement of methyl group at the same side of the chain [15]. In Isotactic polypropylene, methyl group force the chain to prefer helical conformation. As a results of the ordered helical conformation isotactic polypropylene crystalizes easily [16]. During the process of polypropylene, some antioxidant to control oxidation and antistatic agent can be used to dissipate static charges [15]. Atactic polypropylene is obtained as a by product during synthesis of isotactic polypropylene and it can be used as modifier for asphalt and in adhesive industry [17]. Although isotactic polypropylene is rigid solid, both atactic and syndiotactic polypropylenes are soft and disordered materials with low degree of crystallinity. Since atactic polypropylene cannot form helical structure, it is soft and flexible [16].

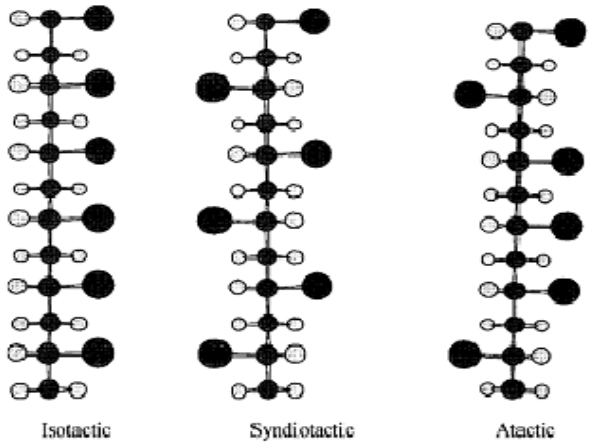

Figure 2.2 Structure of Isotactic, Syndiotactic and Atactic Polypropylene [15]

2.2. Polymer Dielectric for Organic Field Effect Transistor

2.2.1. Polyethylene

Polyethylene (Figure 2.3) is one of the most important commercial polymer in the world due to its excellent chemical resistance, high toughness, ductility, low water absorption, easy process. Polyethylene can be used to make bottles, film, pipe etc [15] .

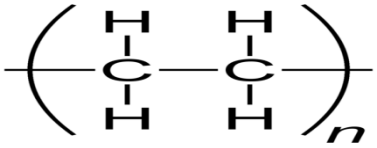

Figure 2.3 Structure of Polyethylene

The most commercial polyethylene's are High Density Polyethylene (HDPE) , Low Density Polyethylene (LDPE) and Linear Low density Polyethylene (LLDPE) [5]. The structures of the different configuration of PE are given in Figure 2.4. Low Density Polyethylene (LDPE) is mostly used to form thin film, packaging industry and as insulator material for wires [5].

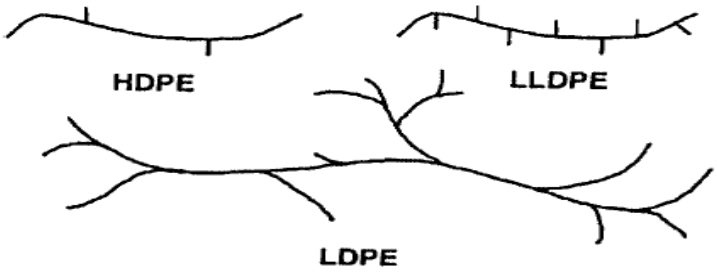

Figure 2.4 Structures of HDPE, LLDPE and LDPE [15]

LDPE is the first synthesized polyethylene in 1939. LDPE has partially crystalline structure and its crystallinity differs between 50 % and 70 %. The melting temperature of LDPE is about between 100 and 120 ^{0}C. LDPE has branched structure and size of the side chains determine the crystallinity of the LDPE. LLDPE has shorter branching than the LDPE. Branches are limited in HDPE in contrast to LLDPE and LDPE. Physical properties of LDPE depend on the degree of crystallinity and molecular weight. The properties of the PE such as tensile strength, opacity, rigidity, chemical strength depend on degree of crystallinity. These properties are increased with decreasing short chain branching. If the crystallinity decreases, permeability to liquid or gases and toughness of the material increase [5].

Highly stable and trap-free dielectrics are crucial in the fabrication of high-performance organic field effect transistors (OFET's) [18,19]. Owing to its excellent insulating properties (band gap of ~8.8 eV)[20], and extremely low conductivity ($\sim 9\times10^{-17}$ $\Omega^{-1}cm^{-1}$)[21] , low toxicity, chemical inertness and stability [15], polyethylene represents an interesting choice for the dielectric layer in organic devices.

2.3. Conductive Fillers

2.3.1. Carbon Nanotubes

Carbon nanotubes (CNT) is one of the most studied material which have good electrical and mechanical properties due to its high aspect ratio. Carbon nanotubes firstly synthesized by Iijima [22] in 1991 during arc evoporation synthesis of fullerene. Its structure is like one or more rolled graphene sheets with several microns in length and about 2-25 nm in diameter. CNTs are very small seamless hollow tubes or cylinders of rolled-up graphene sheets [23]. Structure of a graphene sheet was given in Figure 2.5.

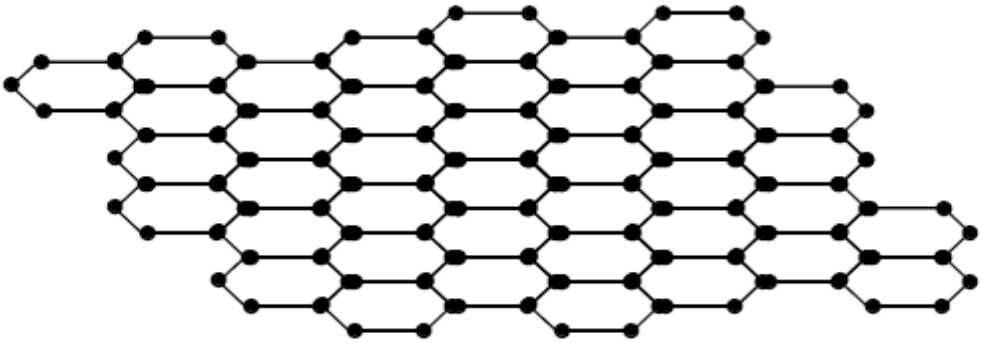

Figure 2.5 Structure of graphene sheet [23]

There are two types of carbon nanotubes: single walled carbon nanotube (SWNT) and multi walled carbon nanotube (MWNT) (Figure 2.6).

Figure 2.6 Structure of multi walled carbon nanotube and single walled carbon nanotube [23].

Due to hexagonal symmetry in graphene sheet, it has different isomers depending on how to planar graphene sheet is folded. Three isomers of Carbon nanotubes are Armchair, Zig-zag and Chiral (Figure 2.7).

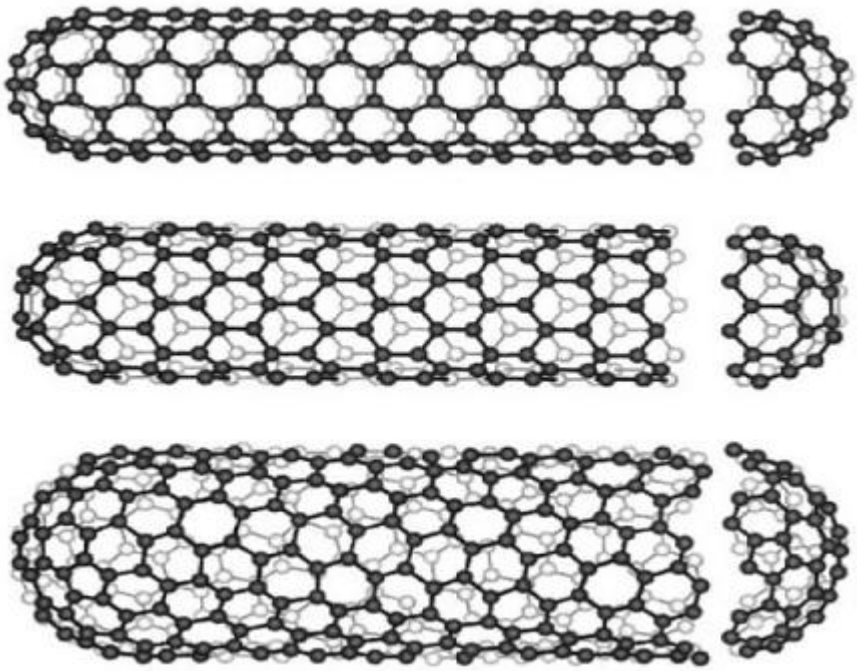

Figure 2.7 Structural isomers of Carbon Nanotubes, armchair (top) zig zag (middle), chiral (bottom) [24]

Due to its isomerism, CNTs have different properties. For example armchair isomer is metallic, zig-zag and chiral can be metallic or semiconductor [23]. CNT is a good candidate to produce nanocomposite with polymers due to its high Young's modulus, aspect ratio [25] and electrical properties [26]. CNTs have wide application area such as biosensors [27], solar cells [28] and fuel cells [29]. One of the disadvantages of the CNT containing polymer composites is tendency of the CNTs to form agglomerate because of strong van der waals interaction. To prevent agglomeration of CNT and have good dispersion in polymer matrix, different methods can be used such as in-situ polymerization [30,31], melt mixing [32,33], surface functionalization [34,35], usage of appropriate compatibilizers [36,37] and solution mixing [38,39]. One of the most widely used method to prevent the agglomeration of CNT in polymer matrix is melt mixing [33]. There are two mostly used methods for the preparation of polymer

/carbon nanotube nanocomposites. These methods are solution mixing and melt mixing.

Bikiaris et al. [40] prepared polypropylene nanocomposites with surface modified CNTs. which were functionalized with HNO_3/H_2SO_4 (1:3 in volume ratio). Polypropylene/CNT composites were prepared with CNTs which prepared with different treatment time with acid. During acid treatment, length of the carbon nanotubes decreased and composites which prepared with surface treated CNT showed higher mechanical properties than the neat CNT /PP composites. Length reduction of CNT decreased the agglomeration ability of the CNTs. Zhou et al. [34] functionalized CNT with silane coupling agent and then grafted 3-methacryloxypropyltrimetoxysilane on CNT. After surface modification, CNT showed good interfacial adhesion with polypropylene and dispersion of the CNT was better than neat CNT.

Kashiwagi et al.[41] studied the thermal and flammability properties of the PP/CNT composites prepared by melt mixing. Addition of the CNT to polymer matrix increased thermal stability of the polymer matrix. Lee et al. [36] studied the effect of compatibilizer on rheological and electrical properties of acid, amine and heat treated CNT. Composites prepared with amine and acid treated CNT showed higher electrical properties than untreated CNT.

Logakis et al. [42] blended PP and CNT at 180 ^{0}C (speed was 200 rpm) for 30 minutes under N_2 atmosphere. They found the percolation threshold as 0.6 vol %.

Prashanta et al. [43] prepared masterbach based composites of PP/CNT. They figured out that addition of CNT, impact resistance of notched samples increased but in contrast with this for unnotched samples impact resistance decreased. CNT addition made crack initiation easier but crack propagation was limited.

Beside melt mixing or solution mixing different techniques can be applied to carbon nanotubes like surface functionalization or usage of appropriate compatibilizers to improve their dispersion in polymer matrix. Surface functionalization with proper functional groups improves the dispersability of carbon nanotubes in polymer matrix or solvent and enhance the ability of the carbon nanotubes to do strong interfacial interaction with polymer [44].

2.3.2. Carbon Black

The primary units of carbon black (CB) are aggregates, which are formed when particles collide and fuse together in the combustion zone of the reactor. Several of those aggregates may be held together by weak forces to form agglomerates. The difference between primary particle, aggregate and agglomerate is presented in Figure 2.8 [45]. CB differs from other forms of bulk carbon such as diamond and graphite (Figure 2.9). CB consists of non parallel plane of the graphite layers [46].

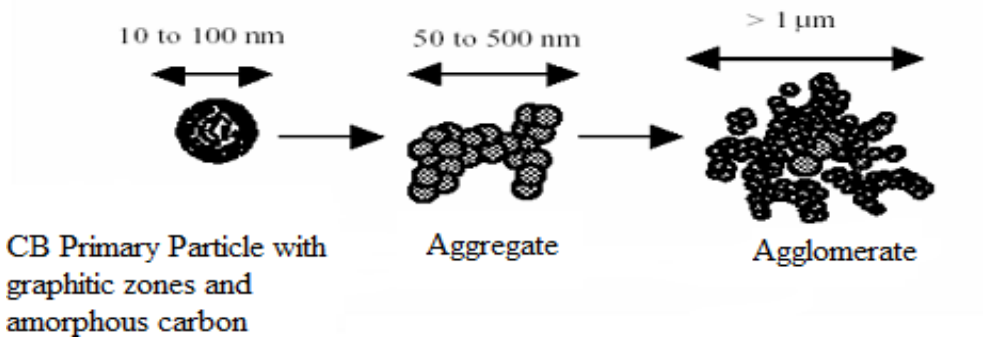

Figure 2.8 Agglomerate and Aggregate sizes of Carbon Black [45]

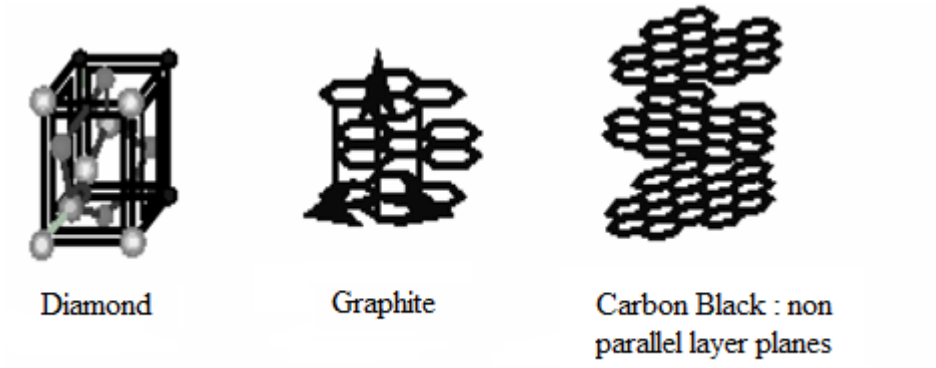

Figure 2.9 Structures of Diamond, Graphite and Carbon Black [46]

Applied shear stress during preparation of composites of CB in polymer matrix break-up agglomerates [24]. By the effect of the shear applied during the production of composites, the ability of the carbon black to form agglomerate should decrease. For many years it has been common practice to improve the electrical conductivity of plastics and rubbers by the incorporation of certain additives like special grades of carbon black [47]. CB is very important filler, especially in the rubber industry. Their fine particle size, high particle porosity, and compatibility with organic materials made them obvious candidates for use as fillers [48]. The strong interaction between polymer and CB particles improves the mechanical properties of the composites [49,50]. The conductivity of a polymer-CB composite depends several factors such as carbon black content, the physical and chemical properties of the carbon black chosen, the chemical structure and crystallinity of the polymer and the process conditions [24,51].

Decrease in the electrical resistance of the polymer matrix is observed with the addition of the carbon black to the polymer matrix. At a concentration known as "electrical percolation threshold", a conductive network is formed by carbon black particles throughout the insulative matrix and the resistivity drops several orders of magnitude [52] . The electrical conductivity of the polymer / CB composites are close to the polymer up to threshold point, after this point carbon black particles form

conductive network in polymer matrix [53,54] and conductivity of the polymer matrix increases several order magnitude [24]. This threshold occurs in the range from 3 to 15 wt % for CB [24].

2.3.3 Fullerene (C_{60})

The fullerenes were discovered in 1985 by Smaliey and Kroto while performing mass-spectroscopy analysis of carbon vapor. They observed the presence of even-numbered clusters of carbon atoms in the molecular range of C_{30} – C_{100}. Fullerenes are cage like spherolites which consist of five membered rings (pentagons) and six membered rings (hexagons). The most known structures of fullerenes are C_{60}, C_{70}, C_{78}, C_{76} and C_{84}. The first synthesized and the most stable fullerene is C_{60} (Figure 2.10) which consist of sixty carbon atoms arranged to form twenty hexagons and twelve pentagons. This structure gives it the appearance of a soccer ball. Each hexagon is connected to alternating pentagon and hexagon, and each carbon atom is shared by one pentagon and two hexagons. Its hybridization is partially sp^3 and partially sp^2.

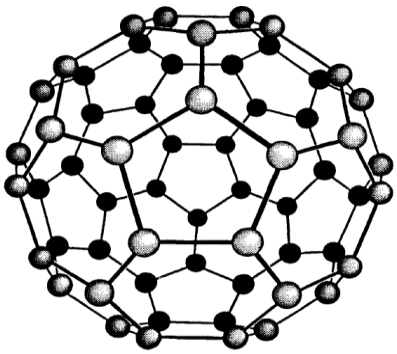

Figure 2.10 Structure of C_{60} [55]

C_{60} aggregates can be considered as softest of the solid phases of carbon. However, they can be compressed to the 70 % of its original volume [55]. The colors of the fullerene family vary according to their molecular weight and symmetry. Their colors in solution with respect to fullerene type are magenta (C60), port-wine red (C_{70}), brown (C_{76} and C_{78}), and yellow-green (C_{84}). C_{60} is insoluble or sparingly soluble in most solvents and that is why it is hard to handle [56]. Because of this problem different groups studied to obtain soluble fullerene derivatives.

Fullerenes and fullerene derivatives have been shown to possess interesting photonic, electronic, superconducting, magnetic, lubrication and biomedical properties due to their structure [57]. Low solubility and poor miscibility of fullerenes limit its application and its ability to form self aggregate cause phase separation problems [58,59].

Surface functionalization of the fullerenes and carbon nanotubes to improve their compatibility has become important subject in recent years [60]. Since fullerenes and carbon nanotubes have no hyrogen atoms or other groups on their surface, they cannot undergo substitution reaction. For this reason they need surface modification in order to do further functionalization on their surface [58].

2.4. Composites and Nanocomposites

Composites are made with the combination of two materials to give the unique properties of materials in one material [61]. The properties of the composites depend on the type of the filler, matrix and interface between filler and polymer chains. Interface between polymer and filler is important to provide better load transfer. Size, shape, orientation and dispersion of the filler are other factors affecting the properties of the composites [62].

The reinforcement length scale is in micrometers, and the interface of fillers is close to the bulk polymer matrix. In the case of nanocomposites, where the length scale of the reinforcement (nanoparticles) is in nanometer scale, they have ultralarge interfacial area per volume, and the distances between the polymer and filler components are extremely short. Polymer coils are 40 nm in diameter, and the nanoparticles are on the same order of magnitude as the polymer [63].

Apart from the properties of individual components in a nanocomposite, interfaces play an important role in enhancing or limiting the overall properties of the system. Due to the high surface area of nanostructures, nanocomposites present many interfaces between the constituent intermixed phases. Special properties of nanocomposite materials often arise from interaction of its phases at the interfaces. An excellent example of this phenomenon is the mechanical behavior of nanotube-filled polymer composites. Although addition nanotubes could conceivably improve the strength of polymers (due to the superior mechanical properties of the nanotubes), poor interaction serves only to create weak regions in the composite, resulting in no enhancement of its mechanical properties [64].

2.5. Conductive Polymer Composites

Polymeric materials can be intrinsically conductive due to their conjugated bonds or doping with an appropriate material. If the polymer is not conductive (polymers which have no conjugated structure), conductive polymer composites can be prepared with addition of a conductive filler such as metal powder, carbon black and graphite. Structures of some conjugated polymers are given in Figure 2.11. By addition of conductive filler, conductivity of the polymeric material increases by several orders of magnitude. This conductivity increase depends on the concentration and the character of the filling material. Conductivity of the material depends on the interaction of filling material and polymer chains. By mixing the filler with polymer,

conductive layers of filler are formed in polymer matrix and as a result volume resistivity of the material decreases. Charge transfer in polymer matrix can be achieved by the formation of chemical linkages between filler and polymer or direct interaction of fillers with each other. Chemical linkage between polymer chain and filler is more favourable because this allows the free motion of charge carrier along the chain [1].

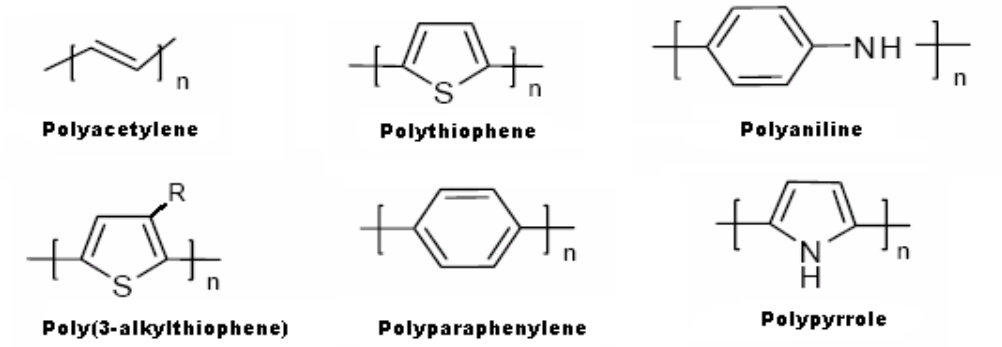

Figure 2.11 Structures of some conjugated polymers

2.6. Band Theory

Materials have specific or quantized energy levels according to quantum theory. According to their conductivities materials can be classified as conductor, semiconductors and insulators. Figure 2.12 shows the energy bands of the solid materials. The energy difference between valance band (Lowest occupied molecular orbital) (LUMO) and conduction band (Highest unoccupied molecular orbital) (HOMO) is named as band gap. For the materials that show metallic character conduction band and valence band overlaps and as a result of this property they show high conductivity. The band gap for insulator material is wide and thus they do not conduct electricity [65].

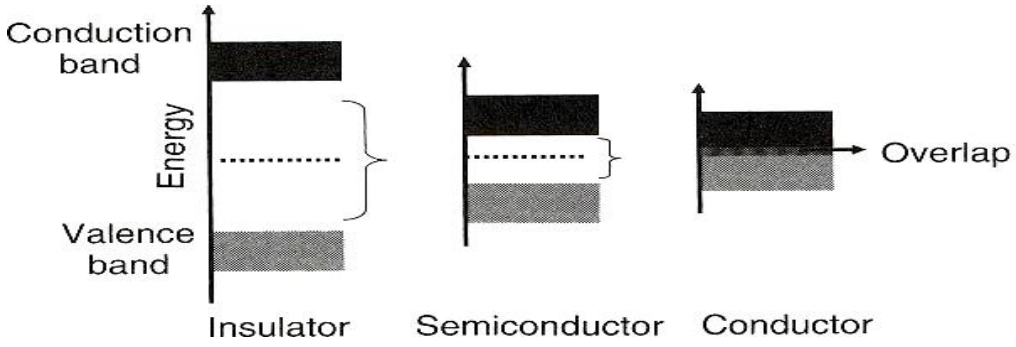

Figure 2.12 Energy Levels of Insulator, Semiconductor and Conductor [65].

2.7. Principles of Organic Field Effect Transistors

An Organic Field Effect Transistor (OFET) is three terminal device which consists of gate, source and drain electrodes. Drain and source electrodes are seperated from gate electrode with an dielectric layer. Semiconductor layer is placed between top electrodes (source and drain) and gate dielectric (Figure 2.13). The geometry of the semiconductor layer can be defined with W (width) and L (length). A few nm thick layer between the semiconductor and dielectric interface is called as channel.

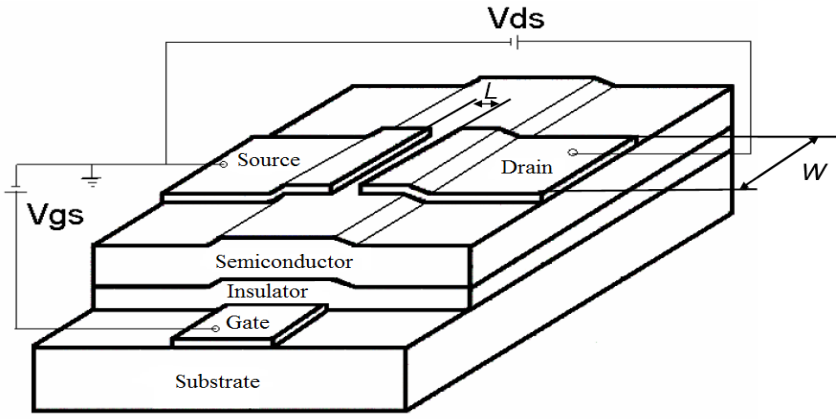

Figure 2.13 Structure of an OFET [66]

Gate electrode can be metal or conducting polymer. Voltage is applied to gate electrode and drain electrode. Source electrode is grounded and used as charge injection electrode. The voltage difference between gate and source electrode is named as V_{gs} while voltage difference between drain and source is called as V_{ds}. If positive voltage is applied to V_{gs} and V_{ds}, negative charges (electrons) are injected from source to channel. Positive charges (holes) are injected from source to channel when the negative gate voltage is applied.

When no gate voltage is applied, there are no charge carriers at channel. There can be small current flow from source to drain due to direct injection from source to drain but this is very small current because the resistance of semiconductor is high and the distance between source and drain is high. When negative voltage is applied to gate, positive charges will induce at semiconductor–dielectric interface and p type channel is formed. If the fermi level of the metal is close to HOMO level of the semiconductor, positive charges are injected by electrodes with applied voltage. If the positive voltage is applied to the gate, negative charges are induced at dielectric-semiconductor interface (n type channel is formed) and if the fermi level of the metal electrodes are close to LUMO level of the organic semiconductor, negative charges are injected by source electrode due to applied voltage (Figure 2.14) [67].

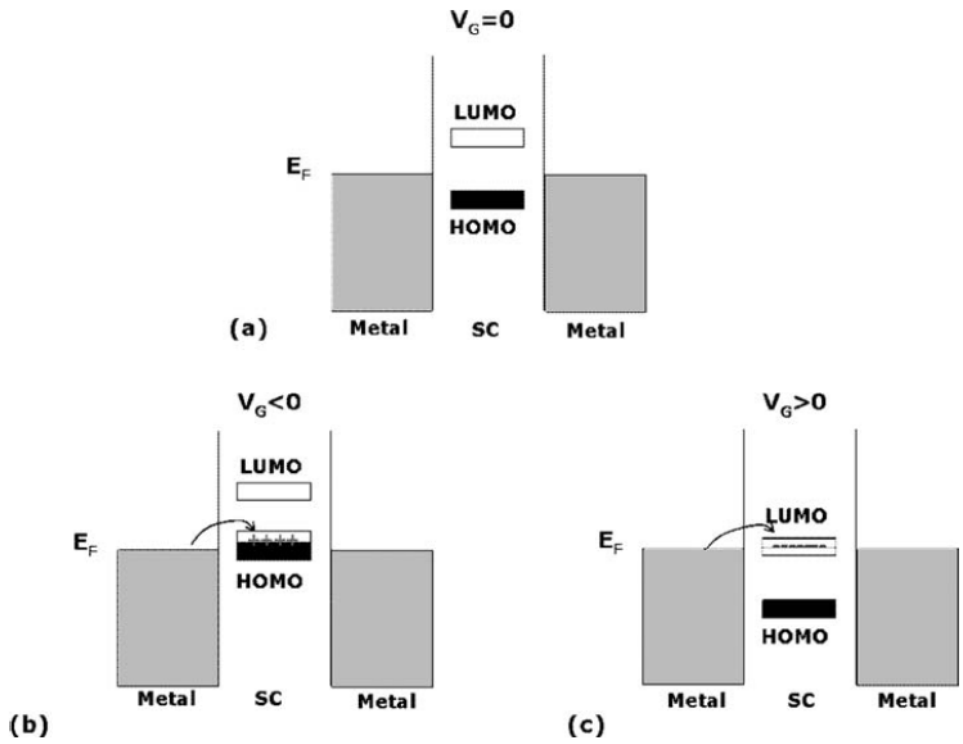

Figure 2.14 Working principle of an OFET [67]

Positive charges or negative charges move to channel in semiconductor layer when voltage is applied to gate electrode and after application of the second voltage between source electrode and drain electrode, holes or electrons move from source to drain.

2.7.1. Device Structures for OFET application

Four different device structures can be possible to build an OFET: bottom-gate bottom-contact, bottom-gate top-contact, top-gate bottom-contact, top-gate top-contact (Figure 2.15). The widely used OFET structure is bottom gate –top contact.

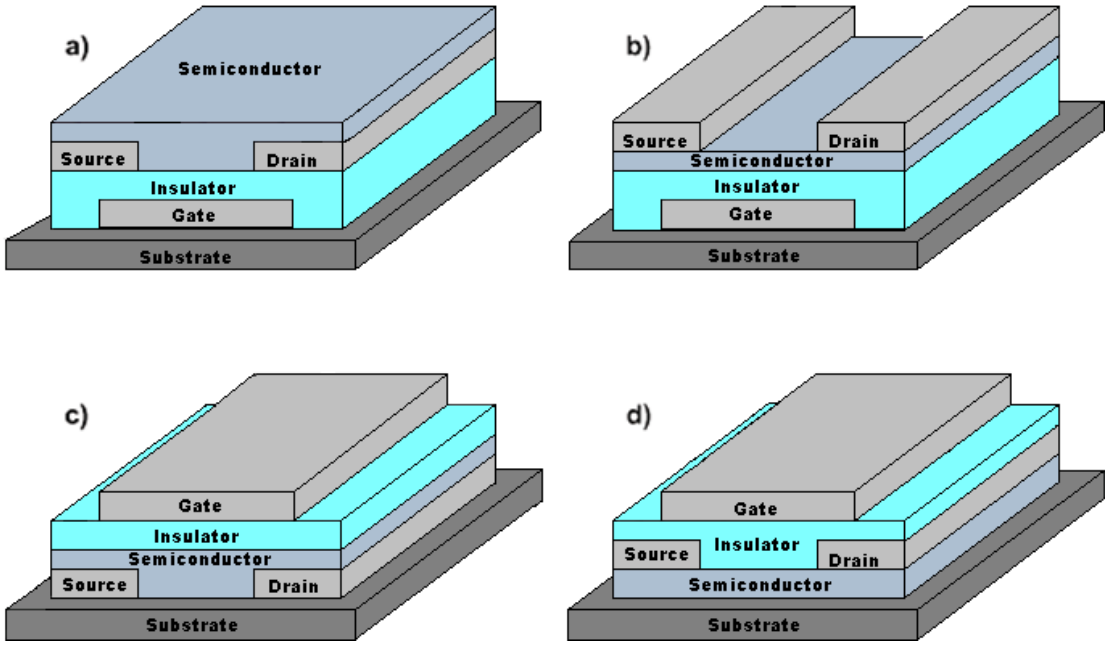

Figure 2.15 Different built structures for OFET's : a) bottom-gate bottom-contact, b) bottom gate top-contact, c) top-gate bottom-contact, d) top-gate top-contact

2.7.2. Characterization of OFET's

The characterization of an OFET can be done with two different measurements. These are transfer and output characteristics. Sweeped gate voltage (V_{gs}) and constant drain voltage are applied to measure transfer characteristic of an OFET device. Figure 2.16 gives the transfer curve of a typical device. It gives the I_{ds} versus to sweeping gate voltage at constant V_{ds}. In output measurement of an OFET, V_{gs} is sweeped while V_{ds} is constant. Figure 2.17 shows the typical plot of I_{ds} versus drain-source voltage (V_{ds}) at different gate voltages.

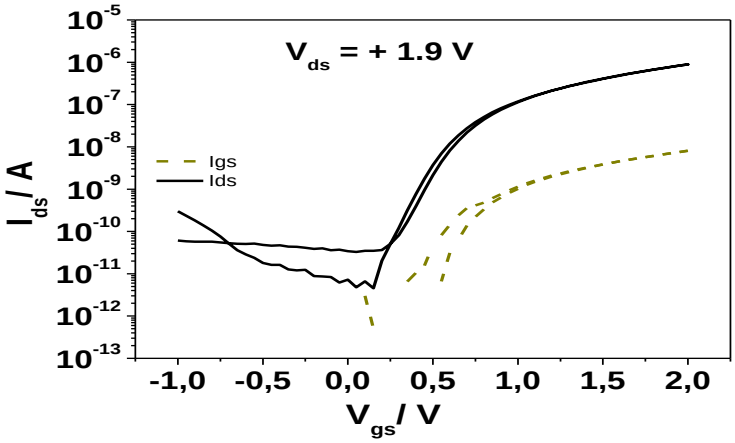

Figure 2.16 Typical transfer curve for an OFET

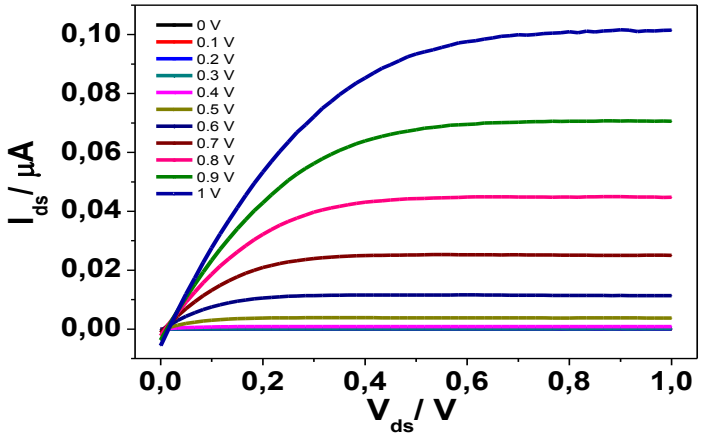

Figure 2.17 Typical output curve for an OFET

2.7.3. Importance of Gate Dielectric for OFET's

Gate insulator is one of the most important part of an OFET. Easy processibility, high capacitance, high dielectric strength, high on /off ratio and low hysteresis are the requirements for gate dieletric [19,68]. Dielectric layer can directly affect the

performance of an OFET device. The interaction between dielectric and organic semiconductor affects the morphology of the organic semiconductor. Beside this surface roughness of the dielectric layer is another important factor for OFET. If the dielectric layer is rough and it contains valleys at interface, these parts behave as charge trap. Field effect mobility is increased with increasing grain size of the organic semiconductor. High gate capacitance is another important property for gate dielectrics. Since high capacitance of the dielectric layer allows the high charge density induce at low voltages. Capacitance of the transistors can be increased by decreasing the thickness of the dielectric layer or with usage of high dielectric constant material [19].

When electric field is applied to dielectric material, material changes its charge distribution. As a result of this field induced polarization, material works as capacitor. Material should have large band gap to be an insulator. If there is an excitation state available material will not work as insulator. But if the applied voltage is higher than breakdown voltage material loses its insulating property [68]. Capacitance of the material between two metal layer is directly proportional with the dielectric constant of the material with the formula of $C = \varepsilon(k/d)$ where C is the capacitance, ε is the vacuum permittivity constant, k is the dielectric constant, d is the thickness of the dielectric layer. Capacitance of the dielectric layer increases with decreasing layer thickness [68].

Decreasing the operation voltage is critically important for some applications of OFETs. Three main factors affecting the operation voltage are: mobility of the semiconductor, capacitance of the dielectric and geometry of the channel. Relation of these factors with operation voltage is given with this formula:

$$I_D = \frac{W}{L} \cdot \mu \cdot C_0 \cdot \left(V_G - V_T - \frac{V_D}{2}\right) \cdot V_D$$

where W is the channel width, L is channel length, C_0 is capacitance per unit area, V_G is gate voltage, V_T is threshold voltage, V_D is drain voltage, μ is the mobility.

Geometry of the channel can be changed to decrease the operation voltage, but the application of this method is limited due to limitations of the shadow mask and printing techniques. Mobility of the semiconductor can not be altered because its intrinsic property of the semiconductor material. The only reasonable way to decrease the operation voltage is increasing the capacitance of the dielectric layer by decreasing thickness of the insulator layer or usage of high dielectric constant material.

2.7.4. Technigues for OFET Preparation

Different techniques can be used during the preparation of device. Spin coating and vacuum evaporation are the most commonly used techniques for the preparation of dielectric and semiconductor layer of an OFET.

Vacuum evaporation of melamin were done by Vladu et al. [69]. They prepared transistor with vacuum processed melamin layer and C_{60} as semiconductor layer. They build transistors working at 15V with 4 orders of magnitude on/off ratio. The advantage of the vacuum evaporation is that it is free from the impurities coming from solvent, which can cause hysteresis. Impurities coming from the dielectric layer can cause hysteresis, too. Egginger et al. [70] worked on the effect of the impurities coming from PVA dielectric on hysteresis. Vladu et al. prepared OFET which consist totaly biodegredable materials [71] . Both spin coating and vacuum evaporation techniques were used in this study. Vacuum evaporation is not useful only for small molecules. It can be also used for the evaporation of the polymers, too. Vacuum evaporation of polyaniline was done by Vladu and coworkers [72]. They prepared devices which contain polyaniline gate dielectric and C_{60} semiconductor layer by

using vacuum evaporation technique. Root mean square roughness (RMS) of 1.75 μm polyaniline film prepared by vacuum evaporation technique was 10 nm.

In this study, chemical vacuum deposition technique was used for evaporation of low density polyethylene gate dielectric, fullerene and pentace layers.

CHAPTER 3

EXPERIMENTAL

In this dissertation, Polypropylene/Carbon Black, Polypropylene/Carbon Nanotube, Polypropylene/Fullerene composites and transistors which are built with the polyethylene gate dielectric were studied. Before preperation of Polypropylene/Carbon Nanotube, Polypropylene/Fullerene composites, carbon nanotube and fullerene were fuctionalized with H_2SO_4/HNO_3. Details of composite preparation ,surface functionalization and transistor preperation were given in experimental part.

3.1. Surface Modification of Carbon nanotube with HNO_3/H_2SO_4

Multi walled carbon nanotube (Nanocyl 7000) purchased from Nanocyl was used in this study. Concentrated H_2SO_4 (95-98 %) and HNO_3 (65 %) were supplied from Merck. Carbon Nanotubes were refluxed with concentrated H_2SO_4-HNO_3 mixture at different ratios (1:1, 1:1.6, (v/v), HNO_3 : H_2SO_4) at 90^0C for 5 h to form a brown suspension (Figure 3.1). The materials were named as CN 1 and CN 2 respectively. Then the suspension was diluted with distilled water (200 mL) and stirred for 2 hours. After this process reaction mixture was filtrated and washed with distilled water. Then the obtained black solid is dried in vacuum owen [73]. The chemical structure of the chemically modified Carbon Nanotube with H_2SO_4/HNO_3 is given in Figure 3.2.

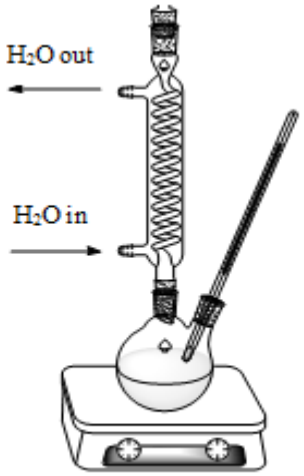

Figure 3.1 Experimental set up for surface modification

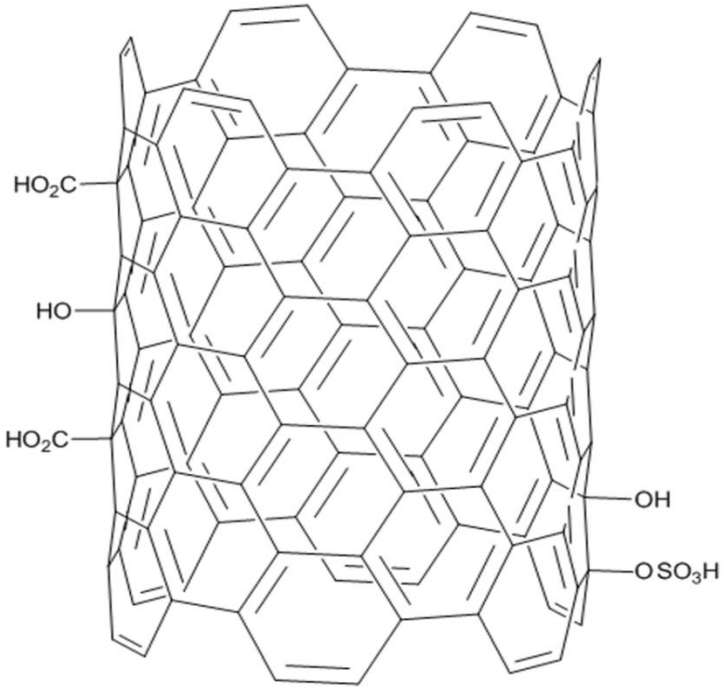

Figure 3.2 Chemical structure of the chemically modified carbon nanotube

3.2. Surface Modification of Fullerene with HNO_3/H_2SO_4

Fullerene was purchased from Acros Organics USA (180-200 mesh). Concentrated H_2SO_4 (95-98 %) and HNO_3 (65 %) were supplied by Merck. Fullerene was refluxed at 130 ^{0}C with a concentrated H_2SO_4-HNO_3 mixture at different concentrations (1:1 and 1:1.6, (v/v), HNO_3 : H_2SO_4) for 5 h. The materials were named as F1 and F2, respectively. Then the mixture was diluted with distilled water to get hydrogen sulfated fullerene from cyclosulfated fullerene and stirred for 3 hours. After filtration the product washed with distilled water and dried under vacuum for 12 h [73]. Reaction of the fullerene with H_2SO_4/HNO_3 was given in Figure 3.3.

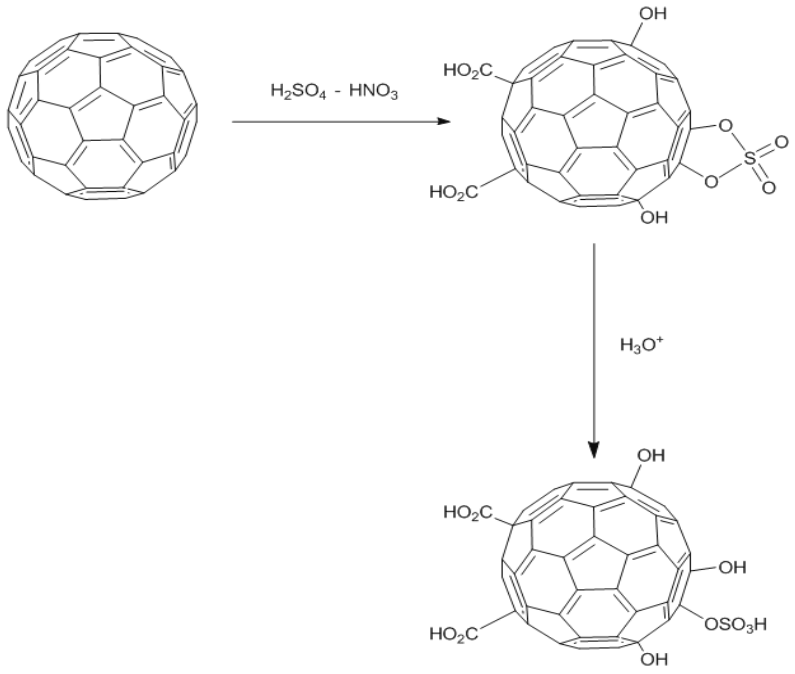

Figure 3.3 Reaction of Fullerene with HNO_3/H_2SO_4

3.3. Composite Preparation

3.3.1. Preparation of Polypropylene / CNT composites

Polypropylene/CNT composites were prepared by using DSM Xplore microcompounder (Figure 3.4) at 210 ^{o}C and 100 rpm for 3 min. Composites were prepared in four different compositions: 0.5, 1.0, 2.0 and 3.0 % (wt/wt). The surfactant, block copolymer and graft copolymer contents in the composites were 2 % wt, 5 % wt and 5 % wt respectively. Triton X-100, PE-block-PEG, MA-g-PP and CTAB were used to increase the dispersion of carbon nanotube particles inside the polypropylene matrix.

Figure 3.4 DSM Explore Microcompounder

3.3.2. Preparation of Polypropylene / Fullerene Composites

Polypropylene / Fullerene nanocomposites were also prepared using DSM Xplore microcompounder (Figure 3.4) Composites were prepared at 210 ^{o}C and 100 rpm for 3 min. Compositions of the fullerene in composites were 0.5, 1.0, 2.0 and 3.0 % (wt/wt). Different compatibilizers like Triton X-100, PE-block-PEG, MA-g-PP, CTAB were used to increase the dispersion of fullerenes in matrix. The surfactant and block copolymer and graft copolymer contents in the composites were 2 % wt, 5 % wt and 5 %wt.

3.3.3. Preparation of Polypropylene /Carbon Black Composites

Polypropylene and carbon black were mixed by using a Brabender Plastic Corder, PLV-151 (Figure 3.5) at 210 ^{0}C and 75 rpm for 10 minutes.

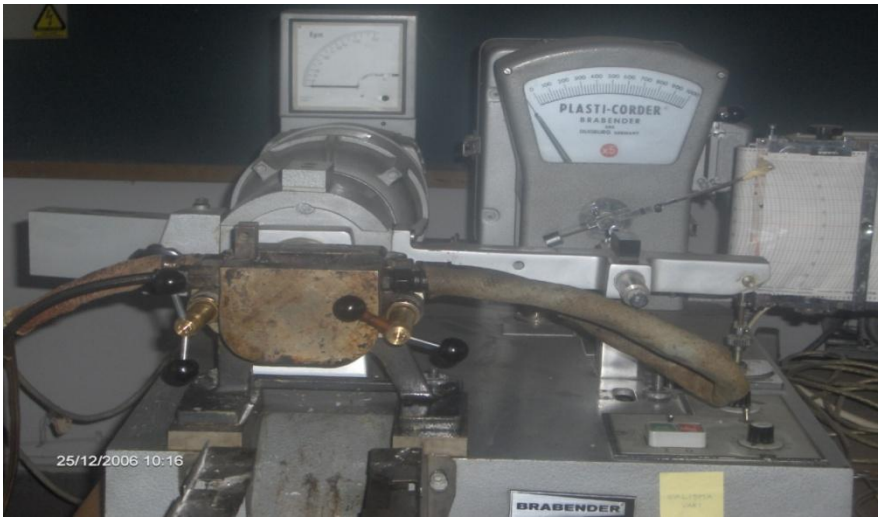

Figure 3.5 Brabender PLV-151 Plasticorder

3.4. Injection Molding

Tensile test samples were prepared with injection molding. The barrel temperature was 210 °C and mold temperature was room temperature. In this study, Micro-injection molding which is produced by Daca Instruments was used (Figure 3.6). Dimensions of the dog bone shaped injection molded test samples were given in Figure 3.7.

Figure 3.6 Daca Injection Molding Instrument

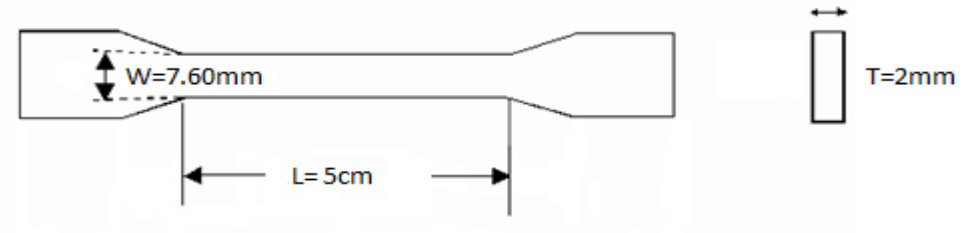

Figure 3.7 Dimensions of the injection molded test samples

3.5. Compression Molding

Rucker PHI hot press machine was used to prepare the compression molded test samples for tensile test. After pressing, compression polymer plates were cooled with cold water. Then dog bone shaped samples were prepared with standard dog bone shaped blade. Dimensions of the compression molded test samples were given in Figure 3.8.

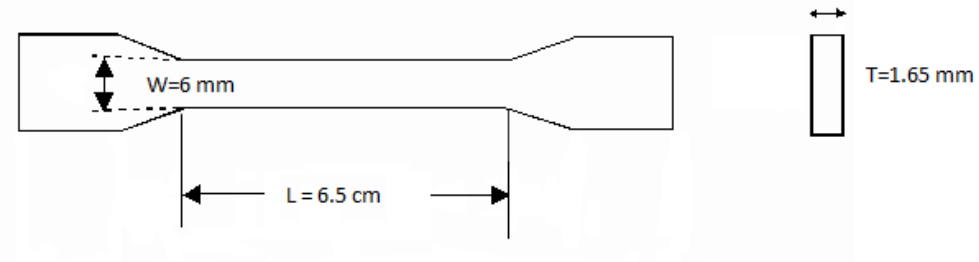

Figure 3.8 Dimensions of the compression molded samples

3.6. Conductivity Measurements

Electrical conductivities of the samples were measured by using four point probe technique. In this method outer two probes apply current to the sample and the inner two probes measure the voltage. The details of the set up were given in Figure 3.9. Conductivity is measured with the formula :

$$\sigma = \frac{\ln 2}{(\pi.\Omega.T)}$$

where T is the thickness and Ω is resistance of the test sample [74]. Compressed circular pellets were used for conductivity measurements.

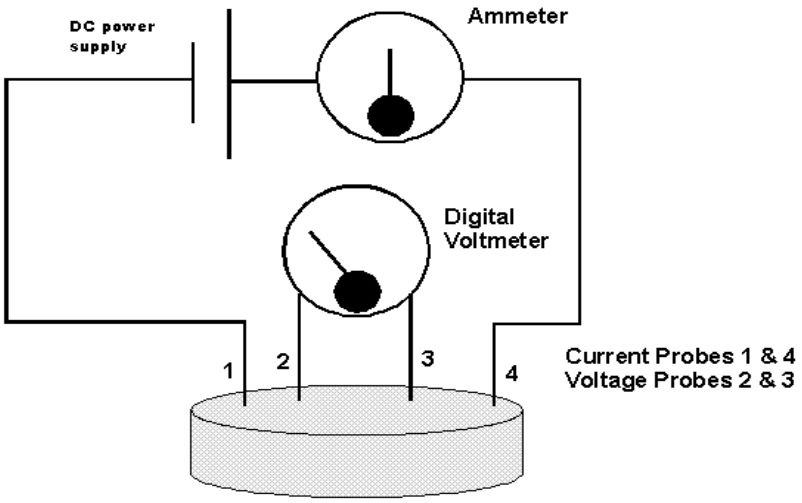

Figure 3.9 Four point probe technique [75].

3.7. Thermal Gravimetric Analysis

Thermal Gravimetric Analysis (TGA) of the composites were done by using Perkin Elmer Pyris 1 TGA at temperature range between 25^0C and 1000 ^{0}C with heating rate of 10 ^{0}C/min. Measurements were done under nitrogen atmosphere.

3.8. Fourier Transform Infrared Spectrometer (FTIR)

FTIR analysis was carried out with Bruker IFS 66/S FTIR spectrometer. The FTIR spectrum of the surface functionalized fullerene and carbon nanotubes were obtained by preparing the pellet of the materials with KBr. FTIR measurements of the vacuum evaporated polyethylene gate dielectric were performed using a Bruker Optics spectrometer (EQUINOX 55) on aluminium-coated glass slides.

3.9. Differential Scanning Calorimetry

Thermal properties of composites were studied with Dupont Thermal Analyst 2000 DSC 910S instrument at the temperature range between 25 ^{0}C - 225 ^{0}C under N_2 atmosphere. Heating rate was 5 ^{0}C /min. Percent crystallinities were calculated from the peak areas.

3.10. Scanning Electron Microscopy (SEM)

The morphological studies of the samples were performed by FEI Quanta 400 F Scanning Electron Microscopy. SEM micrographs of the fracture surfaces of composites were obtained at different magnifications. The fracture surfaces of the samples were coated by a thin layer of gold before investigation. The aim of this study was to observe dispersion of Carbon Black, Fullerene and Carbon nanotube particles in PP matrix

3.11. X Ray Photoelectron Spectroscopy (XPS)

X ray photoelectron spectroscopy was used to confirm the surface functionalization of the carbon nanotubes. XPS analyses of the samples were done by using Mg K Alpha source.

3.12. Zeta Potential

Surface charge of the surface modified and non modified carbon nanotube and fullerene samples were determined with zeta potential measurement. Zeta potentials of the samples were measured by using MALVERN Nano ZS90.

3.13. Transmission Electron Microscopy

TEM analyses of the samples were done by using a JEOL-JSM 1220 Transmission electron microscopy. Solutions of surface functionalized fullerene and carbon nanotube were preperad in water and then the drop of the solution applied on gold grid.

3.14. Tensile Test

Tensile tests were performed with Lloyd LR 30 K universal tensile testing machine according to ASTM D638 (Standard Test Method for Tensile Properties of Plastics). Crosshead speeds for injection molded and compression molded samples were 5 cm/min and 6.5 cm/min, respectively. Dog bone shaped molded samples were used and measurements were done at 24 ^{0}C. 5 kN load cell was used in the measurements.

3.15.Impact Test

Charpy impact test (unnotched) were done by using Pendulum Impact Tester of Coesfield Material Test machine. The test specimens were prepared by injection molding. Bar shaped specimens having size 5.5 cm were used in the experiments.

3.16.Melt Flow Index

Melt flow property measurements were performed by using Coesfield Material Test, Meltfixer LT. The measurement were done at 210 ^{0}C. Materials were allowed to melt for 5 minutes. Then standard weight (2.16 kg) placed on the piston of the instrument

to compress the sample. After that, the weight of the flow sample was reported for 10 minutes.

3.17. Organic Field Effect Transistor Preparation

3.17.1. Preparation of Glass Substrate and Gate Electrode

Glass substrates (15mm x 15mm) were cleaned by using ammonia solution (25% supplied from Merck) and hydrogen peroxide (30% supplied from Merck) in ultrasonic bath at 80 ^{0}C for 15 minutes. Aluminum gate electrodes were prepared by using shadow mask on clean glass substrate. The structure of the gate masks were given in Figure 3.10. Aluminum evaporation was carried out with metal evaporator at 0.5-2 nm/sec evaporation rate under pressure 2x10^{-6} mbar.

Figure 3.10 Structure of gate mask

3.17.2. Aluminum Oxide (Alox) Preparation

Al_2O_3 gate insulator was prepared by anodization of aluminium gate immersed into citric acid solution which is 0.01 M. Steel electrode was used as counter electrode. Current density for the anodization was 0.06 mA/cm^2. After anodization, gate electrodes were washed with distilled water and dried at 180 ^0C two hours under reduced pressure to get rid of water residues. The thickness of the Al_2O_3 layer is proportional with the applied voltage. Experimental set up for Al_2O_3 preparation was given in Figure 3.11.

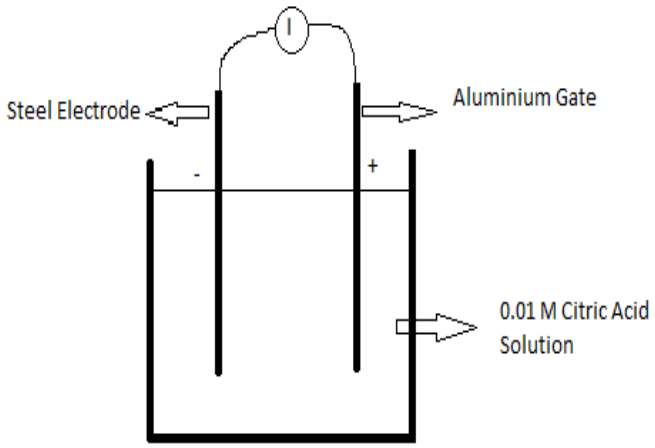

Figure 3.11 Preparation of Al_2O_3 insulator layer

3.17.3. Evaporation of Low Density Polyethylene

Evaporation of Low Density Polyethylene was done with Edwards High Vacuum System (Figure 3.12) at pressure of 10^{-6} torr with evaporation rate of 0.02-0.04 nm/sec. Dielectric layers with different thickness were deposited on gate electrodes.

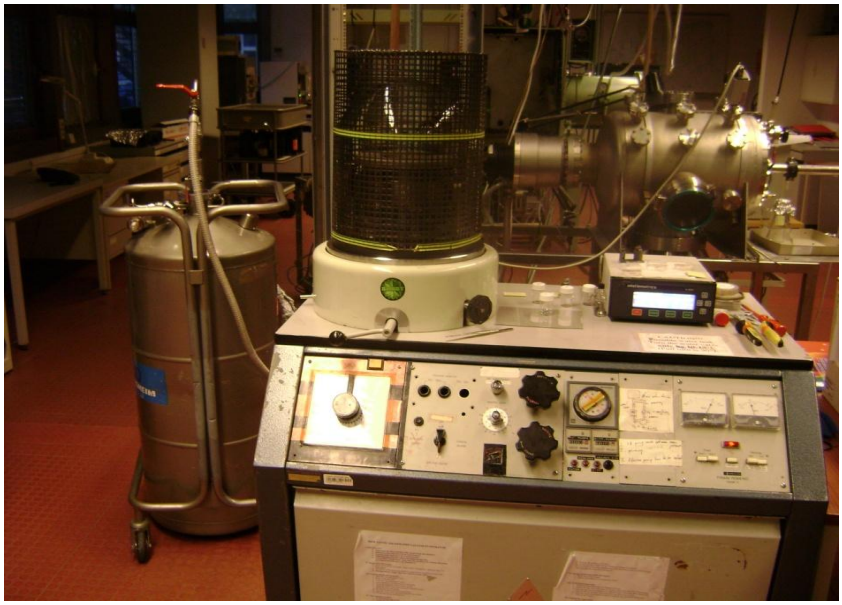

Figure 3.12 Edwards organic evaporator

3.17.4. Evaporation of C_{60} and Pentacene

Semiconductor layers C60 and pentacene were prepared with Edwards High Vacuum System at vacuum (Figure 3.12). Pentacene (normal grade, carbon ≥ 93.5 %) and C60 (sublimation grade, 99.9%) were supplied by Sigma–Aldrich and MER corporation, respectively. The thickness of the deposited semiconductor layers were 100 nm. Semiconductor layers of C_{60} and pentacene were deposited at pressure of 10^{-6} torr with deposition rates of 0.05-0.1 nm/sec and 0.1-0.2 nm/sec, respectively.

3.17.5. Evaporation of Source and Drain electrode

Source and drain electrode were prepared by using shadow masks. Aluminum source and drain electrodes were deposited for the transistors which have C_{60} semiconductor

layer. For the transistors which have pentacene semiconductor layer, Au source and drain electrodes were evaporated. The masks with different channel lengths were used in device fabrication. Structure of source and drain masks were given in Figure 3.13.

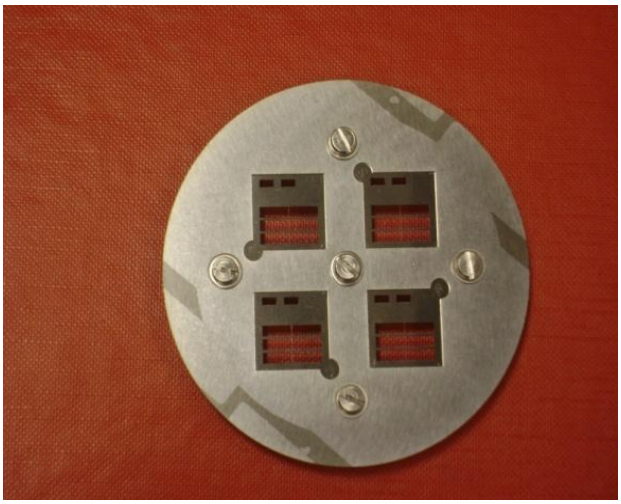

Figure 3.13 Structure of source - drain mask

3.17.6. OFET Characterization

Steady state current voltage measurements were performed with Agilent E5273 A (Figure 3.14) instrument. A picture of transistor measurement set up was given in Figure 3.15. All measurements were done in Mbraun MB200B glove box.

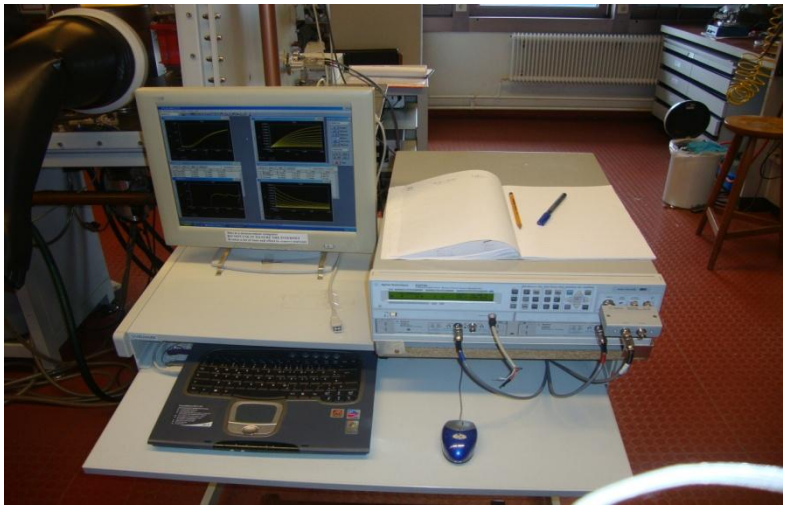

Figure 3.14 Agilent 5273 A Transistor Measurement Device

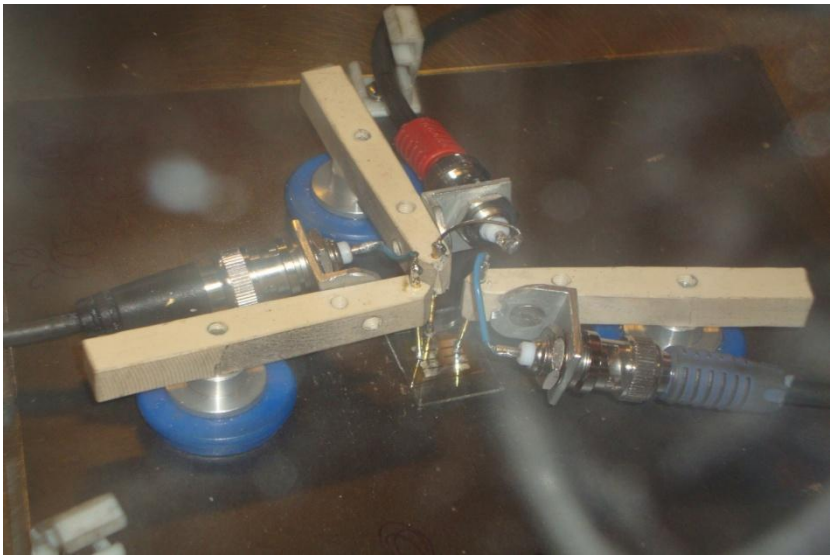

Figure 3.15 Transistor measurement set up

Figure.3.16 Mbraun MB200B Glove box

3.17.7. Dielectric Characterization

Dielectric characterization of the gate dielectrics was performed with metal-insulator-metal capacitors using a Novocontrol Alpha Analyzer (Figure 3.17). Firstly aluminium gate was evaporated on glass substrate then dielectric layer was evaporated on metal surface. After this step another Al layer were evaporated on dielectric layer to form Metal-Insulator-Metal (MIM) structure (Figure3.18).

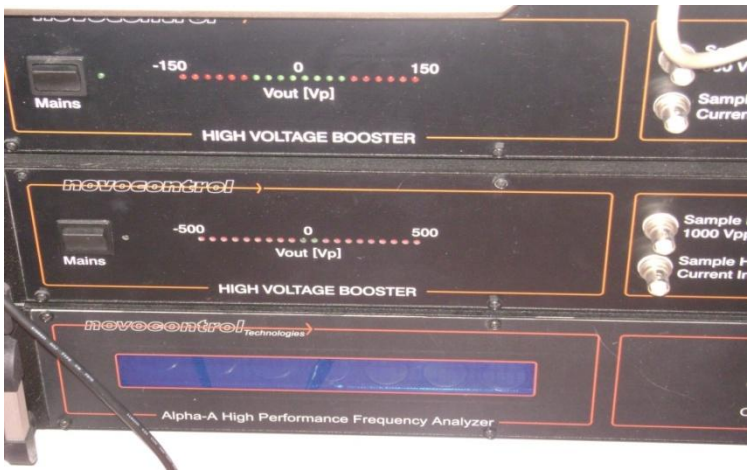

Figure 3.17 Novocontrol dielectric characterization equipment

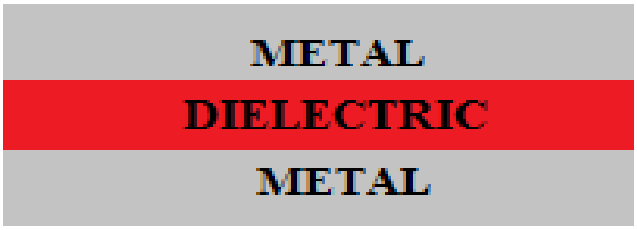

Figure 3.18 MIM structure for dielectric measurements

CHAPTER 4

RESULTS AND DISCUSSION

Results and discussion part of this dissertation is separated into six main parts. Properties of Polypropylene/Carbon Black composites were discussed in the first part. Characterization of surface functionalized carbon nanotubes and fullerenes were given in second and third part, respectively. Fourth and fifth parts include the properties of Polypropylene/Carbon Nanotube and Polypropylene/Fullerene composites, respectively. The last part describes device characteristics of the transistor which are built with the polyethylene gate dielectric.

4.1. Polypropylene / Carbon Black Composites

4.1.1 Melt Flow Index

Figure 4.1 shows melt flow properties of the PP/CB composites. Melt flow index values of the composites decrease with increasing carbon black content since increasing carbon black content increases the viscosity of the composites. A boundary layer, the amount of which depends on filler concentration, of the polymer is formed because of the strong interaction between polymer matrix and carbon black. Polymer molecules are adsorbed on the surface of carbon black particles and this decreases the mobility of the polymer chains. Increasing boundary layer density further increases the viscosity of the samples [76].

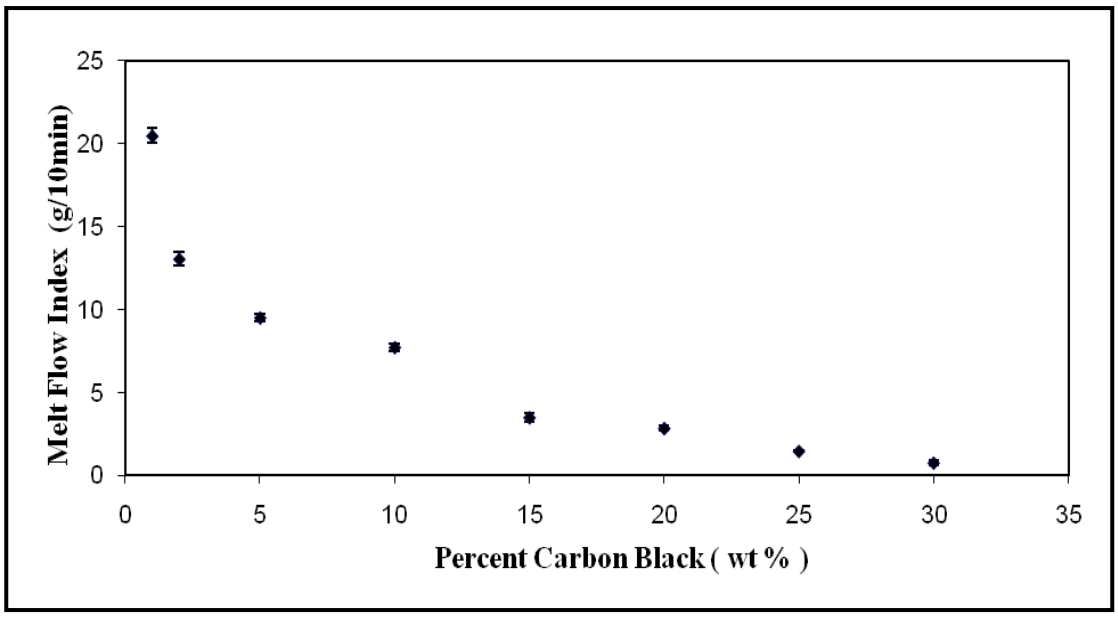

Figure 4.1 Melt flow properties of PP/CB composites

4.1.2. Percent Crystallinity of PP/CB composites

Effect of CB on percent crystallinity of PP was investigated by DSC. Percent crystallinity, calculated from DSC termograms are shown in Figure 4.2. Increasing CB content up to 30 wt% decreases the percent crystallinity from 41 to 33%. Since adding carbon black affects the crystal structure of the polypropylene, deformation occurs in the crystalline structure.

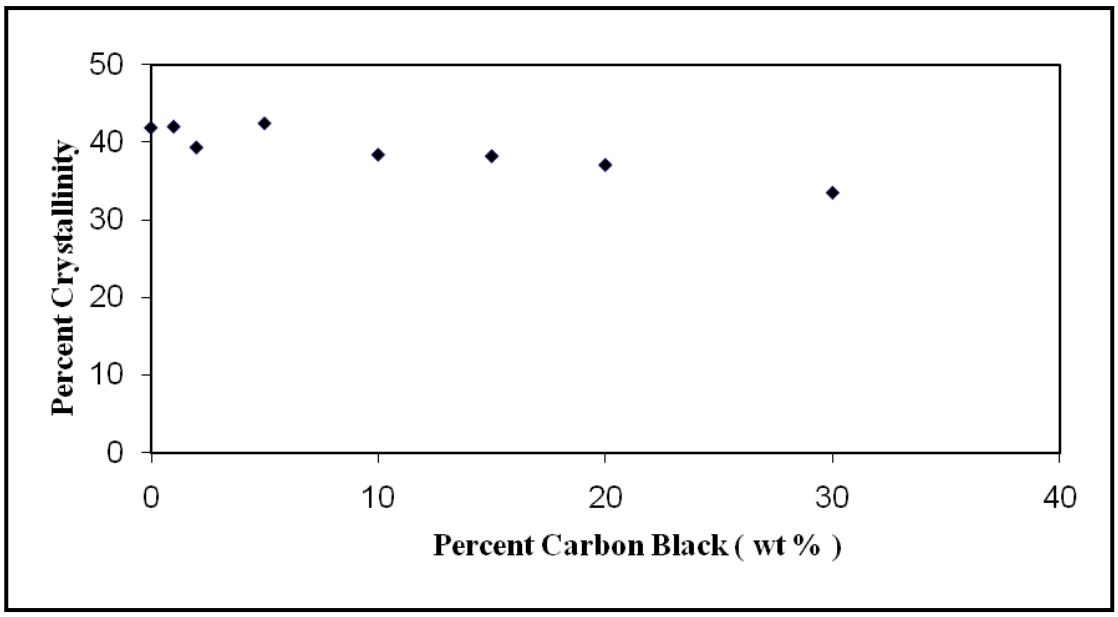

Figure 4.2 Percent crystallinity of the PP/CB composites

4.1.3 Impact Test

The effect of carbon black content on impact properties of composites are shown in Figure 4.3. Impact strength of composites decreases with increasing filler content. The samples which have carbon black lower than 10 wt% do not break with the applied force since the applied energy is absorbed by the polypropylene matrix. Increasing filler content made the composites more brittle. It can also be seen from SEM micrographs of fracture surface of composites that increasing carbon black increases the brittleness of the samples (Figure 4.4(a–d)).

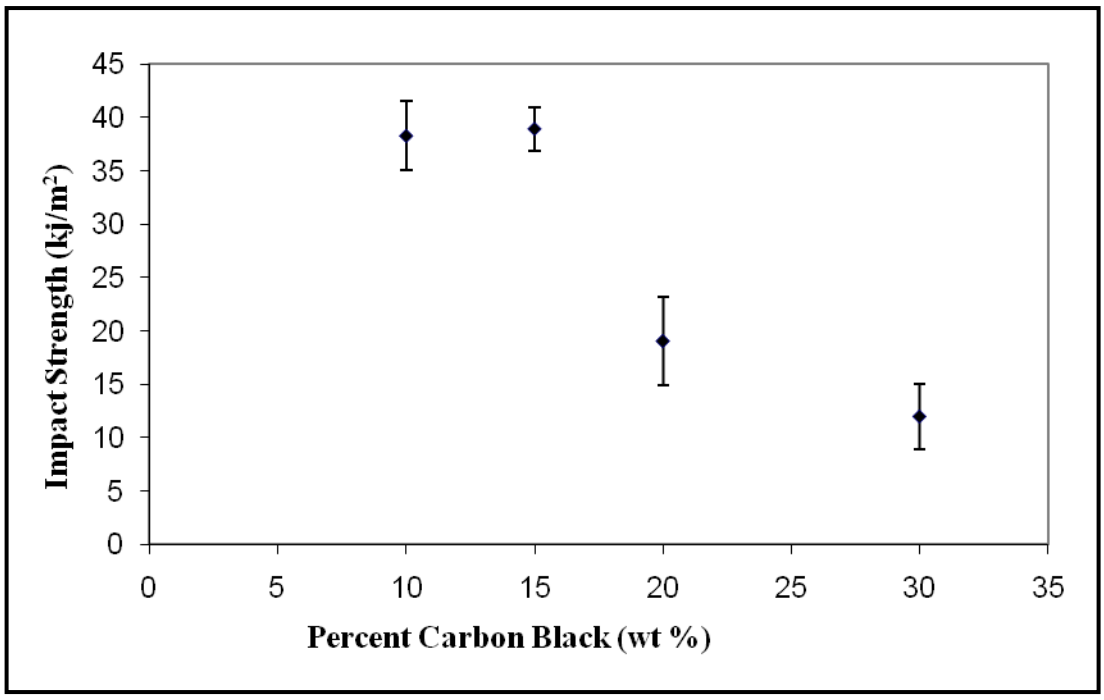

Figure 4.3 Impact test results for PP/CB composites

4.1.4 Scanning Electron Microscopy (SEM)

As can be seen in Figure 4.4(a–d) the estimated size of the carbon black particles are in the range of 100 nm. Dispersion of carbon black in polypropylene matrix becomes more uniform as CB content increases.

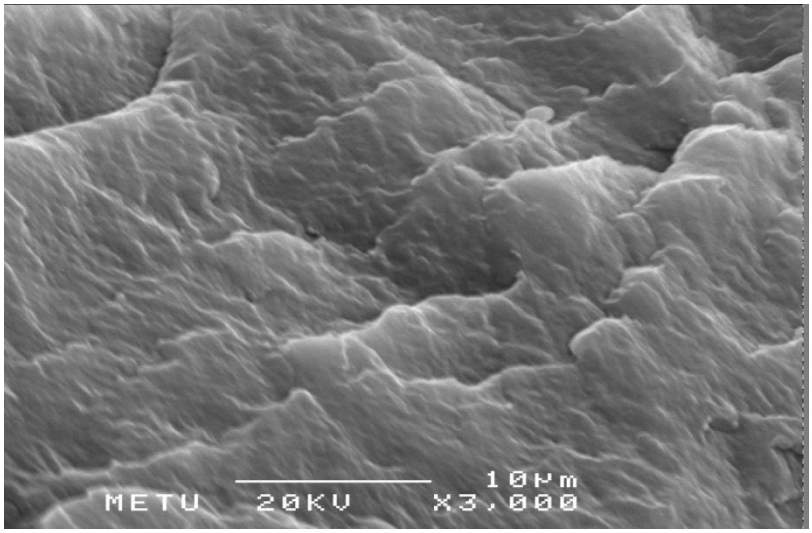

Figure 4.4a Fracture surface of Pure Polypropylene

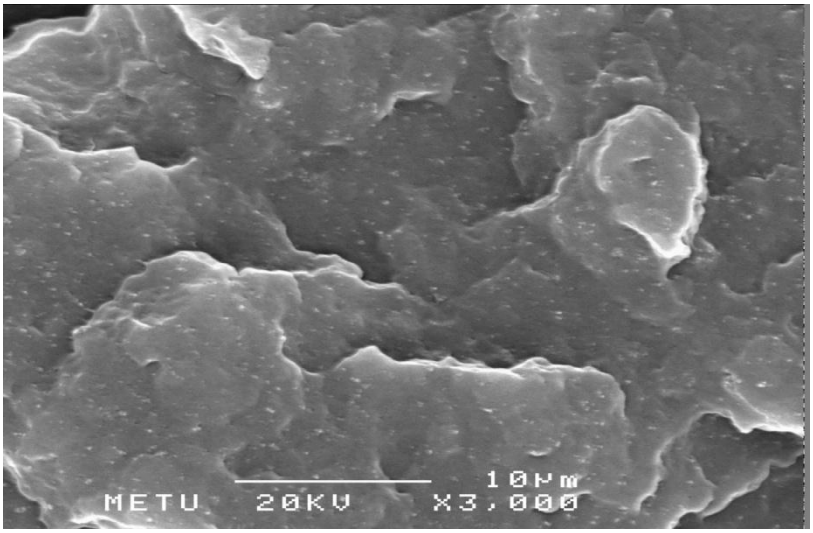

Figure 4.4b Fracture surface of the PP/CB composites containing 5% CB

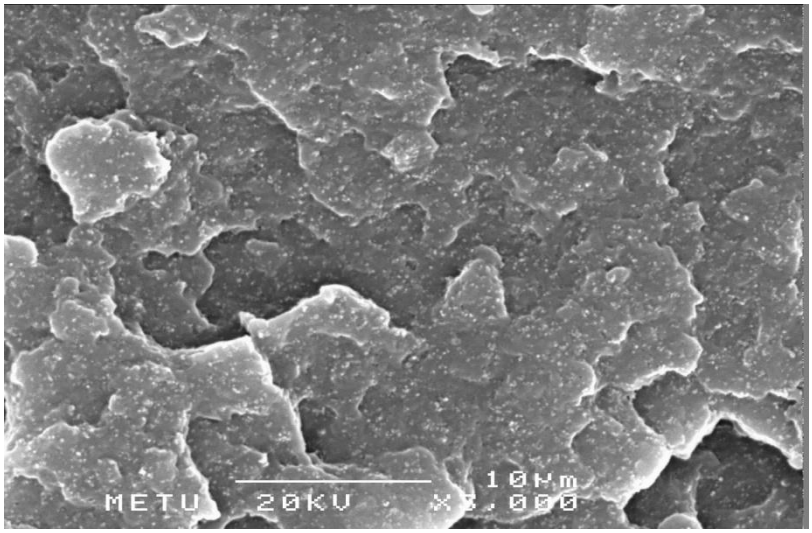

Figure 4.4c Fracture surface of the PP/CB composites containing 15% CB

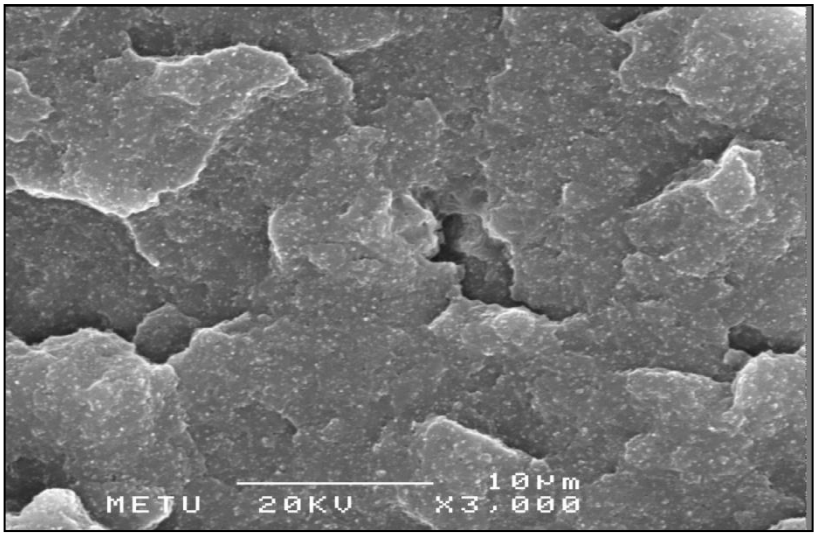

Figure 4.4d Fracture surface of the PP/CB composites containing 30 % CB

4.1.5 Mechanical Properties

The effect of carbon black content on tensile strength and Young's modulus was represented in Figure 4.5 and 4.6, respectively. For compression molded and injection molded samples, an increase was observed in Young's modulus and tensile strength. Young's modulus of the composite increases with increasing carbon black content because carbon black is stiffer than polypropylene. The increase of Young's modulus and tensile strength of the samples prepared by using injection molding is higher than the samples prepared by using compression molding. This result can be explained by the orientation of the polymer chains in the direction of applied force for the samples prepared by injection molding. In compression molded samples there is no orientation of the polymer chains, and mechanical strength of the samples are lower than the injection molded samples.

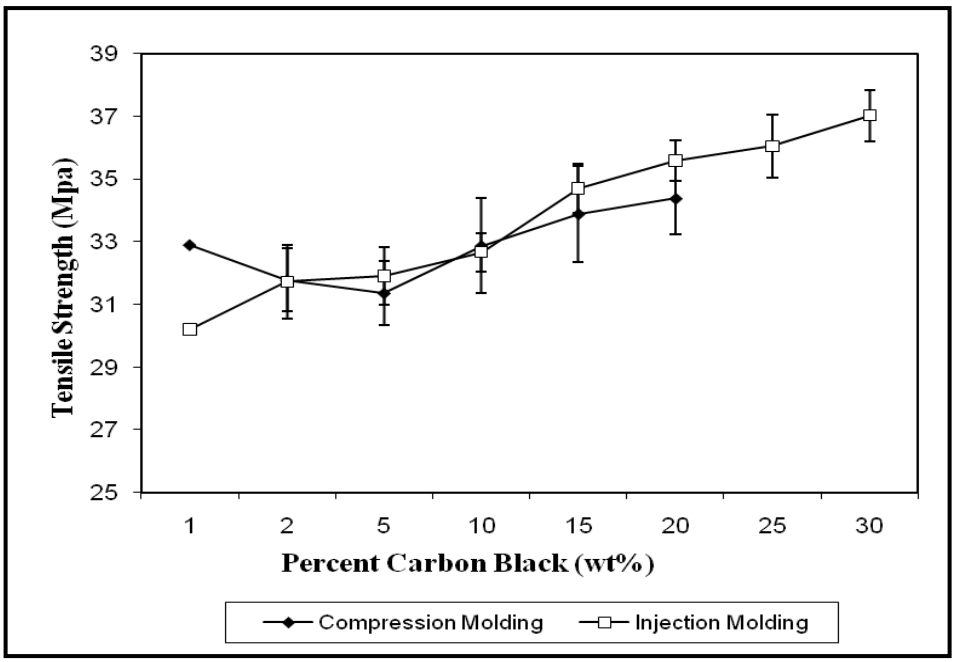

Figure 4.5 Tensile Strength of PP/CB composites

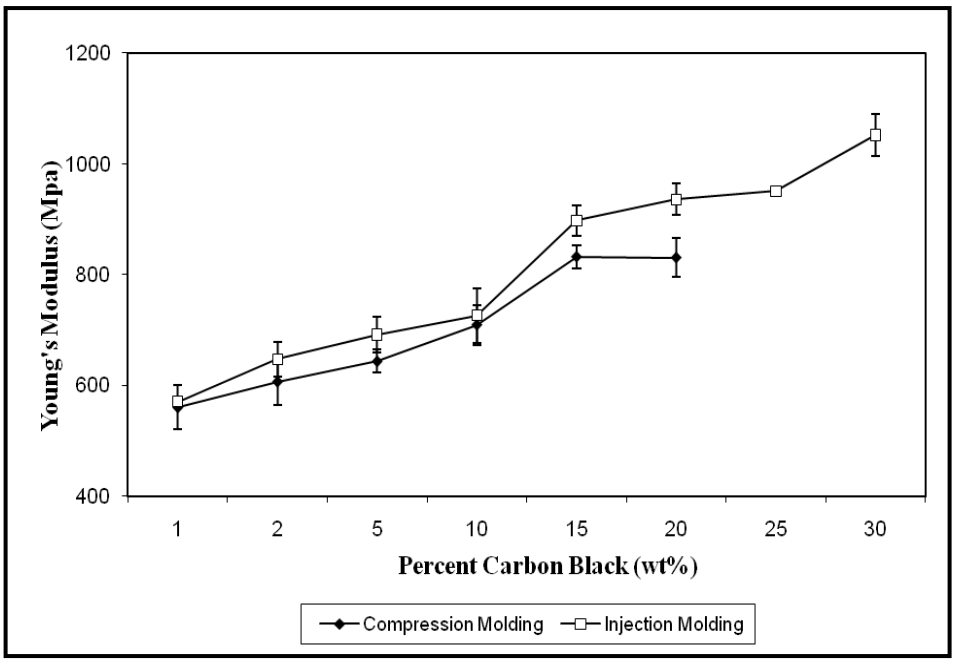

Figure 4.6 Young Modulus of PP/CB composites

Figure 4.7 represents the percent elongation at break with increasing filler content. Percent elongation at break of the samples decreases with the increasing filler content since addition of carbon black restricts the motion of the polymer chains.

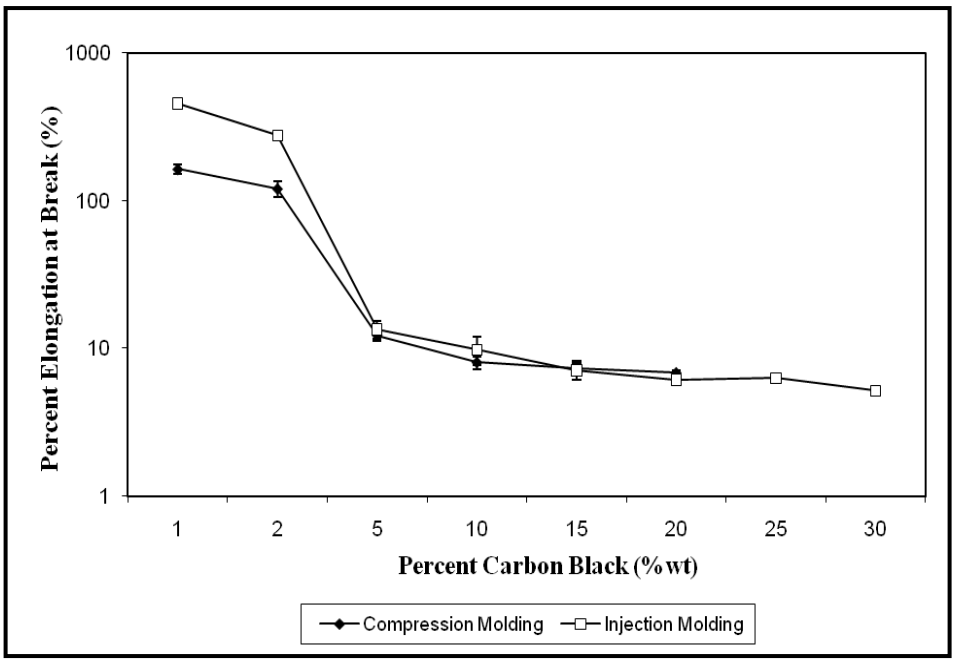

Figure 4.7 Percent elongation at break of the PP/CB composites

4.1.6 Electrical Properties

Addition of conductive carbon black particles in an insulative polymer matrix causes its electrical resistance to decrease. At a concentration known as 'electrical percolation threshold' (Pc) an infinite cluster of conductive carbon black particles extends throughout the insulative matrix and the resistivity drops several orders of magnitude [52,77].

PP is an insulative polymer. The conductivity of pure PP is $1x10^{-16}$ S/cm [77]. As can be seen in Figure 4.8, electrical conductivity increases up to 10^{-6} S/cm upon addition of 2 wt% CB. Electrical conductivity of the samples increases with increasing filler content as shown in this figure. There is an abrupt increase in conductivity for injection molded samples when CB content exceeds 17 %. This value is called a percolation threshold. Percolation threshold value for the compression molded

samples was observed when CB content exceeds 10%. After that point, conductivity increases rapidly because the filler starts to form a conductive layer through the polymer matrix [53]. After the threshold point, carbon black particles agglomerate and this causes the formation of the conducting network [54].

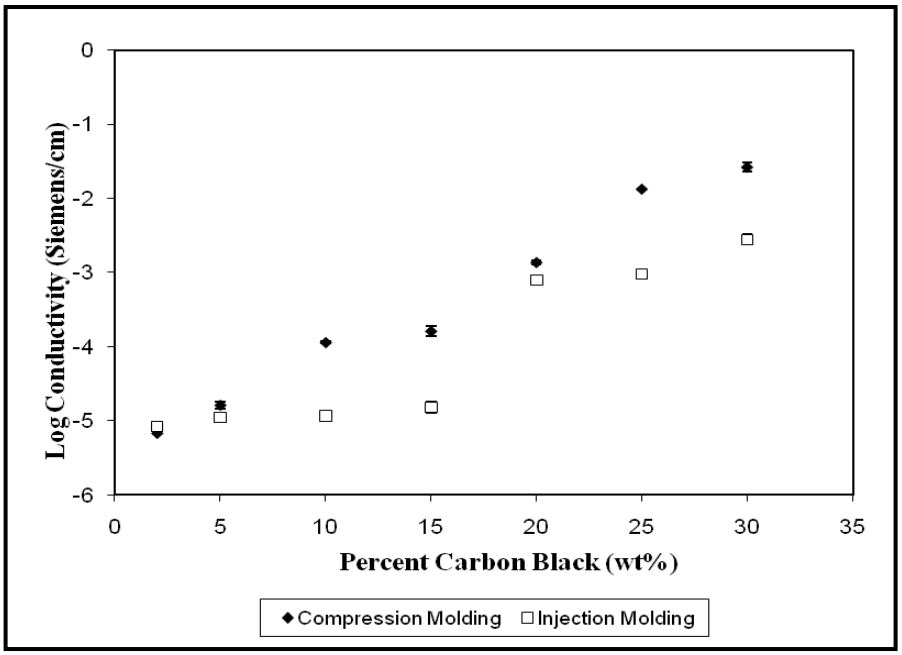

Figure 4.8 Electrical conductivity of the PP/CB composites prepared by compression and injection molding

Effect of the process type on the electrical conductivity is illustrated in Figure 4.8. The increase in electrical conductivity with increasing filler content is more pronounced in the samples prepared by compression molding. Since injection molding causes orientation of fillers and this causes an increase the distance between the CB particles. And as result of this, CB particles cannot form agglomerate and this decreases the electrical conductivity.

In the study of Chodak et al. [78] a relationship between percent elongation and electrical conductivity was proposed. In the present study this relationship was shown

in Figure 4.9 for compression molded and in Figure 4.10 for injection molded samples. Percent elongation at break of the samples decreased with increasing filler content, because polymer chains are absorbed on the surface of the carbon black and the force applied cannot be transported to each point equally and materials become more brittle and hard. The decrease at percent elongation at break is more obvious for the compression molded samples. Addition of the filler content more than the percolation threshold value causes a decrease in the percent elongation at break. After the percolation threshold point, material becomes more brittle [78,79].

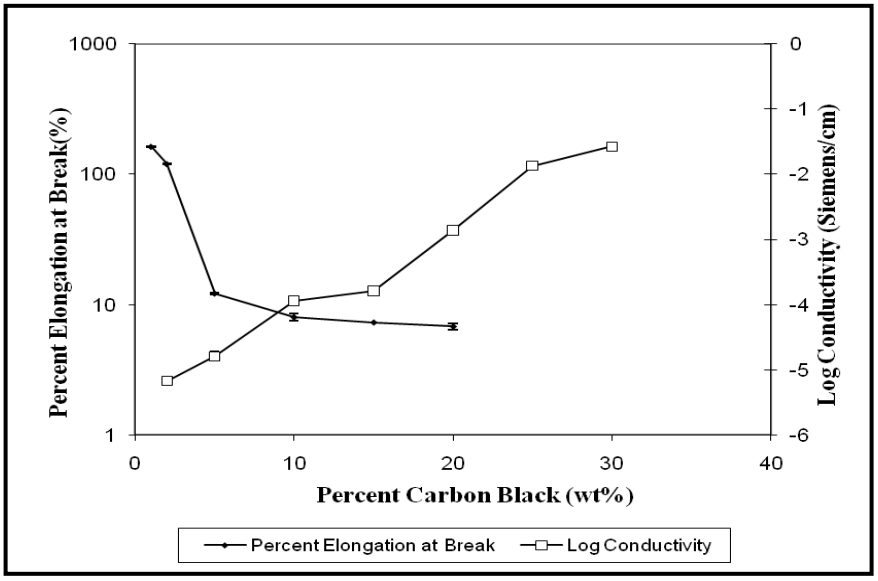

Figure 4.9 The relationship between electrical conductivity and percent deformation at break as a function of carbon black content for composites prepared by compression molding

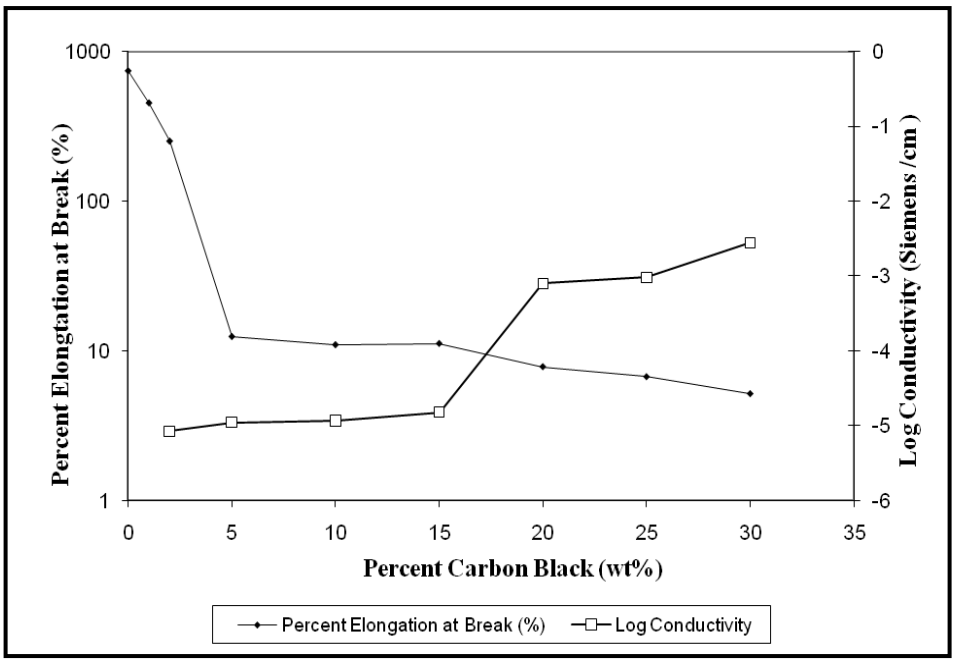

Figure 4.10 The relationship between electrical conductivity and percent deformation at break as a function of carbon black content for composites prepared by injection molding

4.1.7 Thermal Gravimetric Analysis (TGA)

The influence of the amount of carbon black on thermal stability of the composites is given in Figure 4.11. Increasing amount of carbon black increases the thermal stability of the composites. The temperature at which thermal decomposition starts, shifts to higher temperatures [80]. Pure PP decomposes at about 400^0C. Adding 30% CB increases the decomposition temperature to 530^0C.

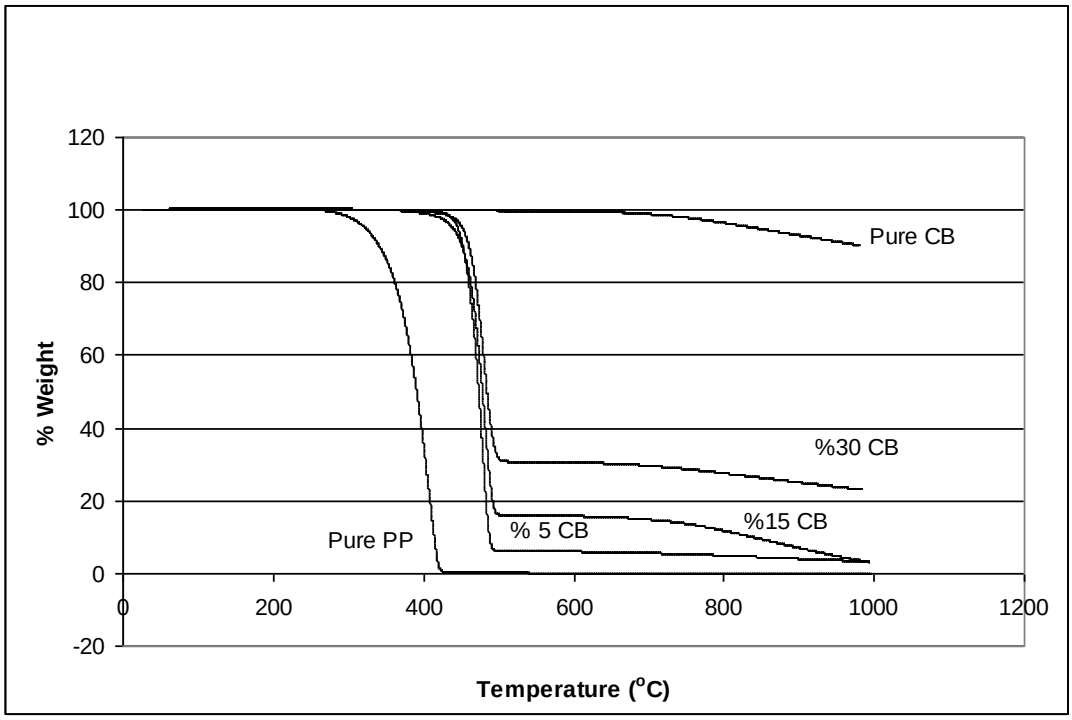

Figure 4.11 TGA of the PP/CB composites

4.2 Surface Modification of Carbon Nanotube

4.2.1 Fourier Transform Infrared Spectroscopy (FTIR)

The FTIR spectrum of the sulfonated Carbon nanotubes are given in Figure 4.12. The FTIR spectrum of the modified carbon nanotube show the charecteristic peak of carbon nanotube at 584-659 cm^{-1}. The carbonyl stretch C=O of a carboxylic acid appears as an intense band from 1709-1698 cm^{-1} and OH streching peak at 3394-3398 cm^{-1}. The characteristic peak of OSO_3H group was observed in the range 1284-1288, 1173 - 1156 cm^{-1} due to the asymmetric and symmetric streching vibrations of S=O groups respectively.

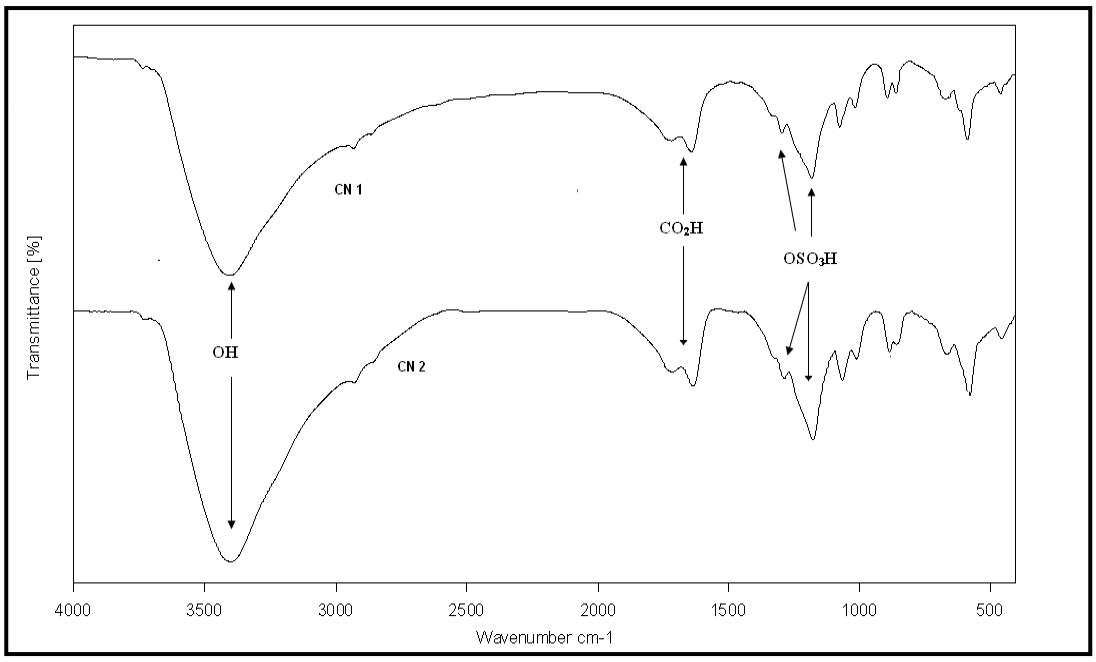

Figure 4.12 FTIR spectrums of CN 1 and CN 2

4.2.2 Elemental Analysis

Elemental Analysis results of the modified carbon nanotubes are given in Table 4.1. Increasing amount of the H_2SO_4 during synthesis increases the $-OSO_3H$ groups in the final product.

Table 4.1 Elemental analysis results of CN 1 and CN 2

	% C	% N	% H	% S	% O
CN 1	51.30	1.14	1.44	2.11	43.99
CN 2	52.81	0.69	1.35	5.49	39.63

4.2.3 Electrical Conductivity

Electrical conductivity of untreated CN and surface modified ones are given in Table 4.2. As can be seen from this table increasing the sulphuric acid content during modification of the material increases the electrical conductivity of the materials due to higher acidic conductivity of hydrogensulfate content on surface [81].

Table 4.2 Electrical conductivity of Untreated CN, CN 1 and CN 2

	Electrical Conductivity (S/cm)
Untreated CN	4.2×10^{-3}
CN 1	2.1×10^{-2}
CN 2	1.2×10^{-1}

4.2.4 X Ray Photoelectron Spectroscopy (XPS)

X ray photoelectron spectroscopy is used to confirm the surface functionalization of the carbon nanotubes. XPS analyses of the samples were done by using Mg K Alpha source. XPS spectra of the samples clearly show the existence of the functional groups on the materials. Figure 4.13 and 4.14 show the XPS spectra of the materials. The peaks coming from the 2p orbital of the sulfur are observed between 168-173 eV. These peaks show that the successive surface functionalization of the material with $-OSO_3H$ groups. The peaks due to carboxylic acid and hydroxyl groups give peak around (O 1s) 530-536 eV and (C 1s) 282-288 eV, respectively.

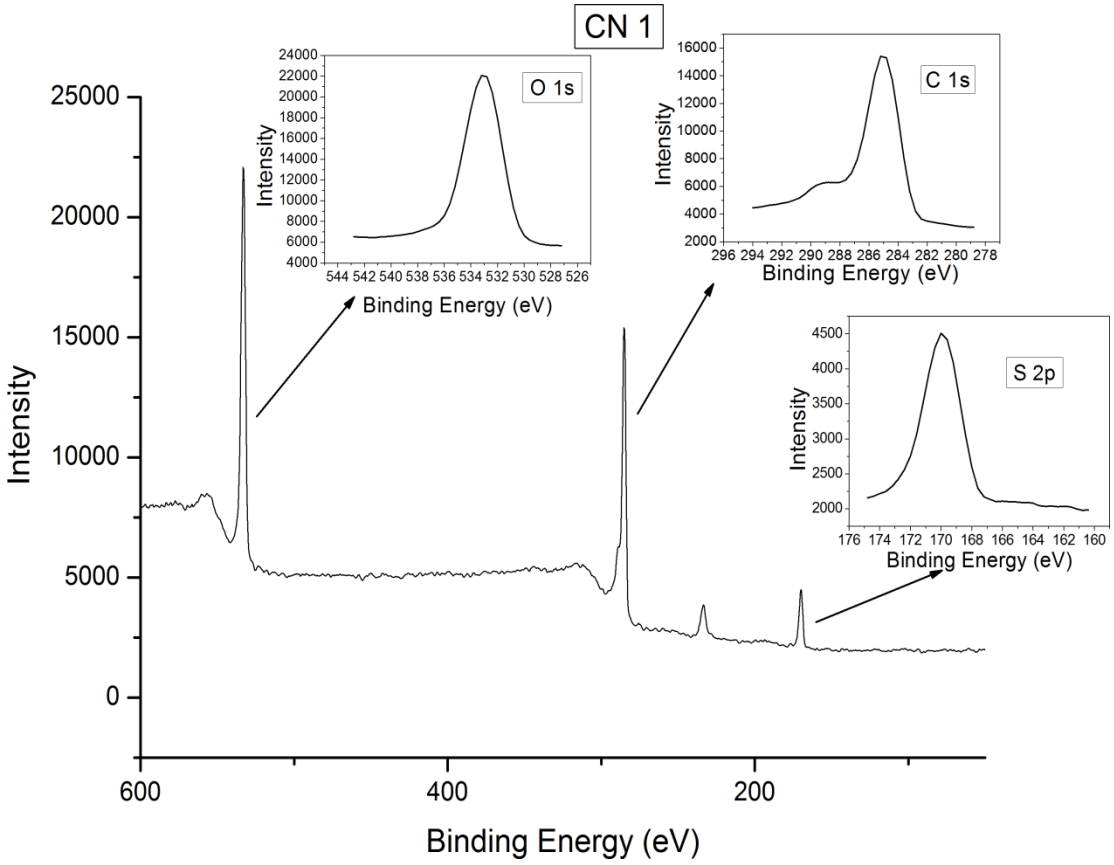

Figure 4.13 XPS spectra of the CN 1

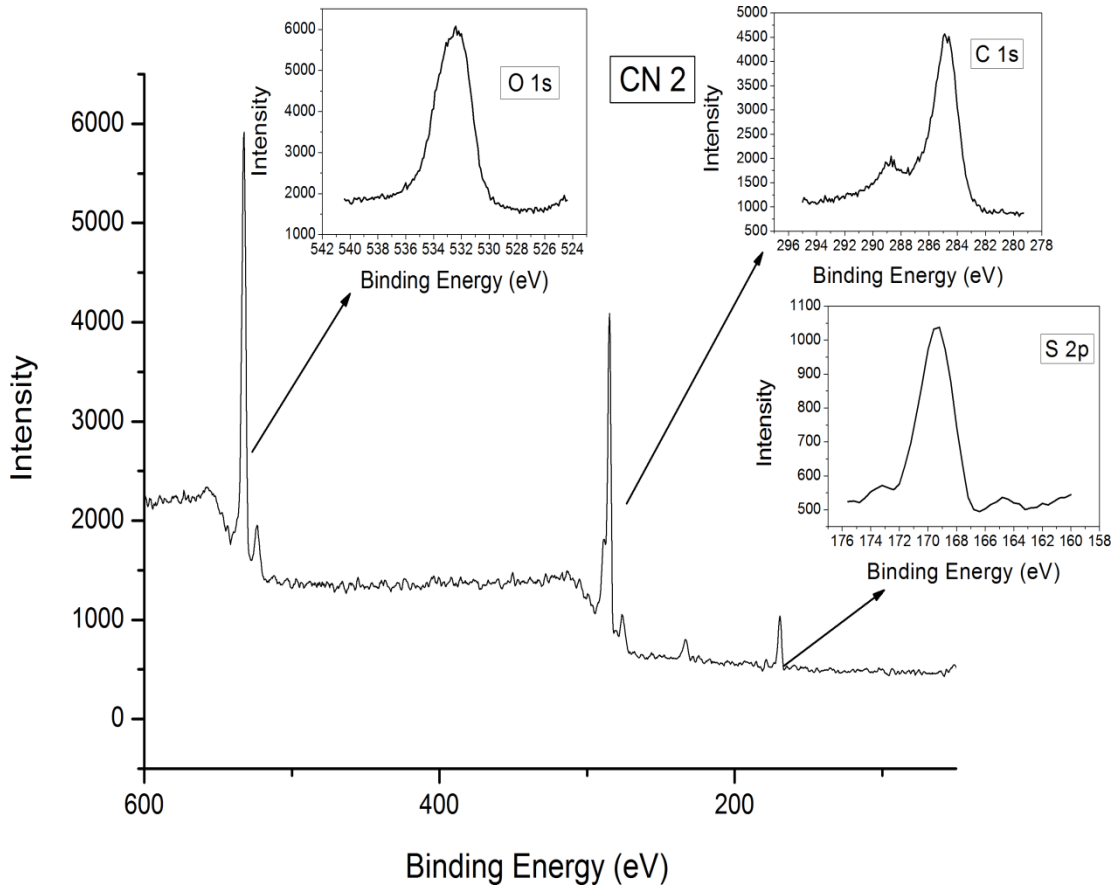

Figure 4.14 XPS spectra of the CN 2

4.2.5 Zeta Potential

Zeta potential is considered as a measure of electrostatic interaction and colloidal stability. The samples which have zeta potential less than – 15mV and higher than + 15 mV have colloidal stability in the solution [82,83]. Zeta potential measurements of the samples were done by using MALVERN Nano ZS90. Zeta potential of the CN and sulfonated carbon nanotubes were measured in water. Zeta potential of the CN, CN 1 and CN 2 samples were found as – 29.3, – 29.6 and - 32.7 mV, respectively.

High zeta potentials are observed for the modified carbon nanotubes. This high value of the zeta potential improves the dispersion of material in the matrix and prevent the agglomeration of the carbon nanotubes.

4.2.6 Scanning Electron Microscopy

The morphology of the functionalized carbon nanotubes were investigated with Scanning Electron Microscopy (SEM). The SEM micrographs of the samples were given in Figures 4.15-4.17. SEM micrographs show that functionalization of the carbon nanotube increases the intermolecular forces like hydrogen bonding and carbon nanotubes seen in more bulky form. The sulfuric acid content during the functionalization increases the bulky form of the samples. As a result of the oxidative treatment, beside the formation of reactive groups on nanotubes, defect sites along the sidewalls and length reduction of the nanotubes into smaller fragments occur [40,84].

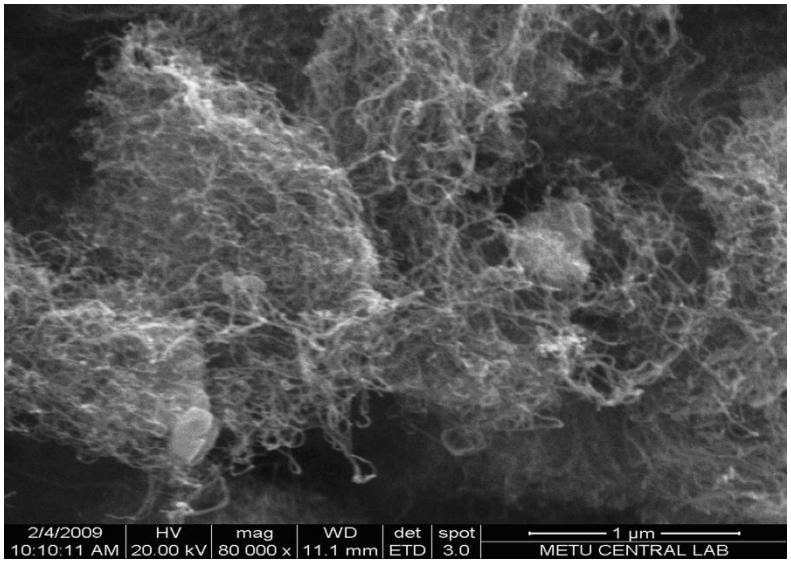

Figure 4.15 SEM micrograph of untreated CN

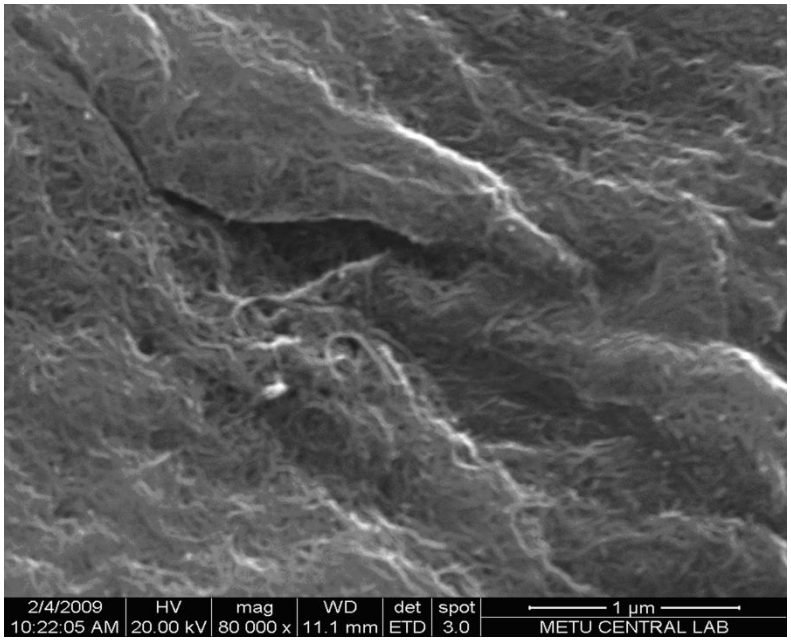

Figure 4.16 SEM micrograph of CN 1

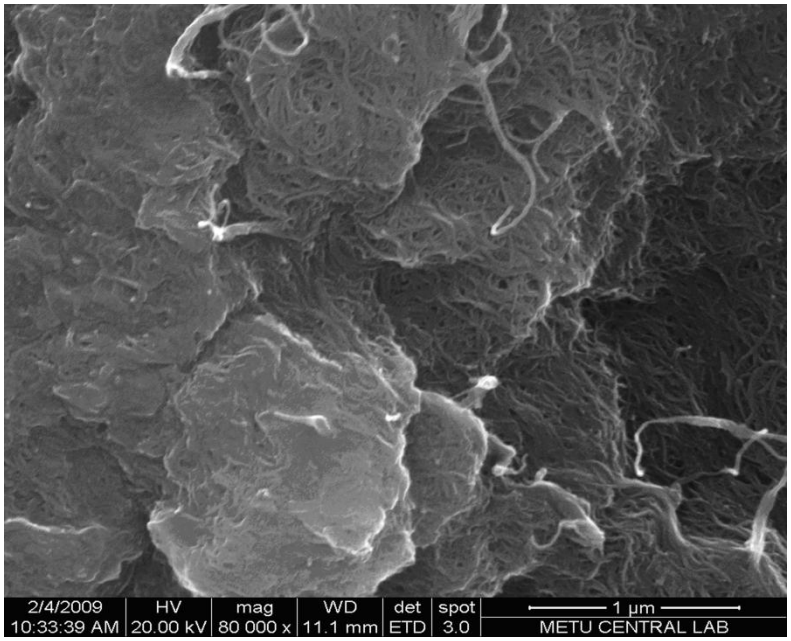

Figure 4.17 SEM micrograph of CN 2

4.2.7 Transmission Electron Microscopy (TEM)

TEM micrograph of the materials are given in the Figure 4.18 and 4.19. As can be seen in TEM micrographs, modification of the carbon nanotube prevent the agglomeration and carbon nanotubes disperse more uniformly. The nanotube lenghts in the CN 1 is smaller than the CN 2 but both the big agglomerate regions and uniformly dispersed parts are observed in CN 1.

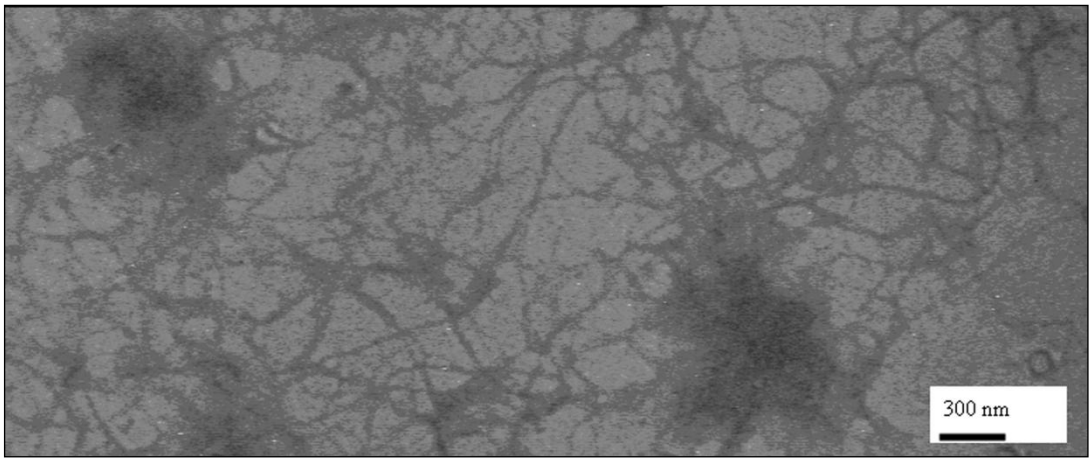

Figure 4.18 TEM micrograph of CN 1

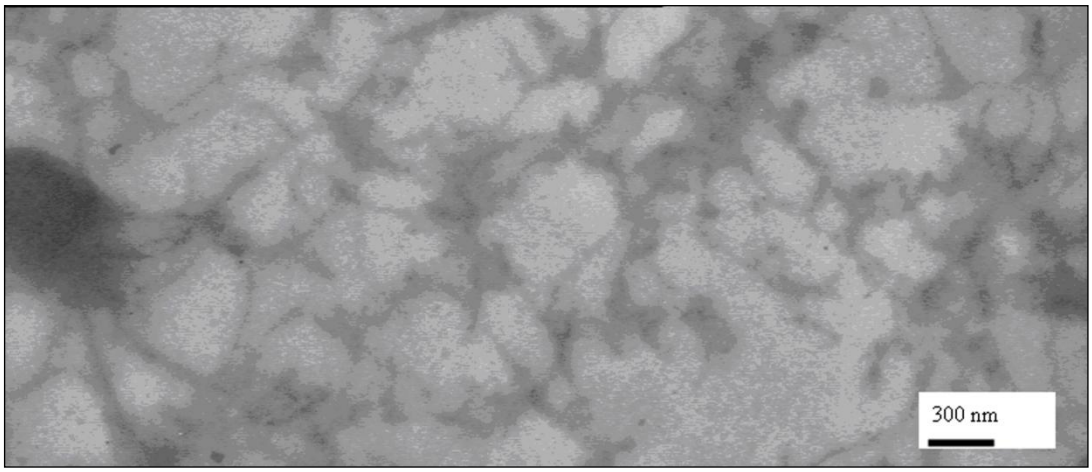

Figure 4.19 TEM micrograph of CN 2

4.3 Surface Modification of Fullerene

4.3.1 Fourier Transform Infrared Spectroscopy (FTIR)

The surface modified fullerene was characterized with FTIR. Figure 4.20 shows the FTIR spectra of the sulfonated fullerenes. The peaks around 1367 -1371 cm^{-1} and 1201-1214 cm^{-1} show the asymmetric and symmetric stretching vibrations of S=O groups respectively. The peaks around the 3428 and 3425 cm^{-1} represent the O-H stretching. The peaks of the C=O stretching were observed around 1698 and 1705 cm^{-1}. The characteristic peaks of fullerene are seen around 566-680 cm^{-1}.

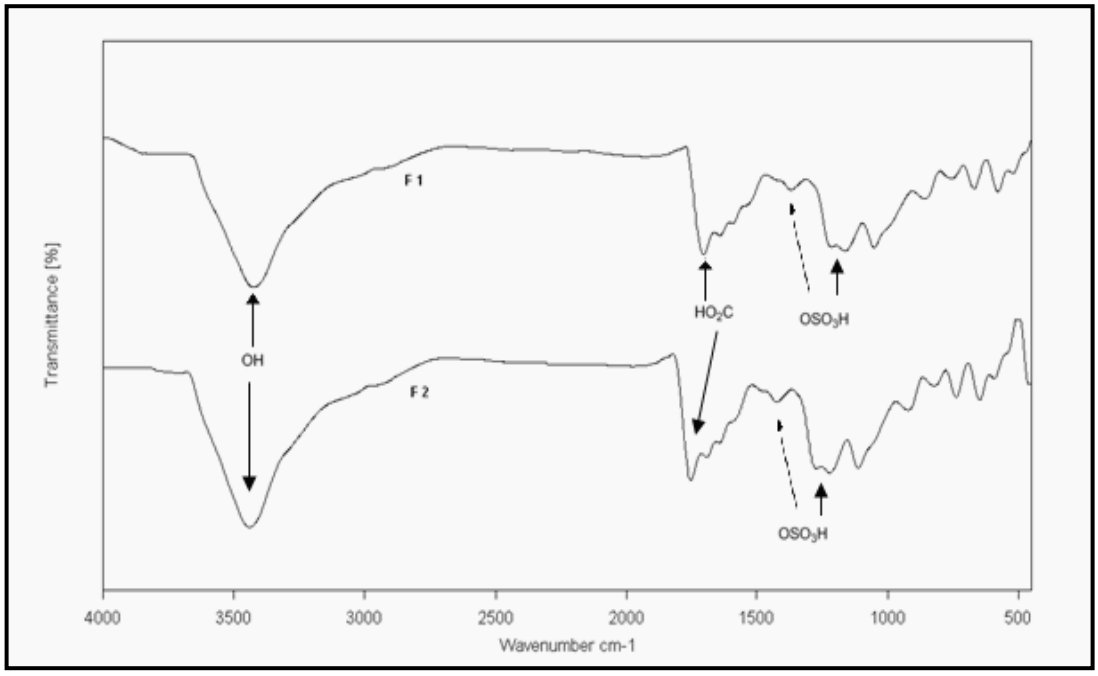

Figure 4.20 FTIR spectrum of F 1 and F 2

4.3.2 X Ray Photoelectron Spectroscopy (XPS)

XPS spectra of the samples clearly show the existence of the functional groups on the materials. Figure 4.21 and 4.22 show the XPS spectra of the materials. The peaks coming from the 2p orbital of the sulfur are observed between 167-172 eV. These peaks show the succesive surface functionalization of the material with $–OSO_3H$ groups. The peaks due to carboxylic acid and hydroxyl groups are around (O 1s) 530-536 eV and (C 1s) 282- 288 eV [85]**.**

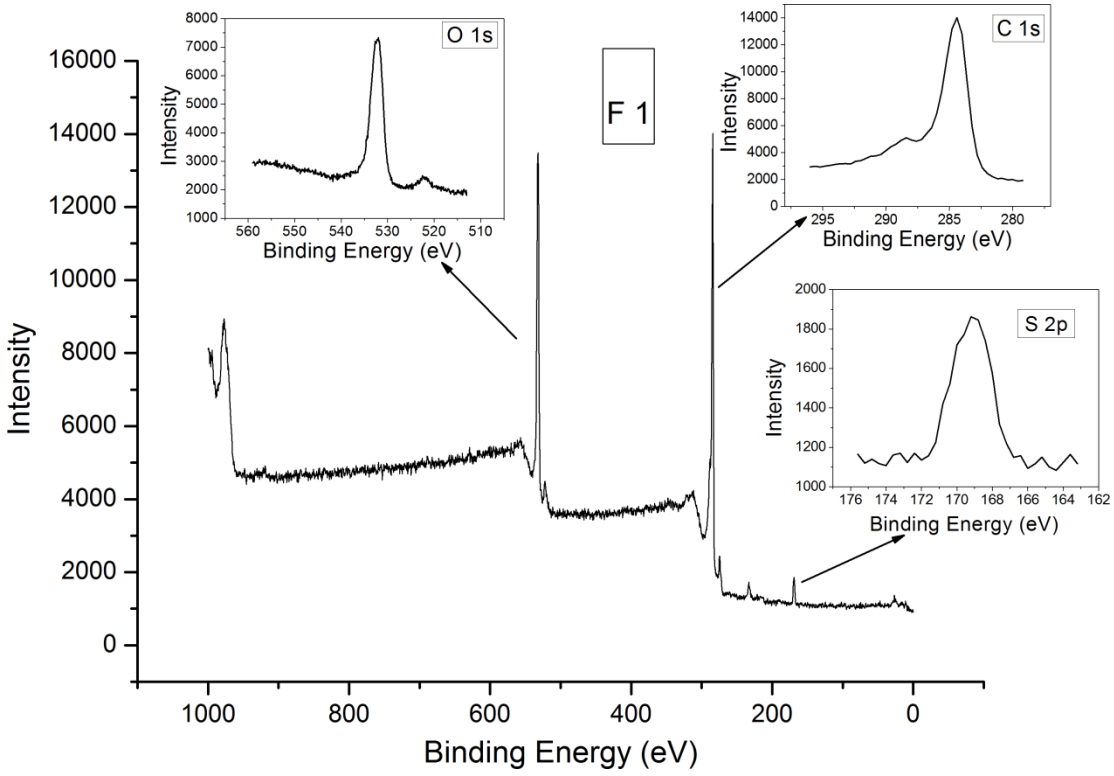

Figure 4.21 ESCA spectrum of F1

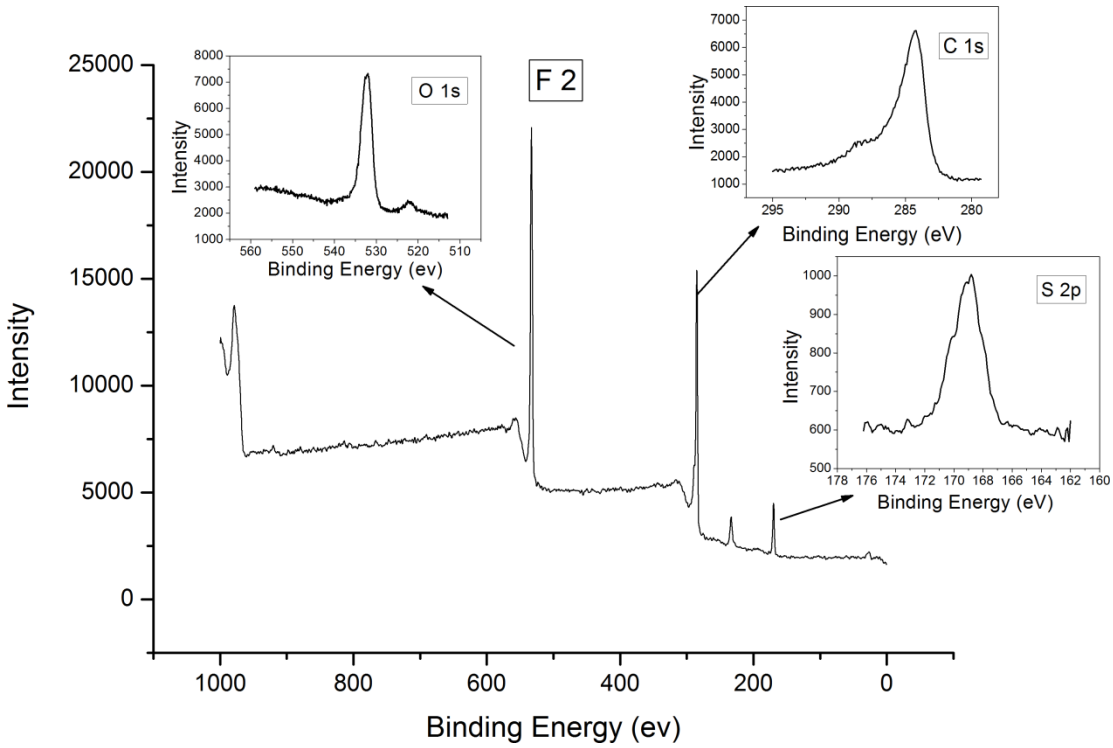

Figure 4.22 ESCA spectrum of F 2

4.3.3 Elemental Analysis

Elemental Analysis results of the sulfonated fullerenes are given in Table 4.3. Increasing amount of the H_2SO_4 during synthesis increases the -OSO_3H groups in the final product.

Table 4.3 Elemental analysis results of surface modified fullerenes

	% C	% N	% H	% S	% O
F 1	80.93	0.59	0.15	2.04	16.28
F 2	78.34	0.63	0.39	2.14	18.48

4.3.4 Electrical Conductivity

Electrical conductivities of the samples are given in Table 4.4. Four Point Probe method was used for conductivity measurements. Increasing the sulphuric acid content during modification of the material increases the electrical conductivity of the materials due to higher acidic conductivity of hydrogensulfate content on surface [81].

Table 4.4 Electrical Conductivity of the F1 and F2

	Electrical Conductivity (S/cm)
F 1	1.78×10^{-2}
F 2	2.72×10^{-2}

4.3.5 Transmission Electron Microscopy

TEM micrographs of neat fullerene and modified fullerenes are given in Figures 4.23, 4.24 and 4.25 respectively. As can be seen from these figures modification of the fullerene improves the dispersion in water and decreases the agglomeration. The particle size is about 50-60 nm for surface modified fullerene (F2). The particle size of the neat fullerene is about 80 nm.

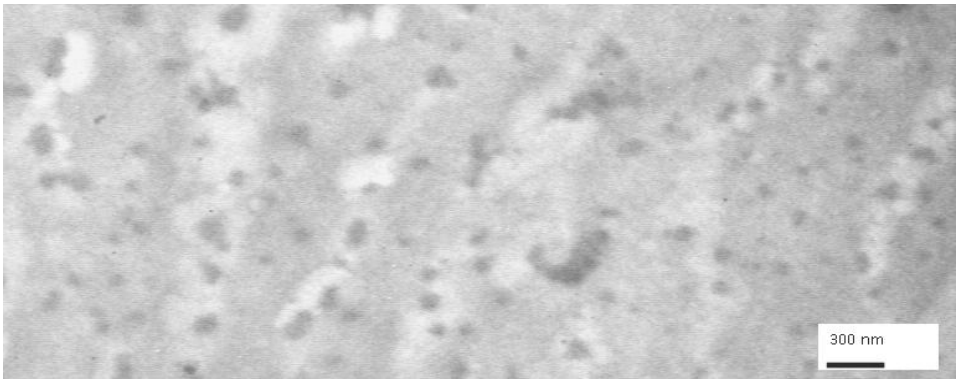

Figure 4.23 TEM micrograph of neat fullerene

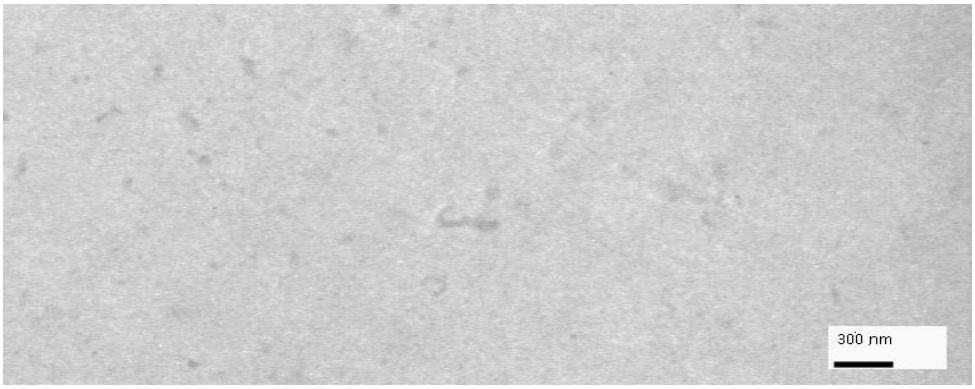

Figure 4.24 TEM micrograph of F1

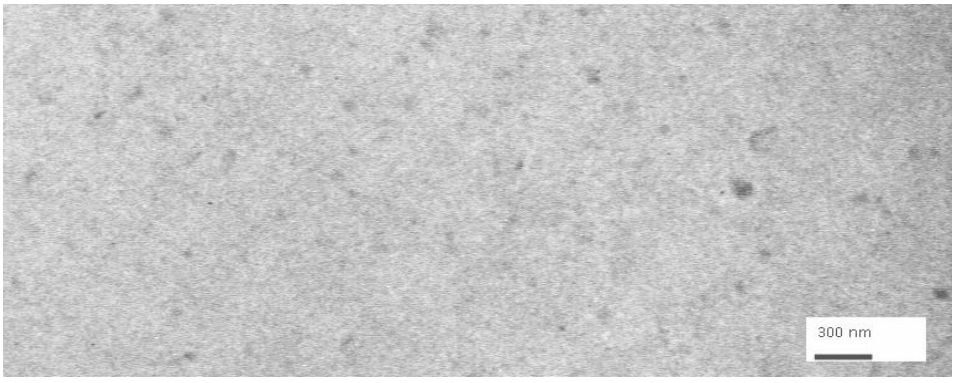

Figure 4.25 TEM micrograph of F2

4.3.6 Zeta Potential

Zeta potential is used as a measure of electrostatic interaction between colloidal particles and shows the colloidal stability of the solution and is a useful parameter to understand the dispersability of particles. If particles have zeta potential smaller than – 15mV or higher than 15 mV, particles are expected to be stable from electrostatic considerations in solution, but colloids have zeta potential between –15 mV and 15 mV can be stabilized with surfactant in solution [82,83,86,87].

Zeta potentials of the F1 and F2 samples were found as – 31.4 and - 40.9 mV, respectively. High zeta potentials are observed at the modified fullerenes. This high value of the zeta potential improves the dispersion of material in the matrix and prevents agglomeration. It can also be seen in the TEM micrograph of the samples.

4.3.7 Scanning Electron Microscopy

SEM micrograph of the pure fullerene and sulfonated fullerenes are given in Figure 4.26, 4.27 and 4.28. SEM micrograph of the pure fullerene shows that fullerenes are in the form of agglomerate about 50-75 nm size. SEM micrographs of the modified fullerenes show that surface modified fullerenes have similar particle size on the average with neat fullerene. On the other hand, because of the modification of the fullerenes, strong hydrogen bonds are formed between the particles, and agglomerates are seen in more bulky form.

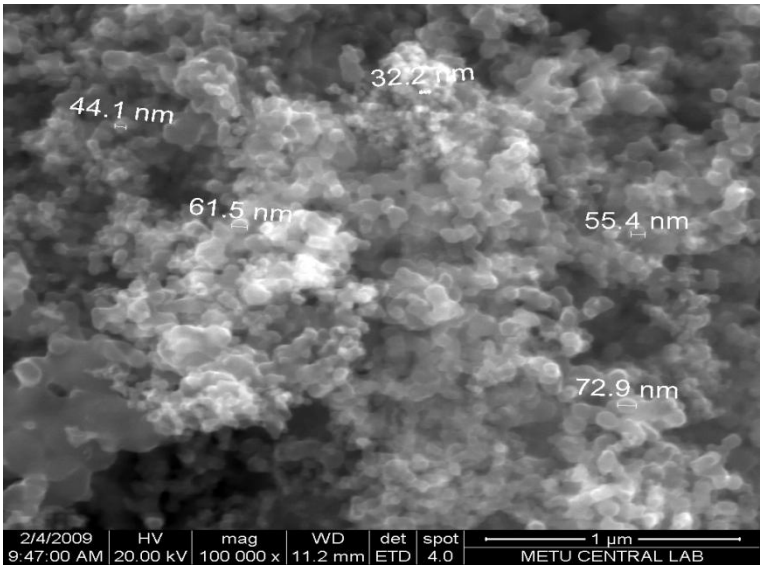

Figure 4.26 SEM micrograph of neat fullerene

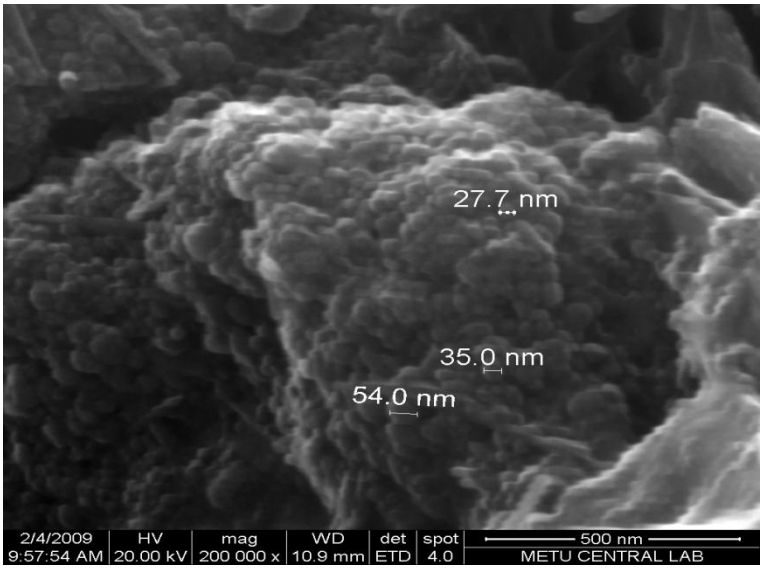

Figure 4.27 SEM micrograph of F1

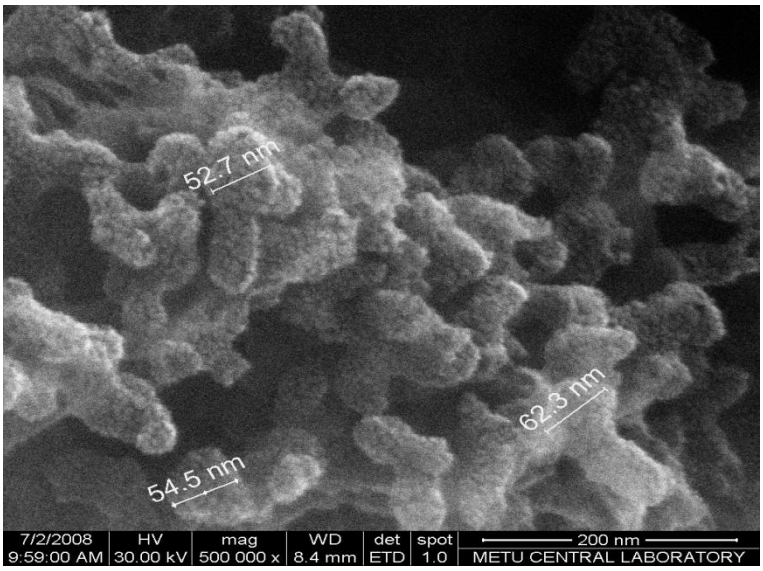

Figure 4.28 SEM micrograph of F2

4.4. Polypropylene/ Carbon Nanotube Composites

4.4.1 Mechanical Properties

Young's Modulus and Percentage elongation at break results of the composites are shown in Figures 4.29 and 4.30, respectively (Stress at break of the composites were given in Appendix A). The mechanical properties of the PP/ neat CNT composites are higher than the PP/surface modified CNT composites. As a result of the oxidative treatment beside the formation of reactive groups, defect sites on sidewall and length reduction will occur [40,84]. Due to the length reduction of the carbon nanotubes, the mechanical properties of the composites which contain modified CNT (m-CNT) have lower Young Modulus than that of unmodified CNT. Because neat CNT with higher aspect ratio will improve the mechanical properties [88,89] and m-CNT shows

poor compatibility with PP. Young's Modulus of the composites increase with increasing CNT content (Figure 4.29). Percentage elongation at break decreases with increasing CNT in the composites (Figure 4.30).

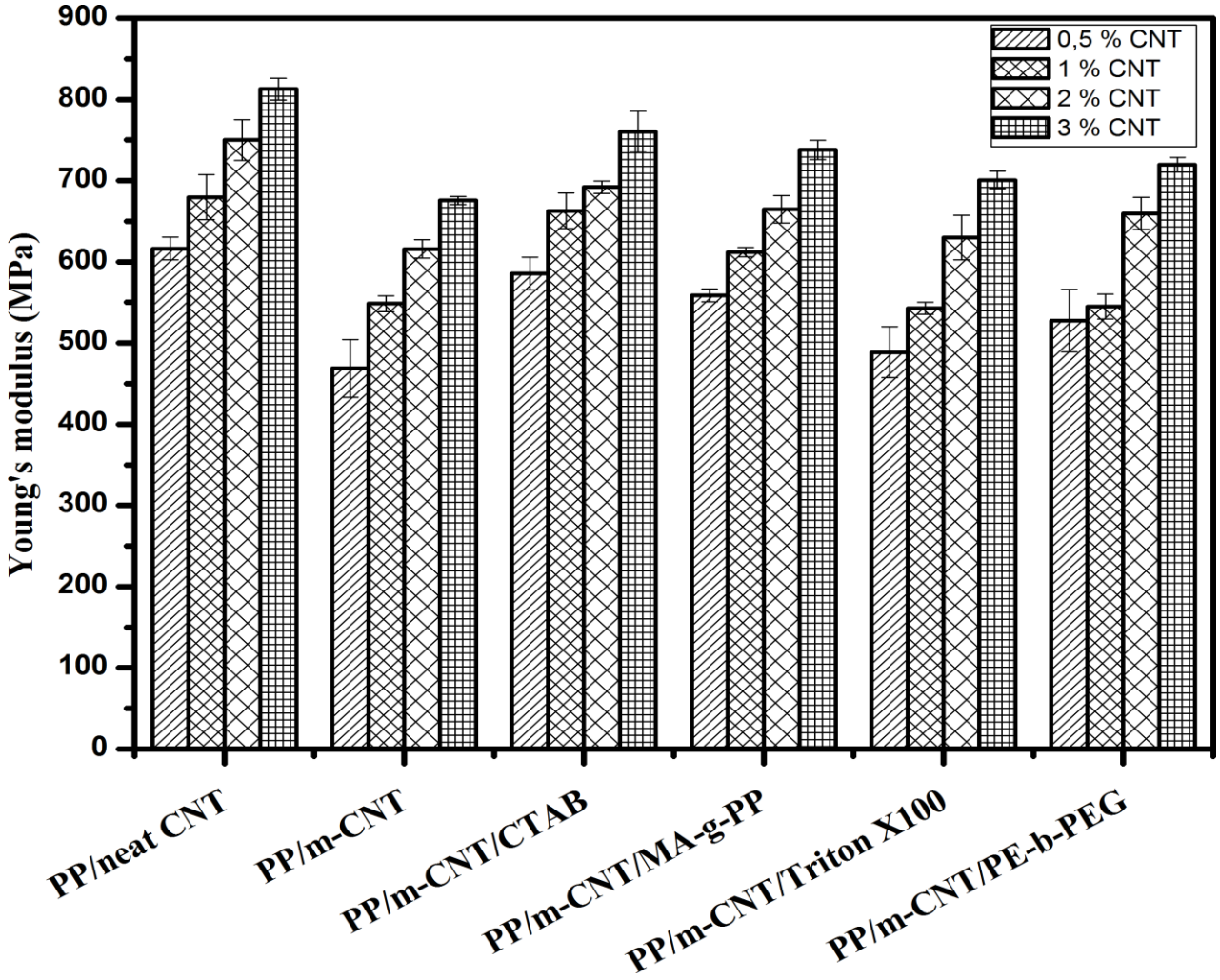

Figure 4.29 Young's Modulus of PP/CNT composites

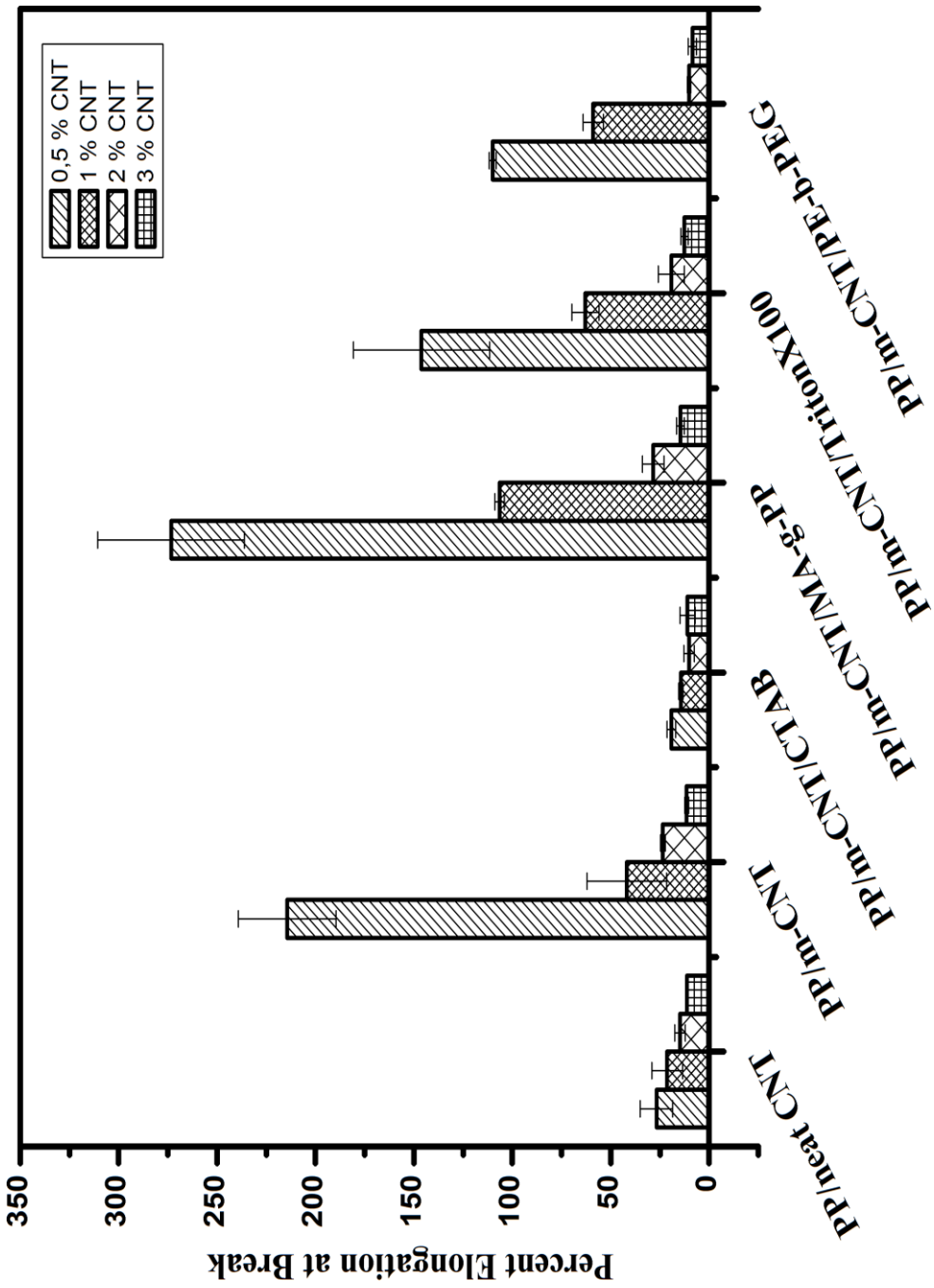

Figure 4.30 Percent elongation at break of PP/CNT composites

The highest mechanical strength and percent elongation at break were observed for composites with MA-g-PP. MA-g-PP is one of the common compatibilizer for the PP composites. Since MA-g-PP has similar backbone with polypropylene matrix and similar functional groups with filler, it increases the compatibility of the filler in PP matrix. Beside this, strong hydrogen bonding between m-CNT and MA-g-PP promotes the compatibility of the m-CNT in polymer matrix. As a results of the MA-g-PP addition percent elongation at break of the composites increased because MA-g-PP is low molecular weight polymer and uncoiling of the MA-g-PP increases the elongation during tensile test.

The composites which contain CTAB have high Young's modulus. CTAB have hydrocarbon chain and positively charged end. Cationic ends of CTAB have good interaction with the negatively charged CNT surface and hydrocarbon parts have similar structure with the polymer matrix and this provides good dispersion in polymer matrix. CTAB have no effect on percent elongation at break like MA-g-PP. Sample which is prepared with CTAB showed brittle tensile behaviour.

Triton X 100 is a non ionic surfactant with hydrocarbon chain and carboxyl groups at one end. Mechanical properties of the composites which are prepared with Triton X-100 and PE-b-PEG are lower than the composites contain CTAB and MA-g-PP. The composites which are prepared by using Triton X-100 and PE-b-PEG showed low mechanical strength due to the poor adhesion of CNT with polymer matrix. Another explanation for this result is the compatibilizers may function as plasticizer.

4.4.2 Electrical Conductivity

Electrical conductivity results are given in Figure 4.31. Electrical conductivities of the composites were measured by using four probe technique. Electrical conductivity of the composites increases with the CNT loading. Electrical conductivity of the

composites contain modified CNT are higher than the non-modified CNT. m-CNT have higher electrical conductivity than the unmodified one due to strong protonic acid groups on their surface [81]. Higher electrical conductivities were obtained for the composites which have good dispersion. The highest electrical conductivities were obtained for the composites which have CTAB and MA-g-PP. This might be attributed to better dispersion of the CNT in polymer matrix. The composites which contain Triton X-100 and PE-block-PEG as compatibilizer showed lower electrical conductivity than the composites with CTAB and MA-g-PP due to poor dispersion. Mechanical properties are also affected by dispersion of CNT in polymer matrix.

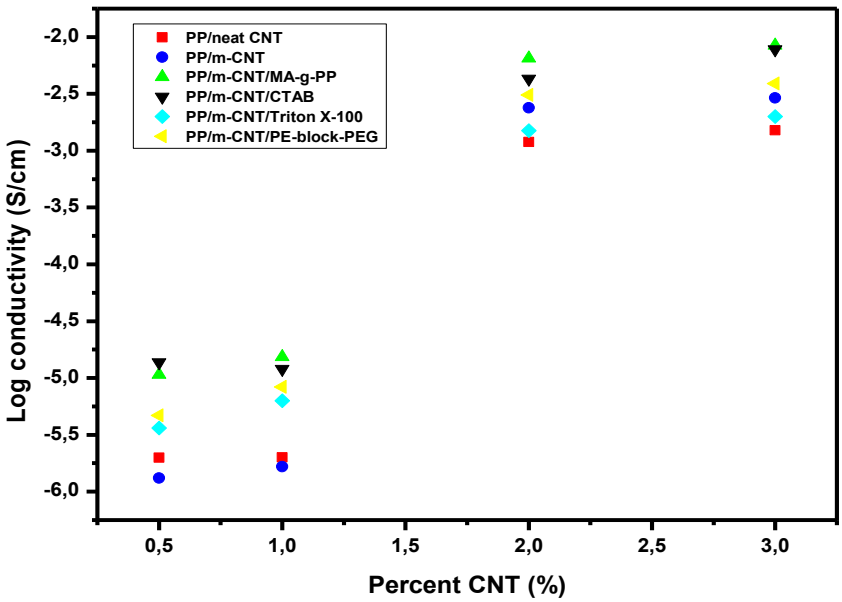

Figure 4.31 Electrical Conductivity of the PP/CNT composites

4.4.3 Scanning Electron Microscopy (SEM)

SEM micrographs of the composites were given in Figure 4.32 a-f. SEM micrographs of the neat CNT and composite which contain CTAB gave smooth fracture surface with individual dispersion of CNT on surface (Figure 4.32 a and

4.32.d). SEM micrographs of the PP/m-CNT/MA-g-PP, PP/m-CNT, PP/m-CNT/TritonX100, PP/m-CNT/PE-block-PEG, (Figure 4.32 b,c,e,f) show rough surface with wide fibriles. This results show similar property with the percent deformation of the composites because they show higher percent deformation at break values than the composites prepared with CTAB. The samples of neat CNT and CTAB percent elongation value are lower than the other composites and they show smooth fracture surface with thin fibrils. Neat CNT have long fibril because of high aspect ratio and agglomerated parts. For the neat CNT long fibrils and close dispersion of carbon nanotubes can be seen in micrograph.

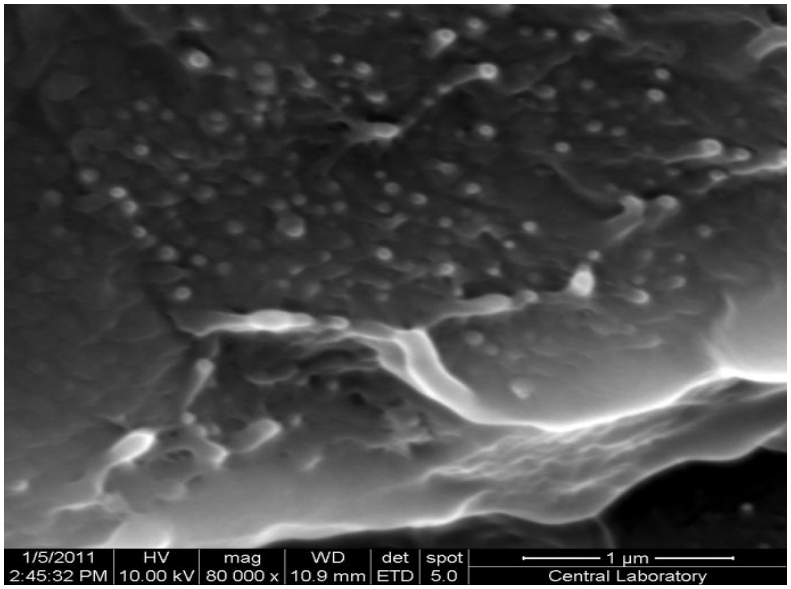

Figure 4.32.a SEM micrograph of PP/m-CNT/ CTAB

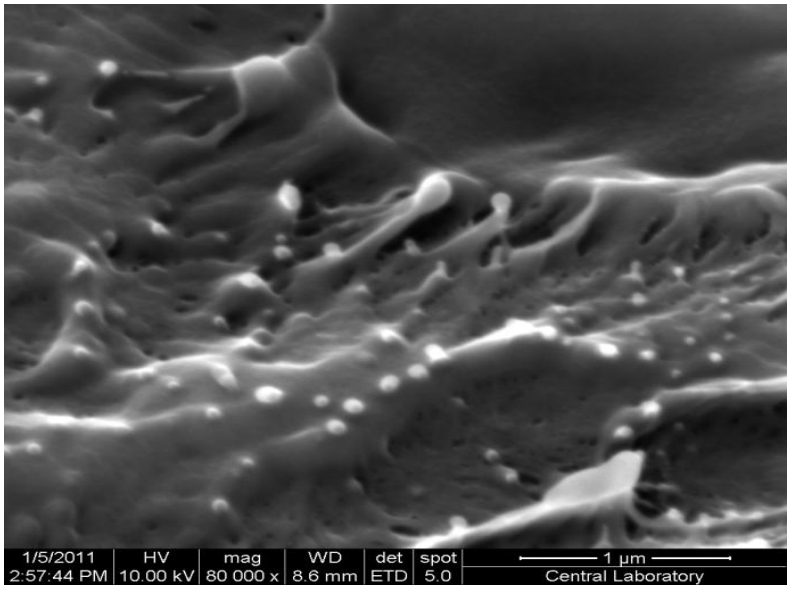

Figure 4.32.b SEM micrograph of PP/m-CNT/ MA-g-PP

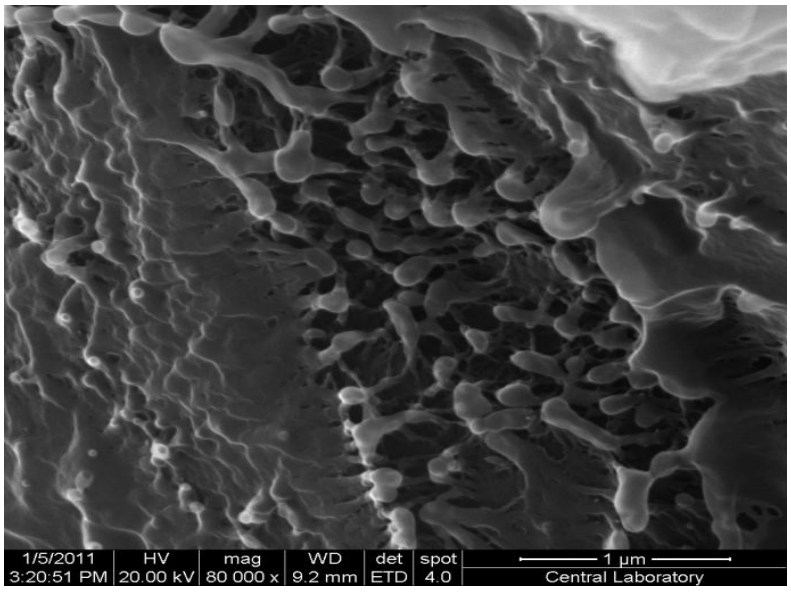

Figure 4.32.c SEM micrograph of PP / m-CNT

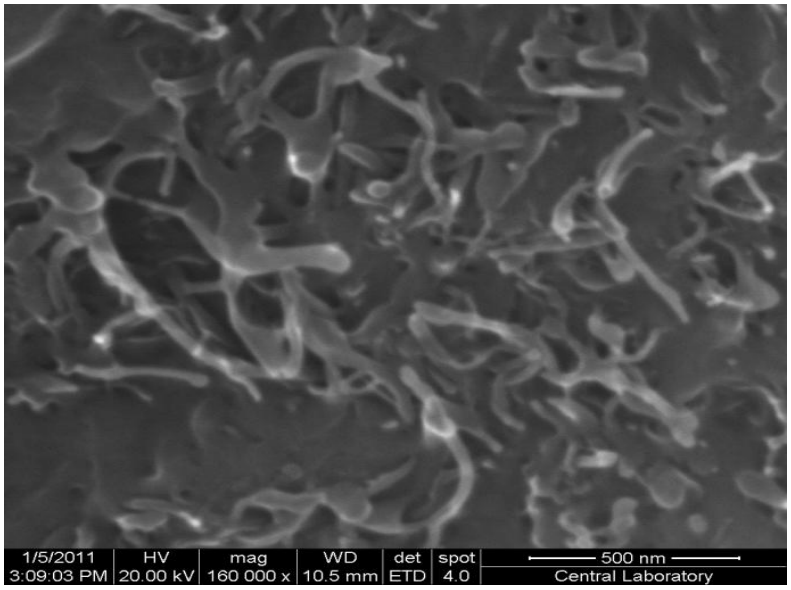

Figure 4.32.d SEM micrograph of PP / neat CNT

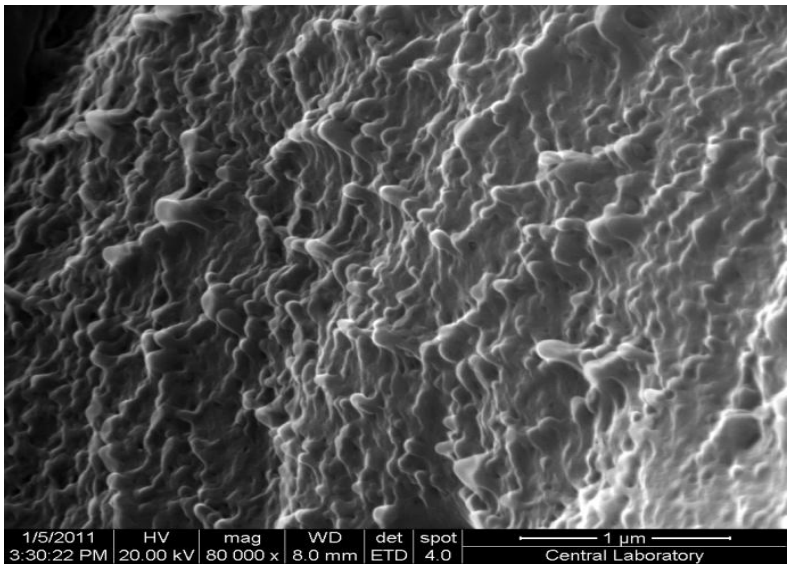

Figure 4.32.e SEM micrograph of PP / m-CNT / Triton X-100

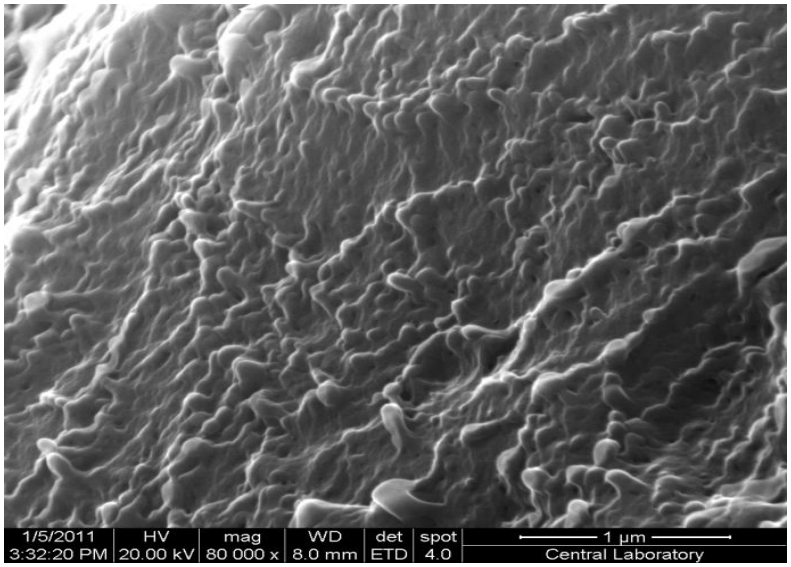

Figure 4.32.f SEM micrograph of PP / m-CNT/ PE-block- PEG

4.4.4 Thermal Gravimetric Analysis (TGA)

The affect of the different dispersants on thermal stability of the composites are given in Figure 4.33. Addition of the 2 % CNT to the polymer matrix increases the thermal stability of PP composites and the temperature at which thermal decomposition starts, shifts to higher temperatures. Pure PP decomposes at about 400 ^{0}C. The best thermal stability was observed for the composites which contain PP-g-MA and CTAB as dispersant. Thermal stability of the composites increase because interfacial interactions between CNT and PP matrix affect the degradation's activation energy of the composites and CNT provide better heat distribution [90], as a result decomposition starts at higher temperatures. Beside the interfacial interactions between CNT and PP, CNT aggregates hinder the penetration of the degradation product from polymer matrix [40].

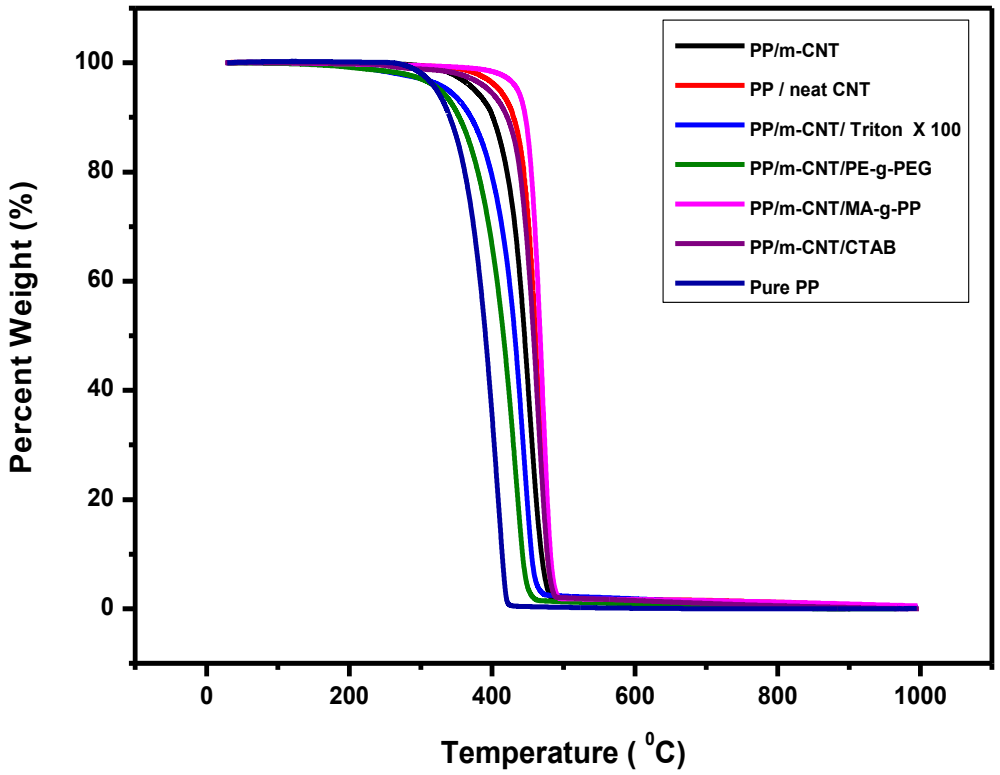

Figure 4.33 TGA of the PP/CNT composites

4.5. Polypropylene /Fullerene Composites

4.5.1 Mechanical Properties

Young's modulus of the composites were given in Figure 4.34. Young's modulus of the composites increased with increasing filler loading. Surface modified fullerene composites which are prepared without compatibilizer have lower Young's modulus value than the PP/neat fullerene composites due to poor dispersion of m-F inside the polymer matrix. The highest Young's modulus results were obtained for the

composites which contain MA-g-PP and CTAB as dispersant. Addition of the MA-g-PP as compatibilizer increased the mechanical properties of the composites because its provides better dispersion of the fullerene particles inside the polymer matrix. Ma-g-PP has similar structure with polymer matrix and similar functional groups with surface modified fullerene particles. Strong hydrogen bonding occurs between functional groups of fullerene and MA-g-PP and this promotes the compability of the fullerene particles in polymer matrix.

Addition of the CTAB compatibilizer showed similar effect on Young's modulus like MA-g-PP. Composites which are prepared with CTAB showed high Young modulus because CTAB is cationic surfactant. Cationic ends of the CTAB and negatively charged surface of the modified fullerene showed good interaction. As a result of the good compatibility of CTAB and fullerene particles, fullerene particles showed good dispersion in polymer matrix.

Young modulus of the composites which is prepared with PE-b-PEG and Triton X-100 are close to the value of neat fullerene composites. Triton X 100 and PE-b-PEG did not show any significant effect on Young Modulus of the composites.

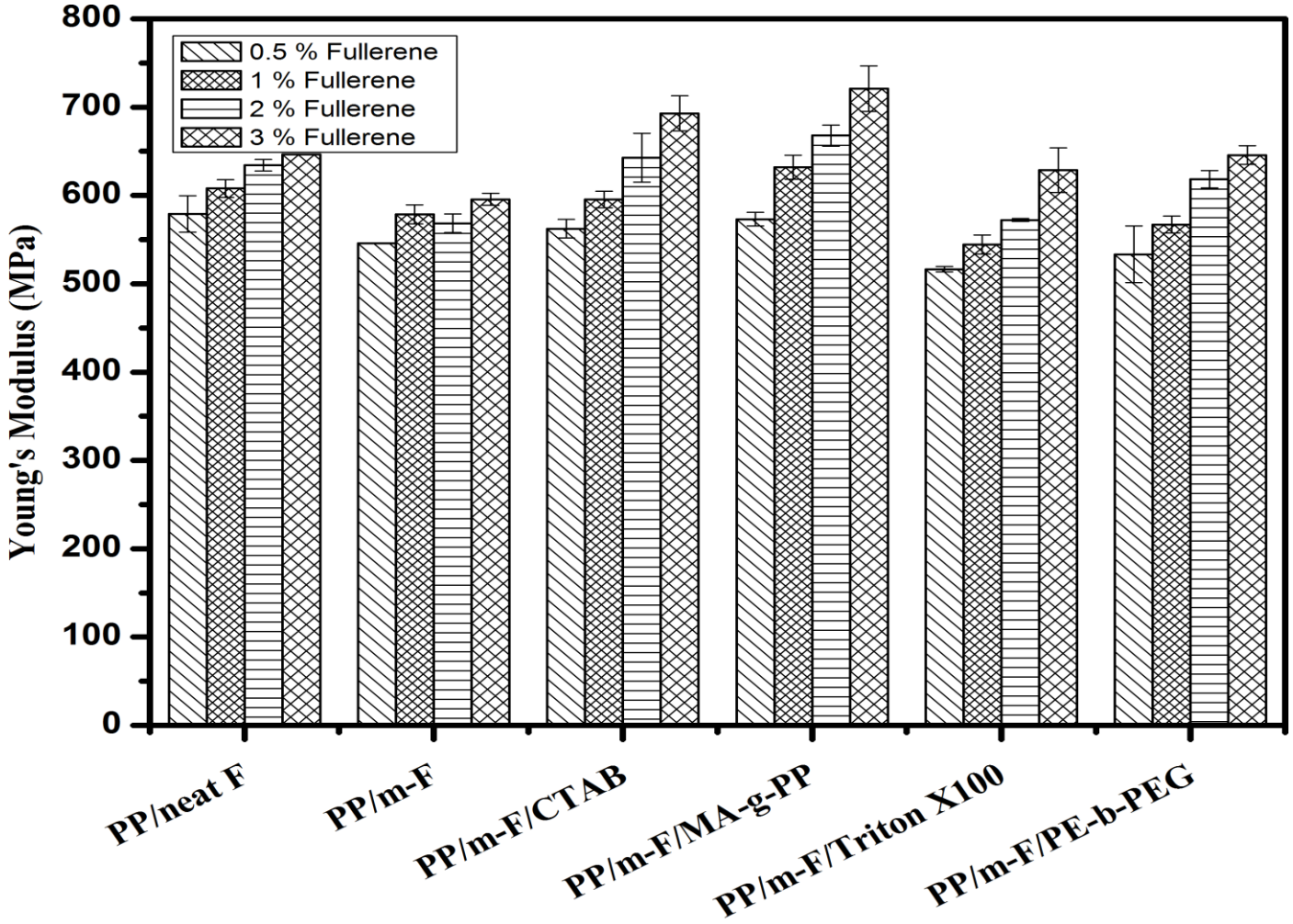

Figure 4.34 Young's Modulus of PP/F composites

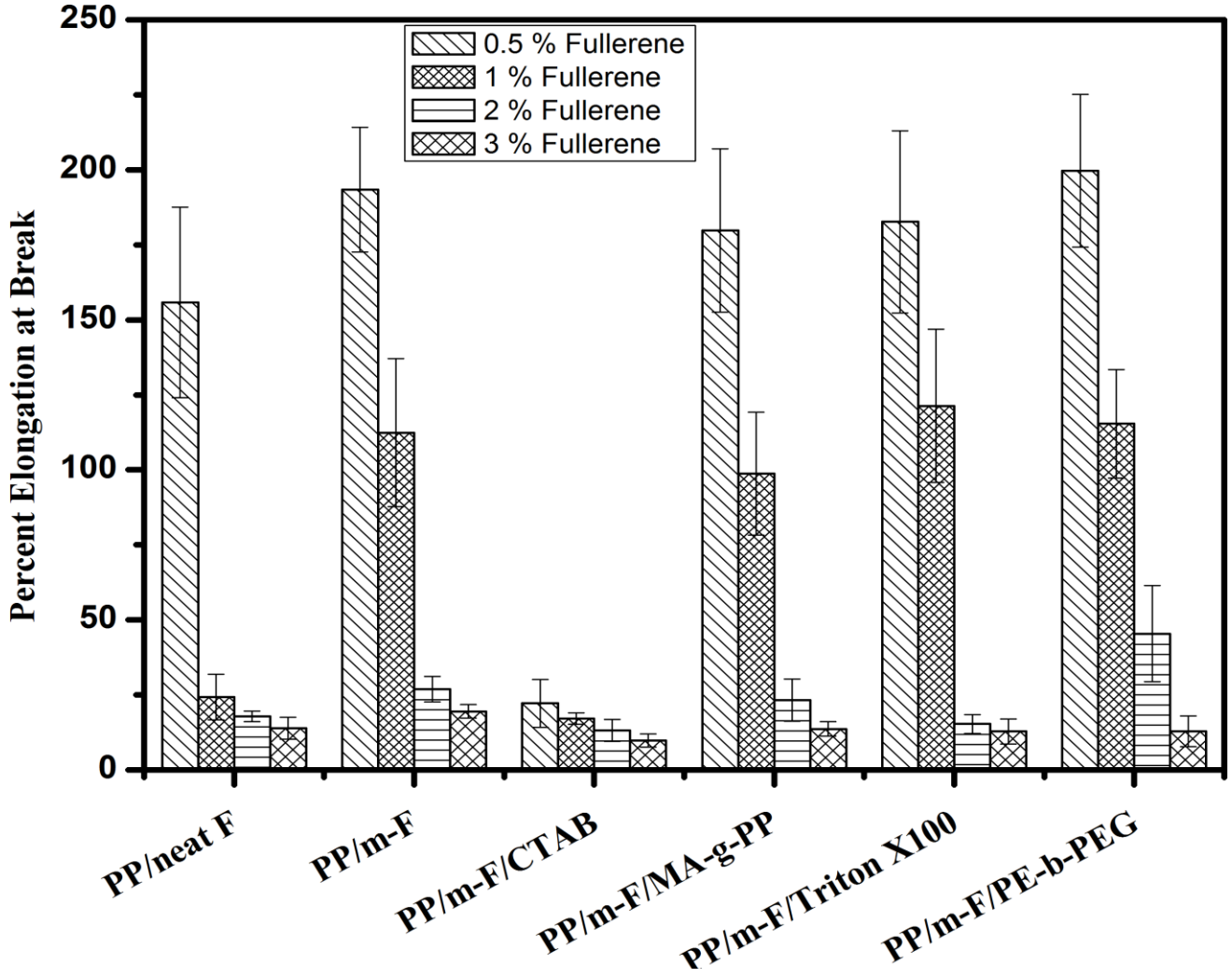

Figure 4.35 Percent elongation at break of PP/F composites

Percant elongation at break of the composites decreases with increasing filler content (Figure 4.35) (Stress at break of the composites were given in Appendix A). The composites which was prepared with PE-b-PEG showed higher percent elongation at break due to its low molecular weight of the compatibilizer. Similar results were obtained for the MA-g-PP. Uncoiling of the low molecular content in the composites increases the percent elongation at break. It can be seen from the percent elongation at break results that addition of fullerene filler to composites does not decrease the percent elongation of the composites at low filler loading. Decrease in the percent elongation is obvious after addition of 2 % fullerene loading. CTAB compatibilizer increased the Young's modulus of the composites but percent elongation of the composites decrease immediately with increasing filler content. The decrease in percent elongation with increasing filler content is slow for the other composites.

4.5.2 Electrical Conductivity

Electrical conductivity measurement results of the Polypropylene/Fullerene composites are given in Figure 4.36. Electrical conductivity of the composites increase with increasing filler content. The composites which were prepared with surface modified fullerene showed higher conductivity values than the composites prepared with neat fullerene. This result can be explained that surface modified fullerenes have strong protonic acid group on their surface and this functional groups makes them more conductive [81]. Another important factor affecting the conductivity of the composites is dispersion of the composites in polymer matrix. The highest conductivity results were obtained with the composites prepared with MA-g-PP and CTAB compatibilizers. Mechanical property measurement result for these composites also support the better dispersion of the fullerene particles with CTAB and MA-g-PP compatibilizers.

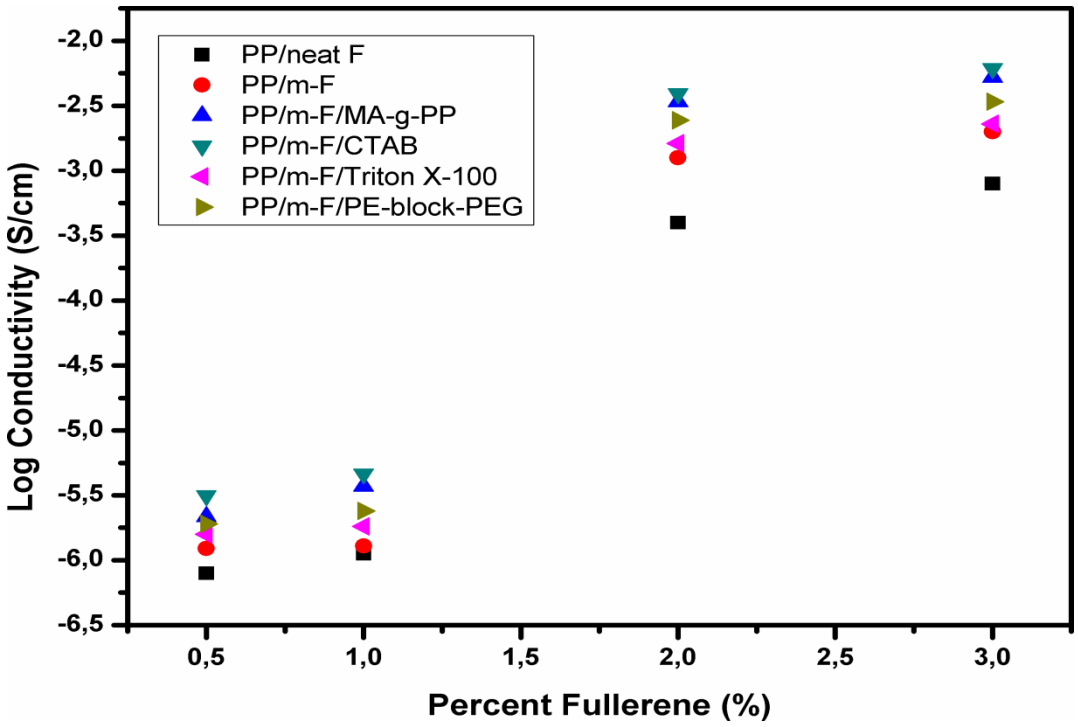

Figure 4.36 Electrical Conductivity of the PP/F composites

4.5.3 Scanning Electron Microscopy

SEM micrographs of the PP/neat fullerene and PP/m-F composites were given in Figure 4.37 a-f. SEM micrographs of the PP/neat F and PP/m-F show that distribution of the neat F is better than the m-F. This result shows that compability of the neat F with polypropylene matrix is better than the m-F. Agglomeration size is around 30-50 nm for neat F. For the m-F, agglomeration size is about 60-100 nm. The agglomeration sizes for the composites which were prepared with MA-g-PP and CTAB compatibilizers were similar to neat fullerene. This result indicate that these compatibilizers provide better dispersion of m-F in polypropylene matrix with the agglomeration size around 40-70 nm. SEM micrographs of the composites which contain PE-b-PEG and Triton X 100 compatibilizers show that agglomeration sizes for these composites are larger like the composites PP/m-F without compatibilizer.

Mechanical properties of the composites also support these results. The mechanical properties of the composites increase with decreasing agglomeration sizes. Mechanical properties of the PP/neat F, PP/m-F/MA-g-PP and PP/m-F/CTAB are higher than the other composites. PP/m-F/MA-g-PP and PP/m-F/CTAB composites showed higher electrical conductivity than the PP/m-F/PE-b-PEG and PP/m-F/Triton X 100 composites. These results also indicate the better dispersion of m-F with MA-g-PP and CTAB compatibilizers.

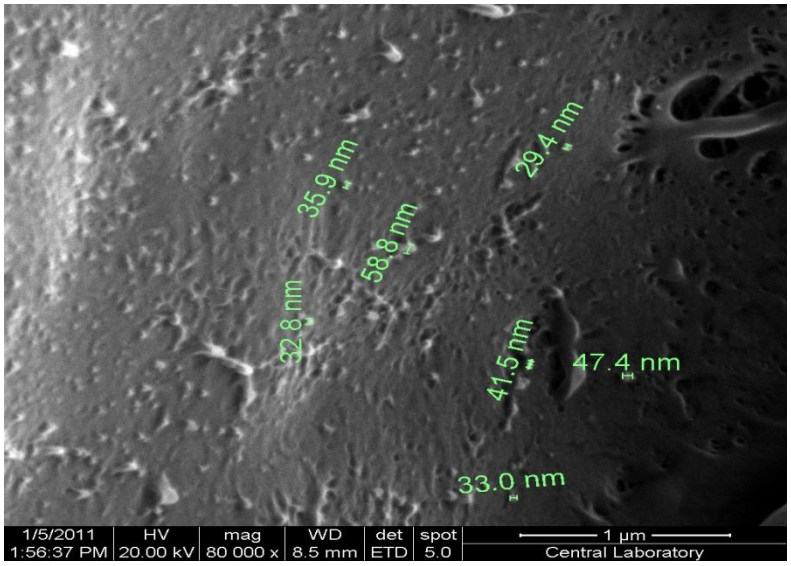

Figure 4.37.a SEM micrograph of PP / neat F

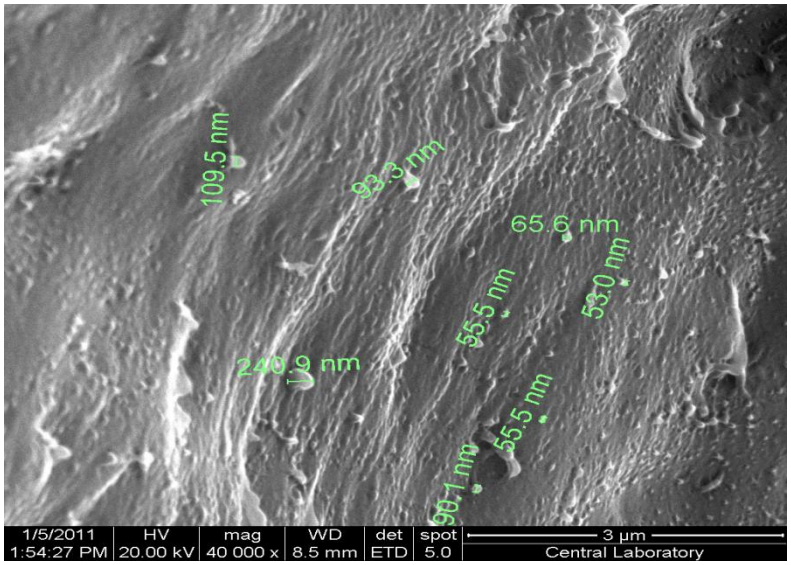

Figure 4.37.b SEM micrograph of PP / m-F

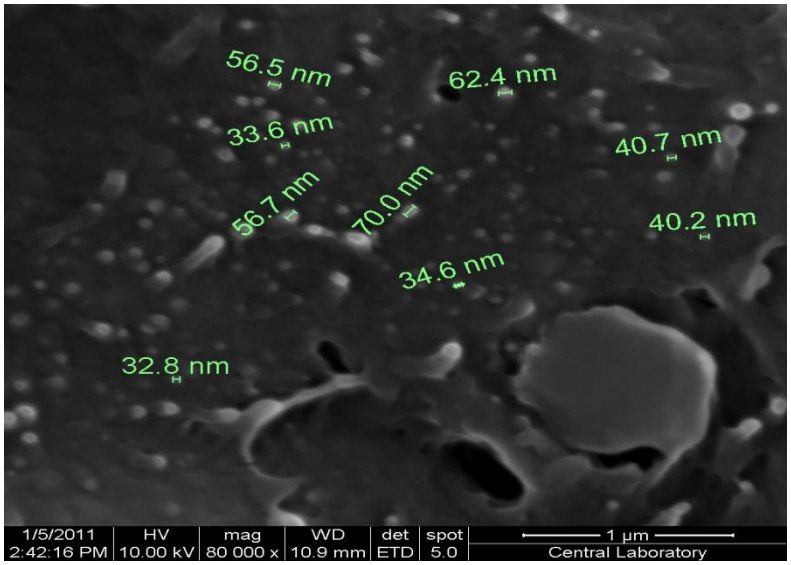

Figure 4.37.c SEM micrograph of PP/m-F/ CTAB

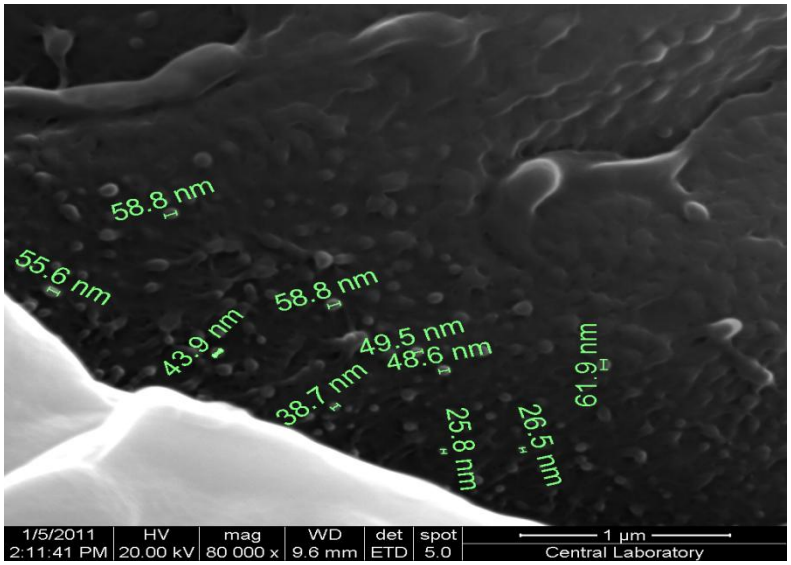

Figure 4.37.d SEM micrograph of PP/m-F/ MA-g-PP

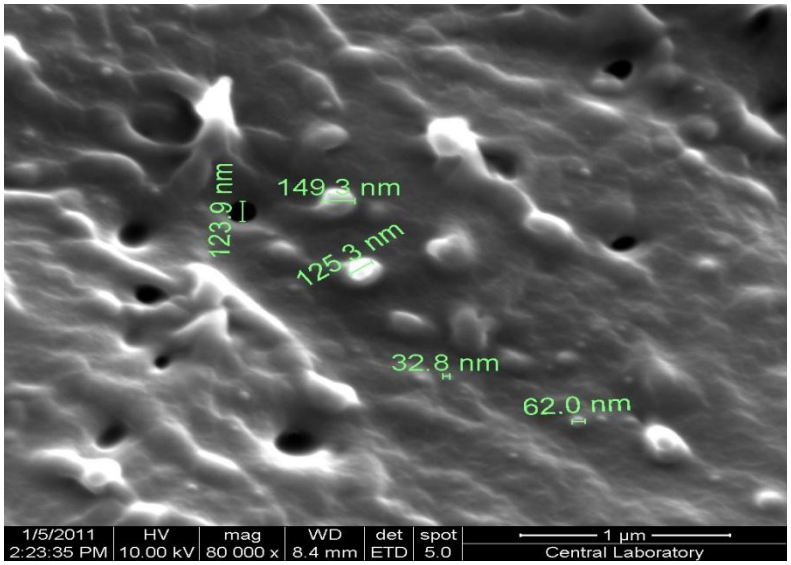

Figure 4.37.e SEM micrograph of PP / m-F / Triton X-100

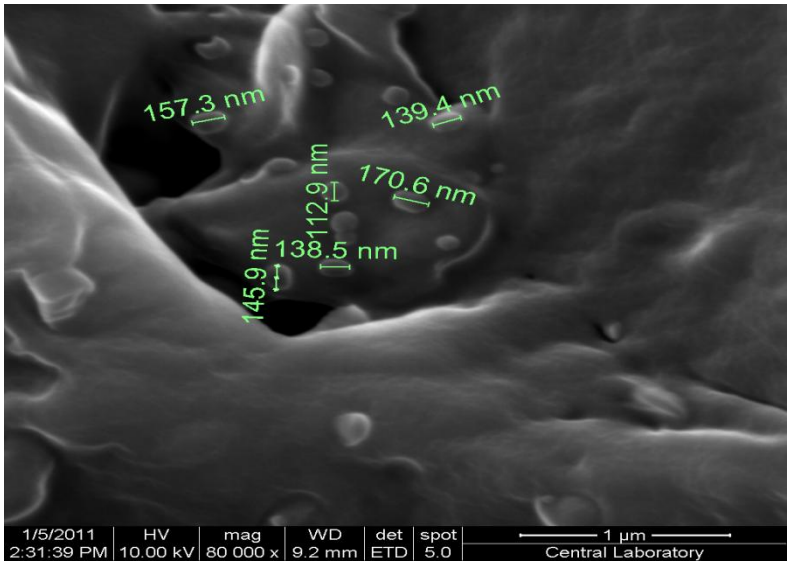

Figure 4.37.f SEM micrograph of PP / m-F/ PE-block- PEG

4.5.4 Thermal Gravimetric Analysis

Thermal Gravimetric Analysis results were given in Figure 4.38. Pure polypropylene decomposes around 400 ^{0}C. Addition of the Fullerene filler increased the decomposition temperature up to 500 ^{0}C. Composites which contain MA-g-PP as compatibilizer starts to decomposize later than the other composites. It is observed that termal properties of the composites prepared surface modified fullerene are close to the composite prepared with neat fullerene. Thermal stability of the composites increase with the addition of fullerene because fullerene addition increases the decomposition activation energy of the polypropylene matrix. Molecular attraction between the polymer matrix and filler increases activation energy of the decomposition. Beside this addition of the filler provide better heat distribution inside the polymer matrix.

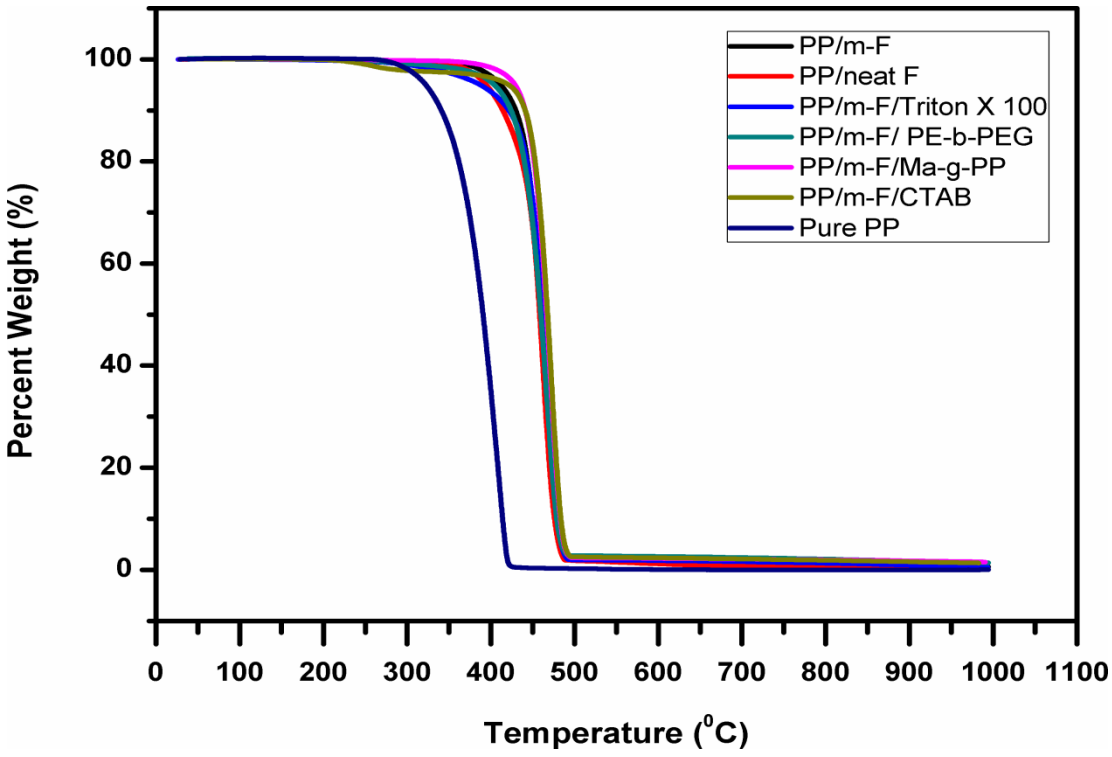

Figure 4.38 TGA of the PP/F composites

4.6 Organic Field Effect Transistors with Polyethylene Gate Dielectric

4.6.1 Fourier Transform Infrared Spectroscopy

Polyethylene was vacuum-processed at a pressure of 10^{-6} torr. Interestingly, compared to polyaniline that sublimes in high vacuum directly from solid phase [72,91] low density polyethylene evaporates from the melt. The crucial steps in producing high quality films of polyethylene are extensively degassing the melt from volatile species and/or impurities before proceeding to the actual evaporation and evaporating the material at a temperature matching exactly the boiling point of polyethylene.

Table 4.5 Observed peaks and literature-reported peaks for polyethylene

Observed Peaks (cm^{-1})	**Vibration Mode**	**Literature reported peaks (cm^{-1})**	
		Gulmine et al. [92]	**Mirzataheri et al.** [93]
2929	CH_2 asymmetric stretching	2919	2918
2858	CH_2 symmetric stretching	2851	2851
1472	scissor (bending) vibration	1473	1464
1373	wagging deformation	1377	1377
1352	wagging deformation	1351	-
1288	twisting deformation	1306	-
721, 730	rocking vibration of $-(CH_2)_n-$	720, 731	719, 720

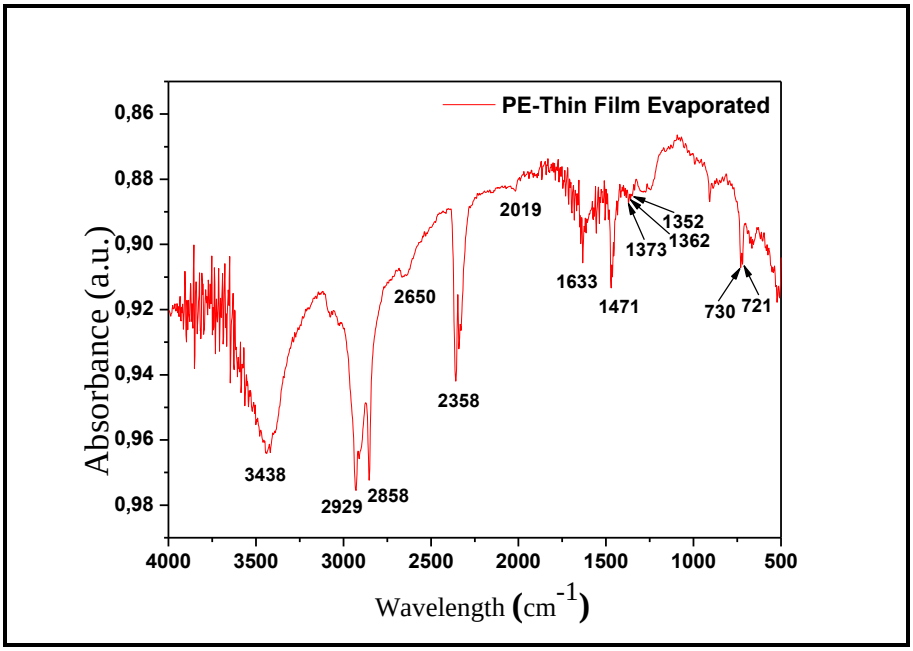

Figure 4.39 FTIR Spectrum of vacuum evaporated polyethylene

Fourier transform infrared spectra of vacuum-processed polyethylene films investigated in this work are shown in Figure 4.39, showing a good correlation to the respective peaks reported in the literature (Table 4.5) [92,93]. The characteristic peaks of CH_2 groups were observed at 2929, 2858 cm^{-1} due to the asymmetric and symmetric stretching vibrations of CH_2 groups respectively. Beside these peaks bending vibration peak was observed at 1472 cm^{-1}.

4.6.2 Atomic Force Microscopy

The atomic force microscopy investigation of vacuum processed polyethylene film is presented in Figure 4.40 a-d. and shows that polyethylene condenses on the aluminum oxide surface as individual islands (Figure 4.40.a) that finaly coalesce and grow with subsequent material deposition (Figure 4.40.c). The evaporation of 10 nm of polyethylene film results in formation of islands with a typical size of 3-4 nm and root-mean-square (rms) roughness measured along the top of each island of ~ 1 nm. The condensed polyethylene islands can be easily smeared out by heating the sample at a temperature above melting point of polyethylene (~110 °C) for 15 minutes (Figure 4.40.b and 4.40.d). Alternatively, the glass slides can be heated *in situ* during the evaporation process of the dielectric material to allow for a complete coverage and passivation of aluminum oxide dielectric.

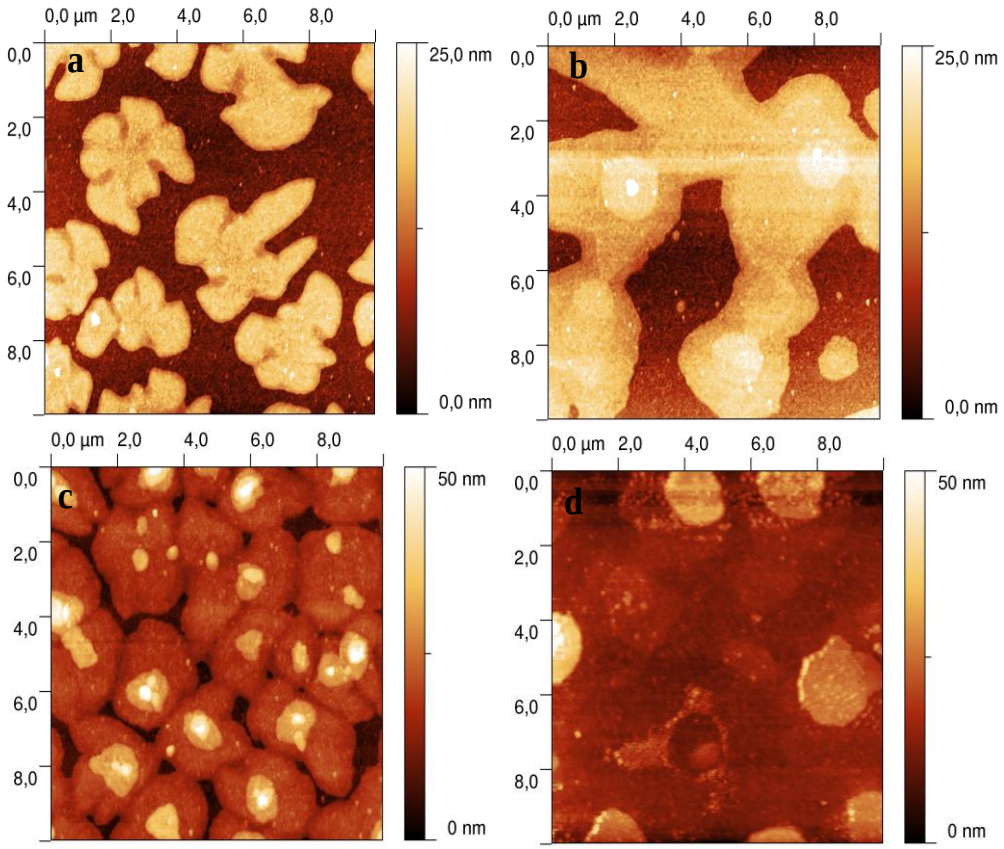

Figure 4.40 Atomic force microscopy of vacuum-processed polyethylene on aluminum oxide gate dielectric showing island formation and growing of the film: a)10 nm thick film; b) 10 nm thick film annealed at 100°C for 15 min; c) 20 nm thick film; d) 20 nm thick film annealed at 100°C for 15 min.

4.6.3 Dielectric Properties

Relative permittivity as a function of probe frequency of ~250 nm thick films of vacuum-processed polyethylene is presented in Figure 4.41. The impedance spectrum shows that vacuum processed polyethylene has a constant capacitance and very low losses over a wide range of frequencies, suggesting that thin films of evaporated polyethylene can act as trap-free charge dielectric layer in organic field effect

transistors. From the dielectric spectroscopy data, a dielectric constant of 2.4 is measured for polyethylene, agreeing closely with reported values [94].

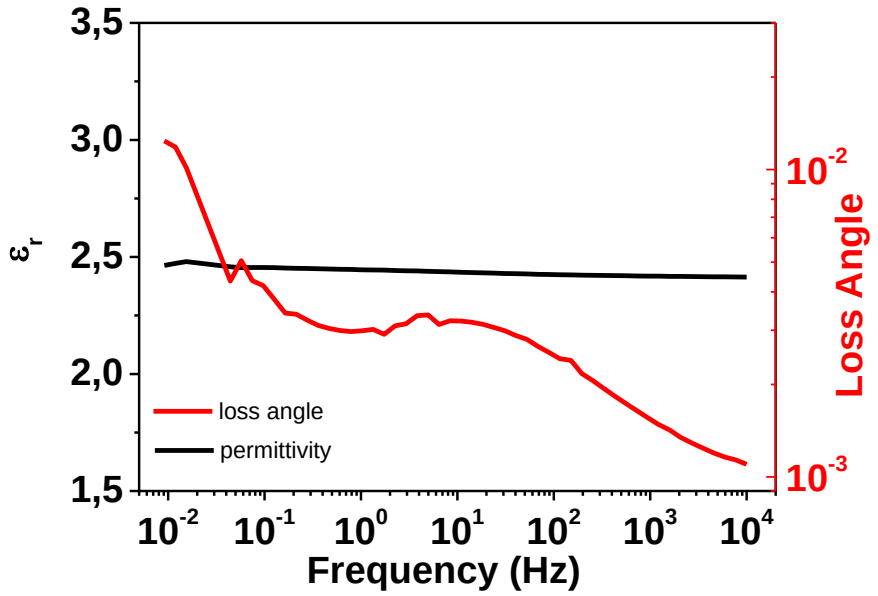

Figure 4.41 Relative permittivity of a 250 nm-thick film of evaporated polyethylene

4.6.4 Characterization of OFET's

Transfer and output characteristics of transistors with 250 nm evaporated polyethylene dielectric and fullerene, C_{60}, semiconductor are presented in Figure 4.42 and 4.43. Despite the roughness of the dielectric layer (rms ~30 nm), the transfer characteristic is hysteresis-free, a fact that was also reported previously for other dielectric materials like adenine, cytosine and thymine [71,95]. The respective OFET dielectric capacitance per unit area, $C_{0d,}$ is ~8.5 nF/cm^2 and the semiconductor mobility calculated in saturation regime is 0.55 cm^2/V·s. Higher performance of transistors are obtained if polyethylene is used as a passivation layer for

electrochemically-grown aluminum oxide dielectric layer. In the example shown in Figures 4.44 and 4.45, 20 nm polyethylene was evaporated on ~ 55 nm-thick aluminum oxide, followed by C_{60}. The dielectric capacitance of the combined dielectric was 60.4 nF/cm^2 and the operating voltage of the OFET was ~0.5 V for a mobility of the semiconductor material of 4.4 cm^2/V·s. Evaporated polyethylene dielectric also affords also a hole transport channel. In an example shown in Figures 4.46 and 4.47, pentacene semiconductor was thermally evaporated on the combined AlO_x-polyethylene dielectric layer, with 8 nm of electrochemically-grown aluminum oxide passivated with 20 nm of polyethylene. Although not fully optimized, the device operating voltage was only 4 V and the semiconductor mobility ~ 0.16 cm^2/V·s, for a dielectric capacitance of 96 nF/cm^2.

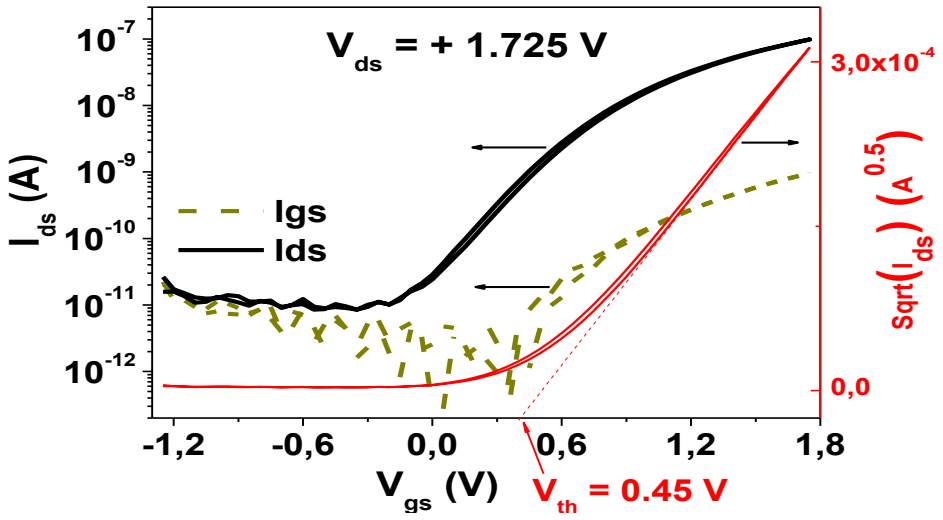

Figure 4.42 Transfer characteristics of field effect transistors with polyethylene dielectric: Channel design: L = 75 µm, W = 2 mm. Dielectric capacitance per area C_{0d} = 8.5 nF /cm^2

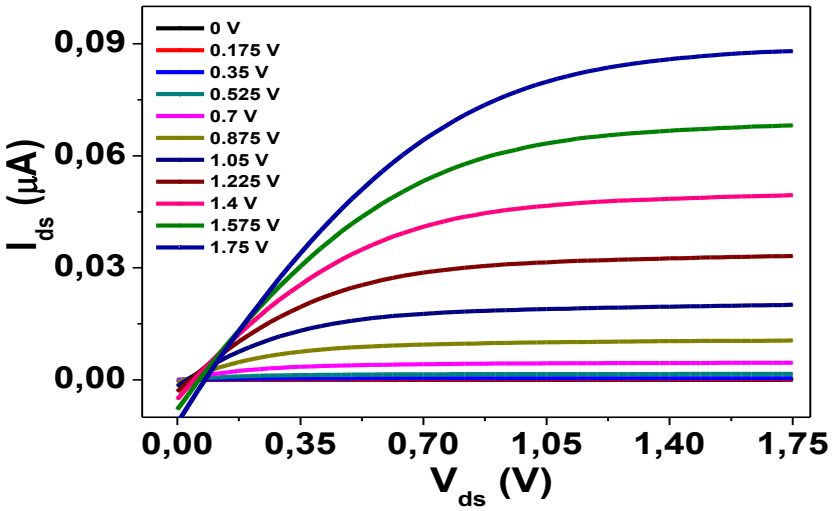

Figure 4.43 Output characteristics of field effect transistors with polyethylene dielectric: Channel design: L = 75 µm, W = 2 mm. Dielectric capacitance per area C_{0d} = 8.5 nF /cm^2

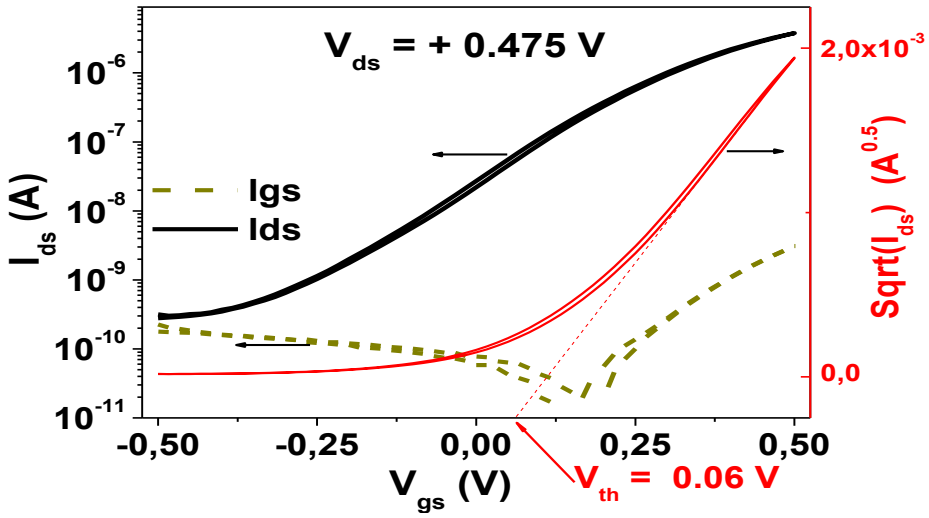

Figure 4.44 Transfer characteristics of field effect transistors with polyethylene dielectric: Channel design: L = 35 µm, W = 7 mm. Dielectric capacitance per area C_{0d} = 60.4 nF /cm^2

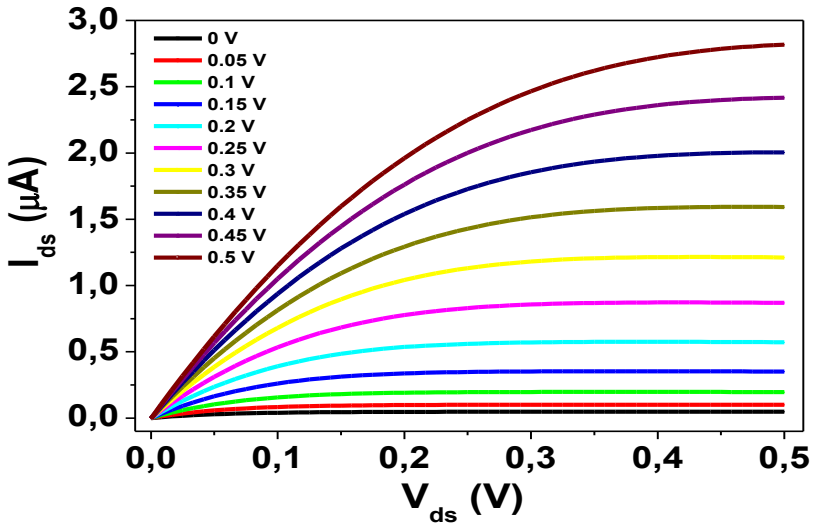

Figure 4.45 Output characteristics of field effect transistors with polyethylene dielectric: Channel design: L = 35 µm, W = 7 mm. Dielectric capacitance per area C_{0d} = 60.4 nF /cm^2

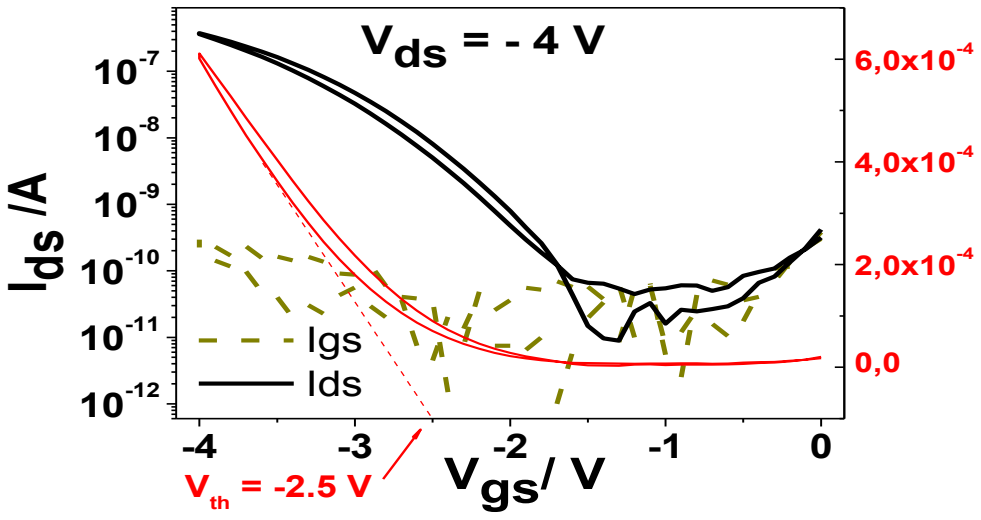

Figure 4.46 Transfer characteristics of field effect transistors with polyethylene dielectric: Channel design: L = 75 µm, W = 2 mm. Dielectric capacitance per area C_{0d} = 96 nF /cm^2

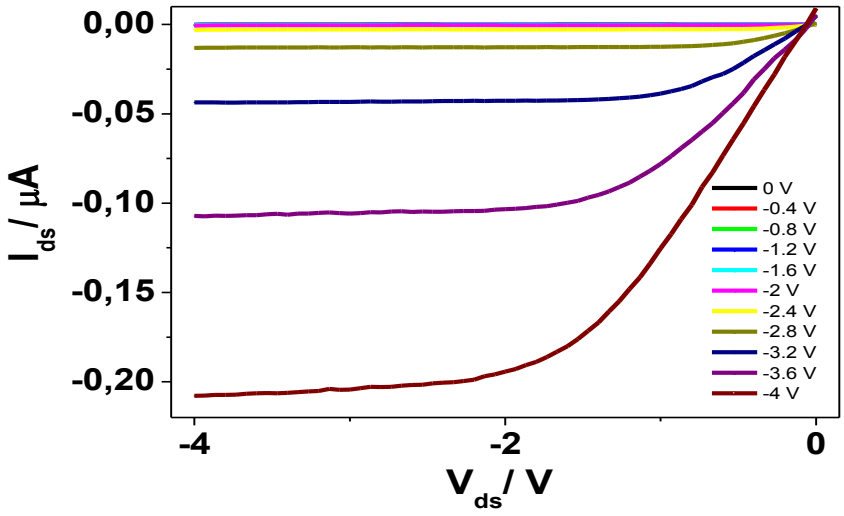

Figure 4.47 Output characteristics of field effect transistors with polyethylene dielectric: Channel design: L = 75 µm, W = 2 mm. Dielectric capacitance per area C_{0d} = 96 nF /cm^2

The fact that evaporated polyethylene dielectric affords both electron and hole channels, suggests that the material can be used for developing ambipolar organic field effect transistors. Such an example is given in Figure 4.48 a-c, where indigo is used as a novel ambipolar semiconductor, evaporated polyethylene is employed as a passivation layer for electrochemically-grown aluminum oxide dielectric for an OFET sample fabricated on drop-cast shellac substrate. The thickness of the layers: aluminum oxide 45 nm, polyethylene 10 nm, indigo 60 nm, gold source and drain electrodes 90 nm. Channel dimensions are L = 75 µm, W = 1 mm. Dielectric capacitance per unit area is C_{od} = 97.4 nF/cm^2.

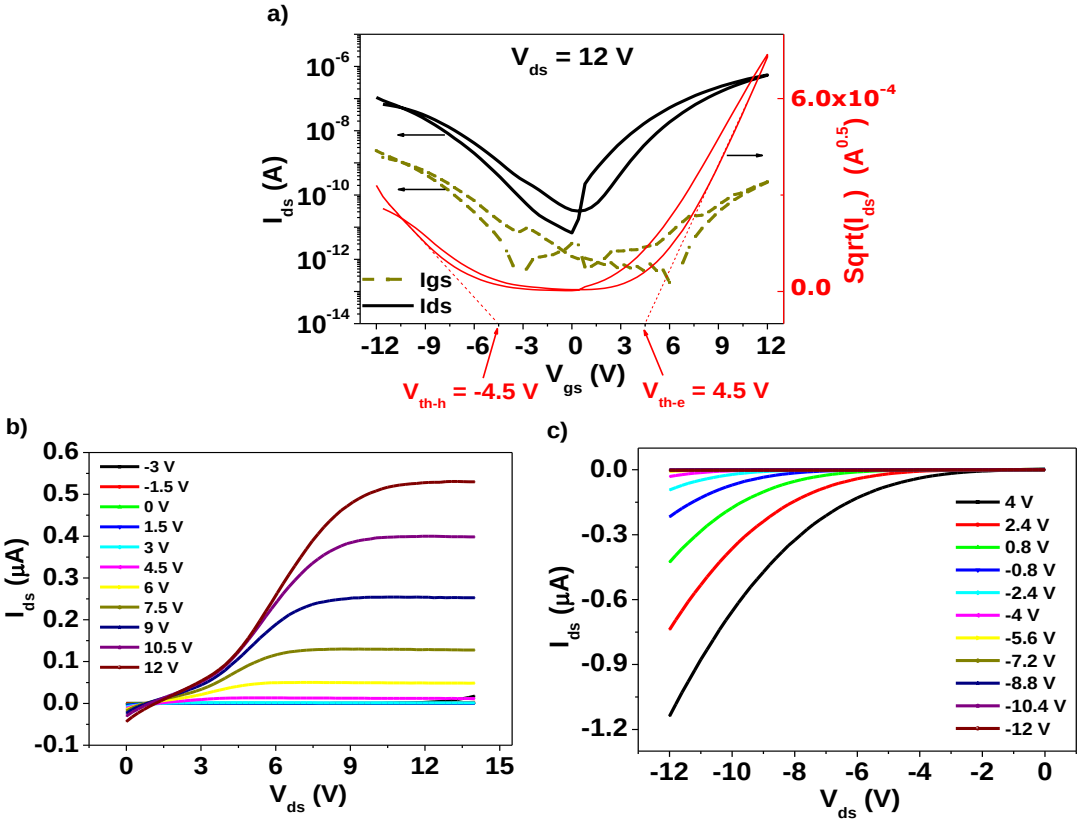

Figure 4.48 a) Transfer and b-c) output characteristics of indigo on evaporated polyethylene passivated aluminum oxide dielectric

The OFET shows clear print of ambipolarity with both electron and hole channel formation and superlinear increase in source drain current at low gate voltages (Fig. 4.48). The calculated electron and hole mobilities are ~ 2x10^{-2} cm^2/Vs and ~5.1x10^{-3} cm^2/V·s, respectively.

CHAPTER 5

CONCLUSION

5.1 Polypropylene / Carbon Black Composites

PP/CB composites were prepared via melt blending PP with CB. Effect of processing type on mechanical and physical properties was investigated. Injection molded samples had better mechanical properties when compared with compression molded samples due to the orientation of the polymer chain in the direction of the applied force. Electrical conductivity increased more in compression molded samples with added carbon black. Percent elongation at break values of the samples decreased with increasing filler content. The relation between percent elongation at break and electrical conductivity was studied. After percolation threshold a sudden increase in electrical conductivity was observed. Increasing filler content after threshold point show negative effect on percent deformation at break. Addition of the carbon black improved the thermal properties of the composites.

5.2 Surface Modification of Carbon Nanotube

In this study the effect of sulfonation amount of CN on electrical conductivity, morphology and dispersion stability in water were studied. The electrical conductivity of the CN increased with increasing sulfonation amount. SEM micrograph of the modified samples showed that after sulfonation CN's were observed in more bulky form due to strong hydrogen bonding between the CN's. Zeta potential of the CN's increased with surface modification. The zeta potential of the

CN were measured as lower than -15mV. This result show that modified CN can form stable dispersion in water.

5.3 Surface Modification of Fullerene

The effect of sulfonation degree of fullerenes on electrical conductivity, morphology and dispersion stability in water were studied in this work. The electrical conductivity of the fullerene increased with increasing sulfonation degree. SEM micrographs of the material show that treatment with acid does not effect on particle size. TEM micrographs of the samples show that after functionalization, materials have good dispersion in water. Zeta potential of the fullerene's increased with surface modification. The zeta potential of the surface modified fullerenes were found as lower than -15mV. This result shows that modified fullerenes can form stable dispersion in water.

5.4 Polypropylene/ Carbon Nanotube Composites

In this study, the electrical, mechanical and thermal stability of PP/neat CNT and PP/m-CNT composites were studied. The effect of surface modification and using different dispersants on these properties were investigated. The best electrical and mechanical properties were observed for the composites which contain CTAB and MA-g-PP as dispersant. CTAB had good interaction with negatively charged m-CNT surface and as a result of this interaction both electrical and the mechanical properties of the composites were good. Addition of MA-g-PP as dispersant increased the Young modulus of the composites and improved the electrical conductivity.

5.5 Polypropylene / Fullerene Composites

Polypropylene/neat F and Polypropylene/m-F composites were prepared via melt blending. The effect of the compatibilizer on mechanical and electrical properties of the m-F were studied. Addition of the CTAB and MA-g-PP compatibilizer improved the mechanical and electrical properties better than the PE-b-PEG and Triton X 100 compatibilizers. Composites which contain m-F without compatibilizer showed lower mechanical properties than the neat fullerene composites. Mechanical properties of the composites increased with decreasing agglomeration size.

5.6 Organic Field Effect Transistors with Polyethylene Gate Dielectric

We demonstrate that vacuum-processed polyethylene represents a good dielectric layer for the development of high performance organic field effect transistors. Polyethylene has excellent insulating properties, given by its high band gap of ~8.9 eV and its extremely low conductivity of ~ 1×10^{-18} S/cm. Its chemical stability is an additional attractive feature. Vacuum-evaporated layers of polyethylene can perform either as a stand-alone dielectric or in combination with aluminum oxide for the attainment of efficient charge transport in OFETs. The best C_{60} devices built in our lab showed operating voltages as low as 0.5 V and field effect mobilities of ~ 3.8 $cm^2/V\cdot s$. In addition, the possibility that both electrons and holes can be transported at the interface polyethylene-organic semiconductor, as demonstrated by indigo, recommends the vacuum-processed polyethylene as a suitable dielectric for the development of ambipolar OFETs and integrated circuits.

REFERENCES

[1] V.E. Gul, *Structure and Properties of Conducting Polymer Composites*, VSP BV, 1996.

[2] L. Chua, J. Zaumseil, J. Chang, and E.C. Ou, "General observation of n-type field-effect behaviour in organic semiconductors," *Nature*, vol. 434, 2005, pp. 194-199.

[3] Y. Ueda, M. Matsushita, S. Morimoto, J. Ping Ni, H. Suzuki, and S. Mashiko, "Structure and crystal growth of low molecular weight polyethylene vapor-deposited on polymer friction-transferred layers," *Thin Solid Films*, vol. 331, Oct. 1998, pp. 216-221.

[4] K. Maki, "Evaporation of polyethylene powder for its thin film growth," *Thin Solid Films*, vol. 188, Jul. 1990, pp. 355-359.

[5] R. Ebewele, *Polymer Science and Technology*, CRC Press, 2000.

[6] H.G. Karian, *Handbook of Polypropylene and Polyropylene composites*, Marcel Dekker Inc., 2003.

[7] R. Stewart, V. Goodship, F. Guild, M. Green, and J. Farrow, "Investigation and demonstration of the durability of air plasma pre-treatment on polypropylene automotive bumpers," *International Journal of Adhesion and Adhesives*, vol. 25, Apr. 2005, pp. 93-99.

[8] W. Hufenbach, R. Böehm, M. Thieme, a Winkler, E. Mäder, J. Rausch, and M. Schade, "Polypropylene/glass fibre 3D-textile reinforced composites for

automotive applications," *Materials & Design*, vol. 32, Sep. 2010, pp. 1468-1476.

[9] P. Tos, S. Artiaco, S. Coppolino, L.G. Conforti, and B. Battiston, "A simple sterile polypropylene fingernail substitute.," *Chirurgie de la main*, vol. 28, Jun. 2009, pp. 143-5.

[10] C. Mao, "Introduction of anticoagulation group to polypropylene film by radiation grafting and its blood compatibility," *Applied Surface Science*, vol. 228, Apr. 2004, pp. 26-33.

[11] J.-M. Thomassin, I. Huynen, R. Jerome, and C. Detrembleur, "Functionalized polypropylenes as efficient dispersing agents for carbon nanotubes in a polypropylene matrix; application to electromagnetic interference (EMI) absorber materials," *Polymer*, vol. 51, Jan. 2010, pp. 115-121.

[12] Y. Kanbur and Z. Kucukyavuz, "Electrical and Mechanical Properties of Polypropylene/Carbon Black Composites," *Journal of Reinforced Plastics and Composites*, vol. 28, Oct. 2008, pp. 2251-2260.

[13] S. Bao and S. Tjong, "Mechanical behaviors of polypropylene/carbon nanotube nanocomposites: The effects of loading rate and temperature," *Materials Science and Engineering: A*, vol. 485, Jun. 2008, pp. 508-516.

[14] J. Thomason, "The influence of fibre length and concentration on the properties of glass fibre reinforced polypropylene: 5. Injection moulded long and short fibre PP," *Composites Part A: Applied Science and Manufacturing*, vol. 33, Dec. 2002, pp. 1641-1652.

[15] A.M.M. Baker and J. Mead, "Thermoplastics," *Handbook of Plastics, elastomers and composites*, C.A. Harper, ed., McGraw-Hill Professional, 2004.

[16] R.A. Petrick, *Polymer Structure Characterization (From Nano to Macro Organization)*, The Royal Society of Chemistry, 2007.

[17] E.C. Carraher, *Polymer Chemistry*, Mercel Dekker ,Inc., 2003.

[18] J. Zaumseil and H. Sirringhaus, "Electron and ambipolar transport in organic field-effect transistors.," *Chemical reviews*, vol. 107, Apr. 2007, pp. 1296-323.

[19] J. Veres, S. Ogier, G. Lloyd, and D. de Leeuw, "Gate Insulators in Organic Field-Effect Transistors," *Chemistry of Materials*, vol. 16, Nov. 2004, pp. 4543-4555.

[20] K.J. Less and E.G. Wilson, "Intrinsic photoconduction and photoemission in polyethylene," *Journal of Physics C: Solid State Physics*, vol. 6, 1973, pp. 3110-3120.

[21] J.F. Fowler, "X-Ray Induced Conductivity in Insulating Materials," *Proceedings of the Royal Society A: Mathematical, Physical and Engineering Sciences*, vol. 236, Sep. 1956, pp. 464-480.

[22] S. Lijima, "Helical microtubules of graphitic carbon," *Nature*, vol. 354, 1991, pp. 56-58.

[23] S.G. Shonaike, G.O. Advani, *Advanced Polymeric Materials (structure and Property Relatioship)*, CRC Press, 2003.

[24] M. Xanthos, *Functional Fillers for Plastics*, WILEY-VCH Verlag GmbH, 2005.

[25] J. Coleman, U. Khan, W. Blau, and Y. Gunko, "Small but strong: A review of the mechanical properties of carbon nanotube–polymer composites," *Carbon*, vol. 44, Aug. 2006, pp. 1624-1652.

[26] Z. Spitalsky, D. Tasis, K. Papagelis, and C. Galiotis, “Carbon nanotube–polymer composites: Chemistry, processing, mechanical and electrical properties,” *Progress in Polymer Science*, vol. 35, Mar. 2010, pp. 357-401.

[27] J. Wang and Y. Lin, “Functionalized carbon nanotubes and nanofibers for biosensing applications.,” *Trends in analytical chemistry : TRAC*, vol. 27, Jan. 2008, pp. 619-626.

[28] R.A. Hatton, N.P. Blanchard, L.W. Tan, G. Latini, F. Cacialli, and S.R.P. Silva, “Oxidised carbon nanotubes as solution processable, high work function hole-extraction layers for organic solar cells,” *Organic Electronics*, vol. 10, May. 2009, pp. 388-395.

[29] P. Hernández-Fernández, M. Montiel, P. Ocón, J.L.G. de la Fuente, S. García-Rodríguez, S. Rojas, and J.L.G. Fierro, “Functionalization of multi-walled carbon nanotubes and application as supports for electrocatalysts in proton-exchange membrane fuel cell,” *Applied Catalysis B: Environmental*, vol. 99, Aug. 2010, pp. 343-352.

[30] X. Jiang, Y. Bin, and M. Matsuo, “Electrical and mechanical properties of polyimide–carbon nanotubes composites fabricated by in situ polymerization,” *Polymer*, vol. 46, Aug. 2005, pp. 7418-7424.

[31] R. Haggenmueller, F. Du, J.E. Fischer, and K.I. Winey, “Interfacial in situ polymerization of single wall carbon nanotube/nylon 6,6 nanocomposites,” *Polymer*, vol. 47, Mar. 2006, pp. 2381-2388.

[32] C. Teng, C. Ma, Y. Huang, S. Yuen, C. Weng, C. Chen, and S. Su, “Effect of MWCNT content on rheological and dynamic mechanical properties of multiwalled carbon nanotube/polypropylene composites,” *Composites Part A: Applied Science and Manufacturing*, vol. 39, Dec. 2008, pp. 1869-1875.

[33] F. Thiébaud and J.C. Gelin, “Characterization of rheological behaviors of polypropylene/carbon nanotubes composites and modeling their flow in a twin-screw mixer,” *Composites Science and Technology*, vol. 70, Apr. 2010, pp. 647-656.

[34] Z. Zhou, S. Wang, L. Lu, Y. Zhang, and Y. Zhang, “Functionalization of multi-wall carbon nanotubes with silane and its reinforcement on polypropylene composites,” *Composites Science and Technology*, vol. 68, Jun. 2008, pp. 1727-1733.

[35] B. Yang, J. Shi, K. Pramoda, and S. Goh, “Enhancement of the mechanical properties of polypropylene using polypropylene-grafted multiwalled carbon nanotubes,” *Composites Science and Technology*, vol. 68, Sep. 2008, pp. 2490-2497.

[36] S. Lee, E. Cho, S. Jeon, and J. Youn, “Rheological and electrical properties of polypropylene composites containing functionalized multi-walled carbon nanotubes and compatibilizers,” *Carbon*, vol. 45, Nov. 2007, pp. 2810-2822.

[37] S. Bose, A.R. Bhattacharyya, P.V. Kodgire, and A. Misra, “Fractionated crystallization in PA6/ABS blends: Influence of a reactive compatibilizer and multiwall carbon nanotubes,” *Polymer*, vol. 48, Jan. 2007, pp. 356-362.

[38] B. Safadi, R. Andrews, and E. a Grulke, “Multiwalled carbon nanotube polymer composites: Synthesis and characterization of thin films,” *Journal of Applied Polymer Science*, vol. 84, Jun. 2002, pp. 2660-2669.

[39] L. Chen, X. Pang, M. Qu, Q. Zhang, B. Wang, B. Zhang, and Z. Yu, “Fabrication and characterization of polycarbonate/carbon nanotubes composites,” *Composites Part A: Applied Science and Manufacturing*, vol. 37, Sep. 2006, pp. 1485-1489.

[40] D. Bikiaris, A. Vassiliou, K. Chrissafis, K. Paraskevopoulos, A. Jannakoudakis, and A. Docoslis, "Effect of acid treated multi-walled carbon nanotubes on the mechanical, permeability, thermal properties and thermo-oxidative stability of isotactic polypropylene," *Polymer Degradation and Stability*, vol. 93, May. 2008, pp. 952-967.

[41] T. Kashiwagi, "Thermal and flammability properties of polypropylene/carbon nanotube nanocomposites," *Polymer*, vol. 45, May. 2004, pp. 4227-4239.

[42] E. Logakis, E. Pollatos, C. Pandis, V. Peoglos, I. Zuburtikudis, C.G. Delides, a Vatalis, M. Gjoka, E. Syskakis, and K. Viras, "Structure–property relationships in isotactic polypropylene/multi-walled carbon nanotubes nanocomposites," *Composites Science and Technology*, vol. 70, Feb. 2010, pp. 328-335.

[43] K. Prashantha, J. Soulestin, M.F. Lacrampe, P. Krawczak, G. Dupin, and M. Claes, "Masterbatch-based multi-walled carbon nanotube filled polypropylene nanocomposites: Assessment of rheological and mechanical properties," *Composites Science and Technology*, vol. 69, Sep. 2009, pp. 1756-1763.

[44] L. Vaisman, H.D. Wagner, and G. Marom, "The role of surfactants in dispersion of carbon nanotubes.," *Advances in colloid and interface science*, vol. 128-130, Dec. 2006, pp. 37-46.

[45] J.I. Kroschwitz and M.H. Grant, *Encyclopedia of chemical technology*, John Wiley & Sons, Inc., 1995.

[46] C. Silvestre, S. Cimmino, and E. Di Pace, "Crystallizable Polymer Blends," *Polymeric Materials Encyclopedia*, 1996.

[47] J.A. Brydson, *Plastics Materials*, Reed Educational andProfessional Publishing Ltd., 1999.

[48] R.N. Rothon, *Particulate Fillers for Polymers*, Rapra Technology Ltd., 2002.

[49] P.K. Pramanik, D. Khastgir, and T.N. Saha, “Conductive nitrile rubber composite containing carbon fillers: Studies on mechanical properties and electrical conductivity,” *Composites*, vol. 23, May. 1992, pp. 183-191.

[50] D.L.D. Chung, *Carbon Fiber Composites*, Butterworth-Heinemann, 1994.

[51] H. Yui, G. Wu, H. Sano, M. Sumita, and K. Kino, “Morphology and electrical conductivity of injection-molded polypropylene/carbon black composites with addition of high-density polyethylene,” *Polymer*, vol. 47, May. 2006, pp. 3599-3608.

[52] Z. Ranjbar and S. Rastegar, “Morphology and electrical conductivity behavior of electro-deposited conductive carbon black-filled epoxy dispersions near the insulator-conductor transition point,” *Colloids and Surfaces A: Physicochemical and Engineering Aspects*, vol. 290, Nov. 2006, pp. 186-193.

[53] M.L. Clingerman, J.A. King, K.H. Schulz, and J.D. Meyers, “Evaluation of Electrical Conductivity Models for Conductive Polymer Composites,” *Polymer*, 2002, pp. 1341-1356.

[54] H. Zois, L. Apekis, and M. Omastová, “Electrical properties of carbon black-filled polymer composites,” *Macromolecular Symposia*, vol. 170, 2001, pp. 249-256.

[55] H.O. Pierson, *Handbook of Carbon, Graphite, Diamond and Fullerenes*, Noyes Publication, 1993.

[56] F. Langa and J.F. Nierengarten, *Fullerenes :Principles and Applications*, The Royal Society of Chemistry, 2007.

[57] L. Dai, J. Lu, B. Matthews, and A.W.H. Mau, “Doping of Conducting Polymers by Sulfonated Fullerene Derivatives and Dendrimers,” *The Journal of Physical Chemistry B*, vol. 102, Apr. 1998, pp. 4049-4053.

[58] R. Taylor and D.R.M. Walton, "The chemistry of fullerenes," *Nature*, vol. 363, Jun. 1993, pp. 685-693.

[59] H. Peng, J.W.Y. Lam, F.S.M. Leung, T.W.H. Poon, A.X. Wu, N.-T. Yu, and B.Z. Tang, "Synthesis of Fullerene-Containing Sol-Gel Glasses," *Journal of Sol-Gel Science and Technology*, vol. 22, pp. 205-218.

[60] J.H. Bae, A.M. Shanmugharaj, W.H. Noh, W.S. Choi, and S.H. Ryu, "Surface chemical functionalized single-walled carbon nanotube with anchored phenol structures: Physical and chemical characterization," *Applied Surface Science*, vol. 253, Feb. 2007, pp. 4150-4155.

[61] S.K. Mazumdar, *Composites Manufacturing*, CRC Press, 2002.

[62] F.L. Matthews and R.D. Rawlings, *Composite Materials : Engineering and Science*, Chapman & Hall, 1996.

[63] J.H. Koo, *Polymer Nanocomposites*, McGraw-Hill Professional, 2006.

[64] P.M. Ajayan, L.S. Schadler, and P.V. Braun, *Nanocomposite Science and Technology*, WILEY-VCH Verlag GmbH, 2003.

[65] M.S. Freund and B. Deore, *Self Doped Conducting Polymers*, WILEY-VCH Verlag GmbH, 2007.

[66] T.B. Singh, N. Marjanović, P. Stadler, M. Auinger, G.J. Matt, S. Günes, N.S. Sariciftci, R. Schwödiauer, and S. Bauer, "Fabrication and characterization of solution-processed methanofullerene-based organic field-effect transistors," *Journal of Applied Physics*, vol. 97, 2005, p. 083714.

[67] T.B. Singh and N.S. Sariciftci, "Progress in Plastic Electronics Devices," *Annual Review of Materials Research*, vol. 36, Aug. 2006, pp. 199-230.

[68] R. Ponce Ortiz, A. Facchetti, and T.J. Marks, “High-k organic, inorganic, and hybrid dielectrics for low-voltage organic field-effect transistors.,” *Chemical reviews*, vol. 110, Jan. 2010, pp. 205-39.

[69] M. Irimia-Vladu, N. Marjanovic, M. Bodea, G. Hernandez-Sosa, A.M. Ramil, R. Schwödiauer, S. Bauer, N.S. Sariciftci, and F. Nüesch, “Small-molecule vacuum processed melamine-C60, organic field-effect transistors,” *Organic Electronics*, vol. 10, May. 2009, pp. 408-415.

[70] M. Egginger, M. Irimia-Vladu, R. Schwödiauer, a Tanda, I. Frischauf, S. Bauer, and N.S. Sariciftci, “Mobile Ionic Impurities in Poly(vinyl alcohol) Gate Dielectric: Possible Source of the Hysteresis in Organic Field-Effect Transistors,” *Advanced Materials*, vol. 20, Mar. 2008, pp. 1018-1022.

[71] M. Irimia-Vladu, P.A. Troshin, M. Reisinger, L. Shmygleva, Y. Kanbur, G. Schwabegger, M. Bodea, R. Schwödiauer, A. Mumyatov, J.W. Fergus, V.F. Razumov, H. Sitter, N.S. Sariciftci, and S. Bauer, “Biocompatible and Biodegradable Materials for Organic Field-Effect Transistors,” *Advanced Functional Materials*, Sep. 2010, pp. 4069-4076.

[72] M. Irimia-Vladu, N. Marjanovic, A. Vlad, A.M. Ramil, G. Hernandez-Sosa, R. Schwoödiauer, S. Bauer, and N.S. Sariciftci, “Vacuum-Processed Polyaniline-C 60 Organic Field Effect Transistors,” *Advanced Materials*, vol. 20, Oct. 2008, pp. 3887-3892.

[73] R. Yu, L. Chen, Q. Liu, J. Lin, K.-L. Tan, S.C. Ng, H.S.O. Chan, G.-Q. Xu, and T.S.A. Hor, “Platinum Deposition on Carbon Nanotubes via Chemical Modification,” *Chemistry of Materials*, vol. 10, Jan. 1998, pp. 718-722.

[74] N. Bowler and Y. Huang, “Electrical conductivity measurement of metal plates using broadband eddy-current and four-point methods,” *Measurement Science and Technology*, vol. 16, Nov. 2005, pp. 2193-2200.

[75] " Four Point Probe, http://www.imagesco.com/articles/supercond/09.html last accessed 15th April 2011."

[76] Z.S. Petrović, B. Martinović, V. Divjaković, and J. Budinski–Simendić, "Polypropylene–Carbon black interaction in conductive composites," *Journal of Applied Polymer Science*, vol. 49, 1993, pp. 1659-1669.

[77] J. Adler, Y. Meir, A. Aharony, A.B. Harris, and L. Klein, "Low-concentration series in general dimension," *Journal of Statistical Physics*, vol. 58, pp. 511-538.

[78] I. Chodák, M. Omastová, and J. Pionteck, "Relation between electrical and mechanical properties of conducting polymer composites," *Journal of Applied Polymer Science*, vol. 82, 2001, pp. 1903-1906.

[79] M. Omastova, I. Chodak, and J. Pionteck, "Electrical and mechanical properties of conducting polymer composites," *Synthetic Metals*, vol. 102, Jun. 1999, pp. 1251-1252.

[80] E. Jakab and M. Omastova, "Thermal decomposition of polyolefin/carbon black composites," *Journal of Analytical and Applied Pyrolysis*, vol. 74, Aug. 2005, pp. 204-214.

[81] K. Hinokuma and M. Ata, "Proton Conduction in Polyhydroxy Hydrogensulfated Fullerenes," *Journal of The Electrochemical Society*, vol. 150, 2003, p. A112.

[82] Z. Sun, V. Nicolosi, D. Rickard, S.D. Bergin, D. Aherne, and J.N. Coleman, "Quantitative Evaluation of Surfactant-stabilized Single-walled Carbon Nanotubes: Dispersion Quality and Its Correlation with Zeta Potential," *The Journal of Physical Chemistry C*, vol. 112, Jun. 2008, pp. 10692-10699.

[83] B. White, S. Banerjee, S. O'Brien, N.J. Turro, and I.P. Herman, "Zeta-Potential Measurements of Surfactant-Wrapped Individual Single-Walled Carbon Nanotubes," *The Journal of Physical Chemistry C*, vol. 111, Aug. 2007, pp. 13684-13690.

[84] X. Xie, Y. Mai, and X. Zhou, "Dispersion and alignment of carbon nanotubes in polymer matrix: A review," *Materials Science and Engineering: R: Reports*, vol. 49, May. 2005, pp. 89-112.

[85] L.Y. Chiang, L.-Y. Wang, J.W. Swirczewski, S. Soled, and S. Cameron, "Efficient Synthesis of Polyhydroxylated Fullerene Derivatives via Hydrolysis of Polycyclosulfated Precursors," *The Journal of Organic Chemistry*, vol. 59, Jul. 1994, pp. 3960-3968.

[86] H. Hu, A. Yu, E. Kim, B. Zhao, M.E. Itkis, E. Bekyarova, and R.C. Haddon, "Influence of the Zeta Potential on the Dispersability and Purification of Single-Walled Carbon Nanotubes," *The Journal of Physical Chemistry B*, vol. 109, May. 2005, pp. 11520-11524.

[87] Q. Wang, Y. Han, Y. Wang, Y. Qin, and Z.-X. Guo, "Effect of Surfactant Structure on the Stability of Carbon Nanotubes in Aqueous Solution," *The Journal of Physical Chemistry B*, vol. 112, May. 2008, pp. 7227-7233.

[88] A. Montazeri, J. Javadpour, A. Khavandi, A. Tcharkhtchi, and A. Mohajeri, "Mechanical properties of multi-walled carbon nanotube/epoxy composites," *Materials & Design*, vol. 31, Oct. 2010, pp. 4202-4208.

[89] M. Yeh, N. Tai, and J. Liu, "Mechanical behavior of phenolic-based composites reinforced with multi-walled carbon nanotubes," *Carbon*, vol. 44, Jan. 2006, pp. 1-9.

[90] B.B. Marosfői, a Szabó, G. Marosi, D. Tabuani, G. Camino, and S. Pagliari, "Thermal and spectroscopic characterization of polypropylene-carbon nanotube composites," *Journal of Thermal Analysis and Calorimetry*, vol. 86, Oct. 2006, pp. 669-673.

[91] M. Angelopoulos, G.E. Asturias, S.P. Ermer, A. Ray, E.M. Scherr, A.G. Macdiarmid, M. Akhtar, Z. Kiss, and A.J. Epstein, "Polyaniline: Solutions, Films and Oxidation State," *Molecular Crystals and Liquid Crystals Incorporating Nonlinear Optics*, vol. 160, 1988, pp. 151-163.

[92] J.V. Gulmine, P.R. Janissek, H.M. Heise, and L. Akcelrud, "Polyethylene characterization by FTIR," *Polymer Testing*, vol. 21, 2002, pp. 557-563.

[93] M. Mirzataheri and J. Morshedian, "Electron beam performance in the novel solventless LDPE-NVP surface grafting system," *Radiation Physics and Chemistry*, vol. 75, Feb. 2006, pp. 236-242.

[94] M. Zor and C. a Hogarth, "High-field electrical conduction in thin films of polyethylene," *Physica Status Solidi (a)*, vol. 99, Feb. 1987, pp. 513-519.

[95] M. Irimia-Vladu, P.A. Troshin, M. Reisinger, G. Schwabegger, M. Ullah, R. Schwoediauer, A. Mumyatov, M. Bodea, J.W. Fergus, V.F. Razumov, H. Sitter, S. Bauer, and N.S. Sariciftci, "Environmentally sustainable organic field effect transistors," *Organic Electronics*, vol. 11, Dec. 2010, pp. 1974-1990.

APPENDIX A

STRESS AT BREAK OF THE POLYPROPYLENE / CARBON NANOTUBE AND POLYPROPYLENE / FULLERENE COMPOSITES

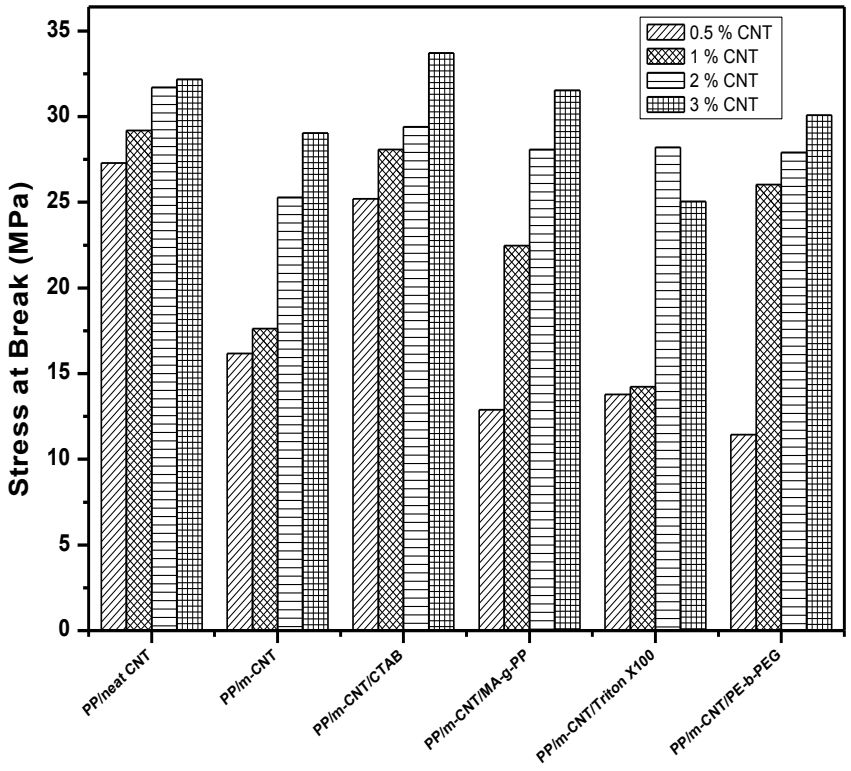

Figure A.1. Stress at Break of the Polypropylene/Carbon Nanotube Composites

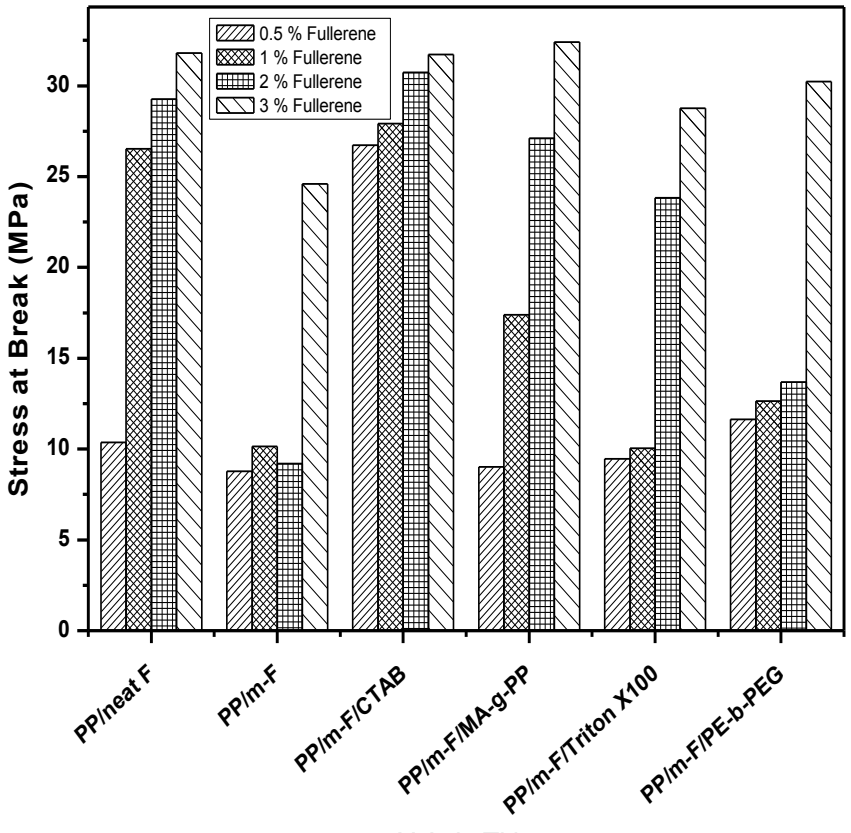

Figure A.2. Stress at Break of the Polypropylene/Fullerene Composites

APPENDIX B

STRESS VS STRAIN CURVES FOR POLYPROPYLENE / CARBON NANOTUBE AND POLYPROPYLENE / FULLERENE COMPOSITES

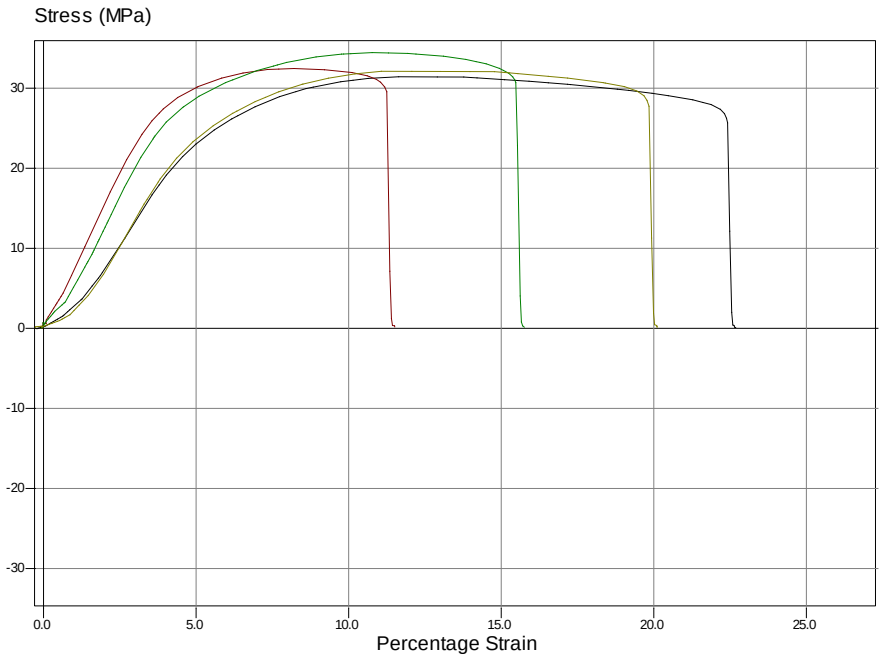

Figure B.1. Stress vs strain curves of PP/CNT composites

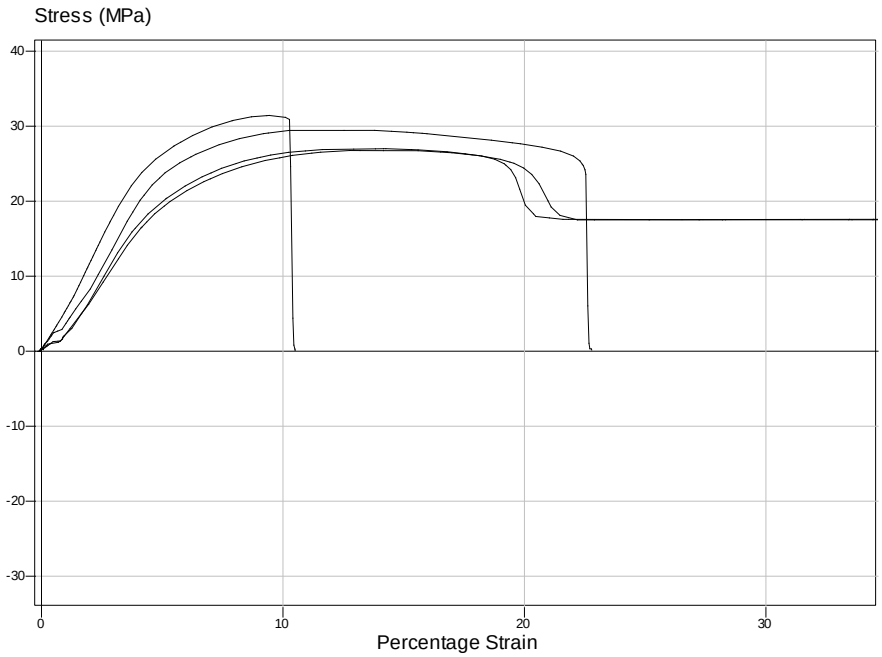

Figure B.2. Stress vs strain curves of PP/m-CNT composites

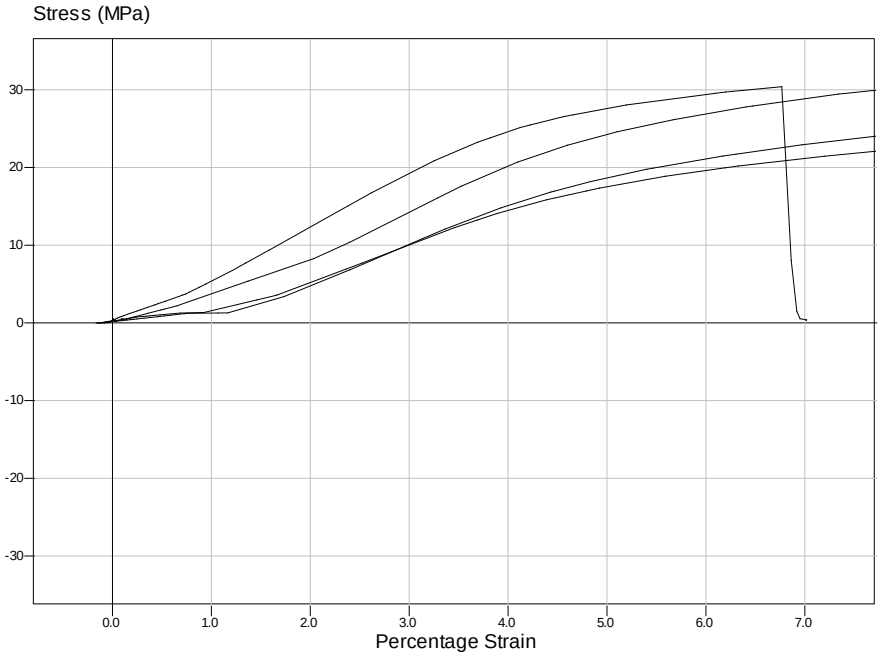

Figure B.3. Stress vs strain curves of PP/ m-CNT/ PE-b-PEG composites

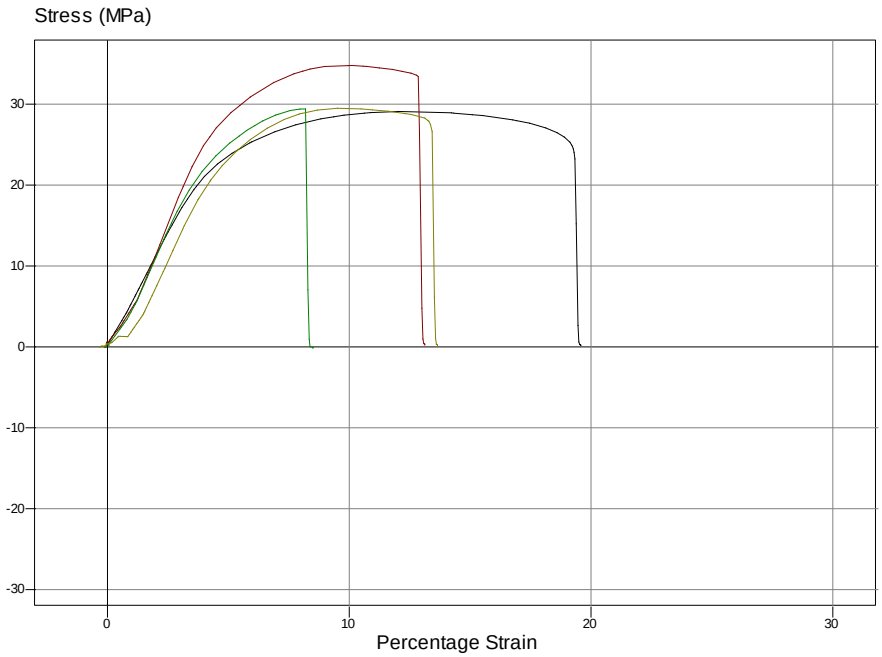

Figure B.4. Stress vs strain curves of PP/ m-CNT/ CTAB composites

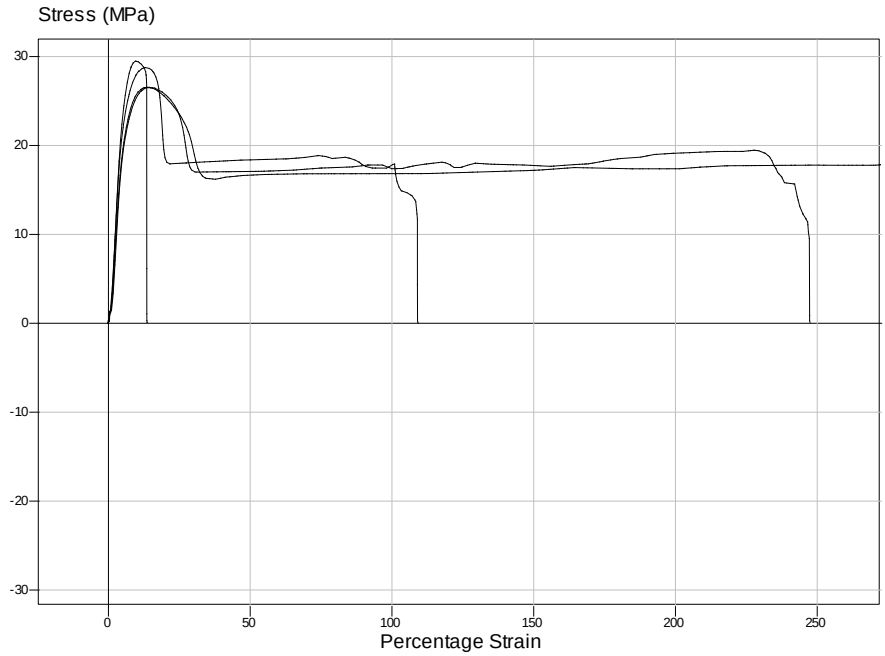

Figure B.5. Stress vs strain curves of PP/ m-CNT/ MA-g-PP composites

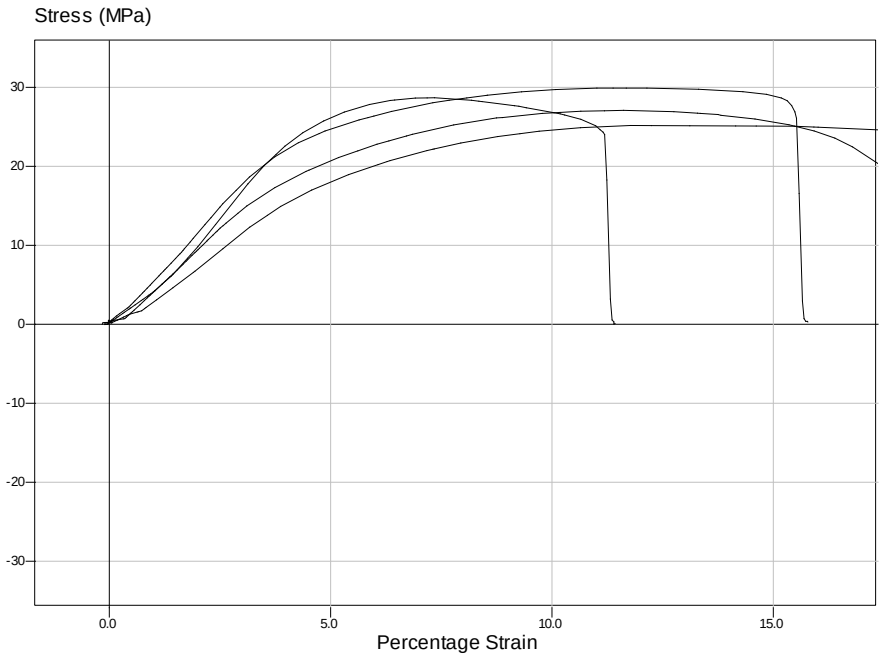

Figure B.6. Stress vs strain curves of PP/m-CNT/Triton X-100 composites

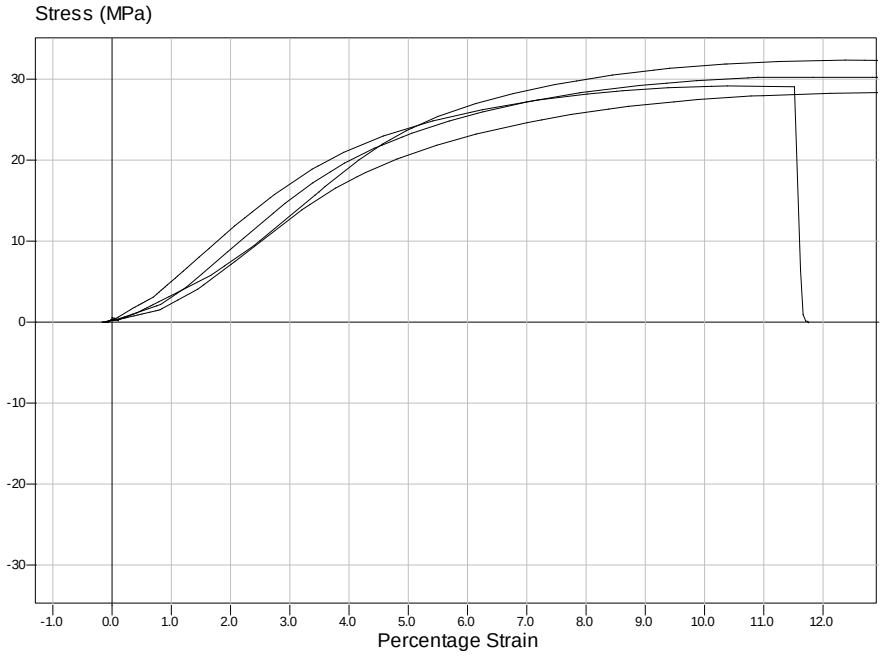

Figure B.7. Stress vs strain curves of PP/neat F composites

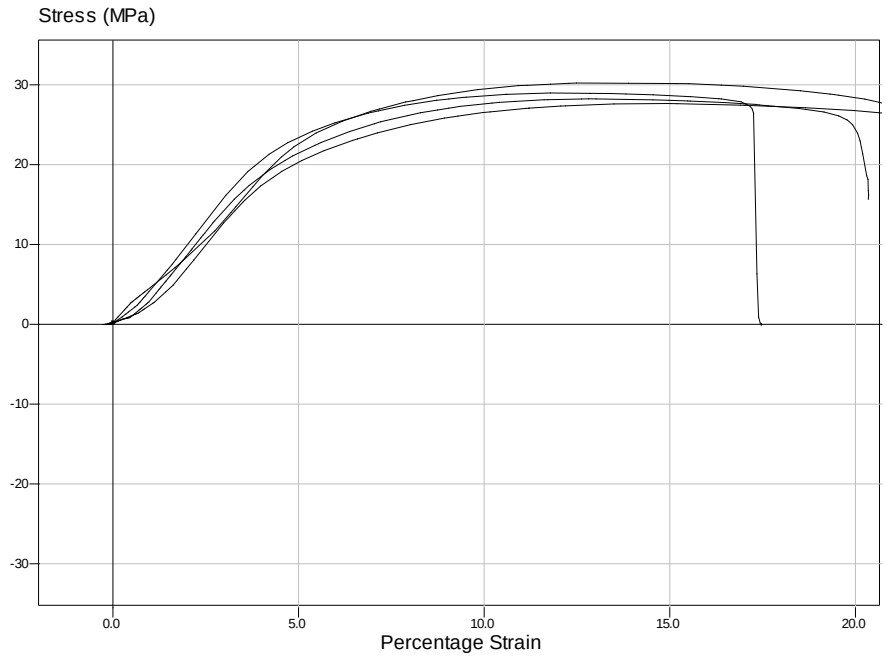

Figure B.8. Stress vs strain curves of PP/ m-F composites

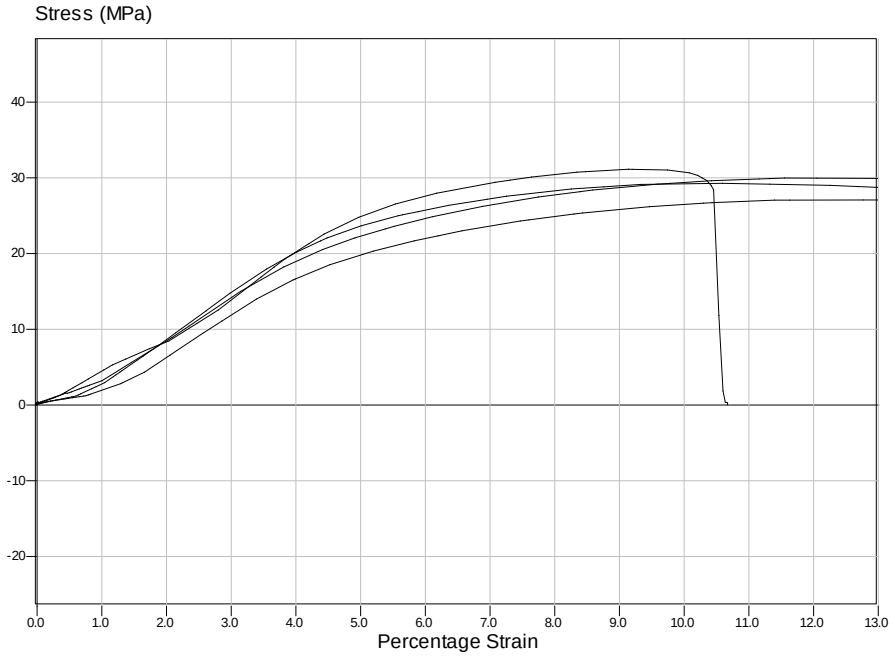

Figure B.9. Stress vs strain curves of PP/ m-F/ PE-b-PEG composites

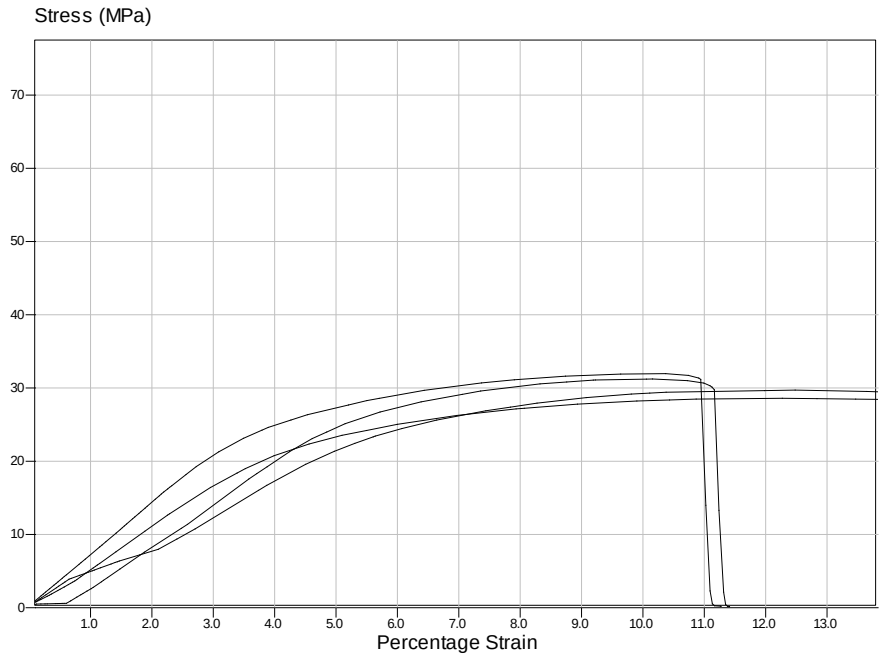

Figure B.10. Stress vs strain curves of PP/ m-F/ CTAB composites

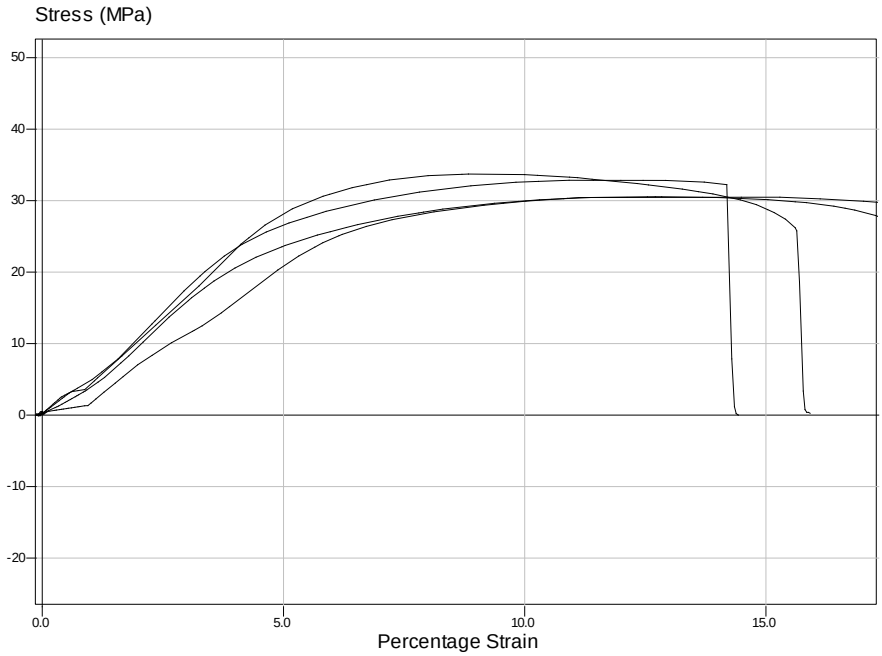

Figure B.11. Stress vs strain curves of PP/ m-F/ MA-g-PP composites

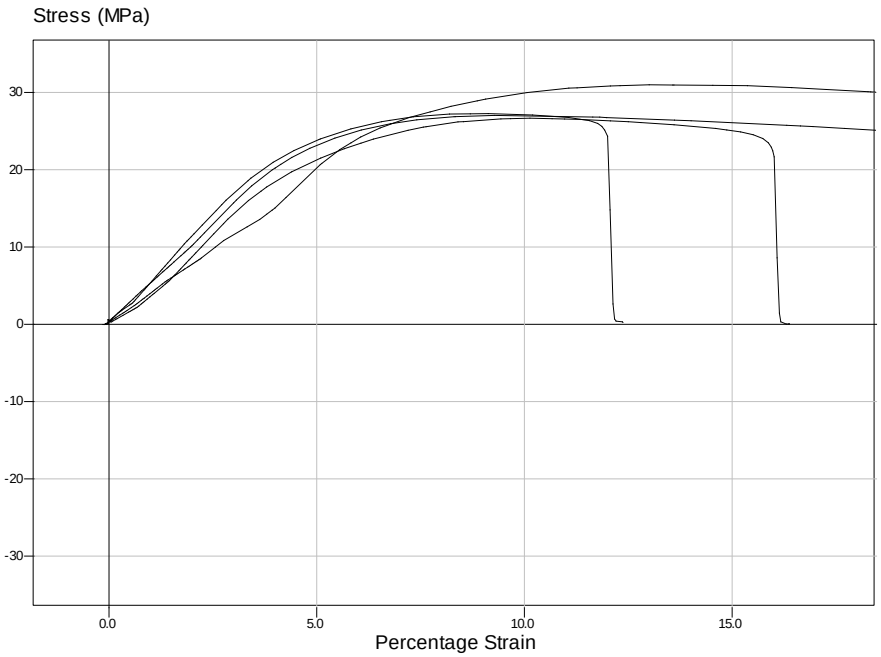

Figure B.12. Stress vs strain curves of PP/ m-F/ Triton X-100 composites

CURRICULUM VITAE

PERSONAL INFORMATION

Name & Surname: Yasin Kanbur

Nationality: Turkish

Date and Place of Birth: 24.10. 1979- Germany

EDUCATION

Degree	Institution	Year
B.Sc.	METU, Chemistry	2002
High School	Ankara Gazi Lisesi	1996

WORK EXPERIENCE

Place	Position	Year
METU, Dept. of Polym. Sci. Tech	Teaching Asistant	2004-2011
MEB	Teacher	2002-2004

FOREIGN LANGUAGES

Advanced English

PROJECTS

1- İletken Polimer Nanokompozitleri, TÜBİTAK 105T217, 01.09.2005-01.01.2008

PUBLICATIONS

1- Yasin Kanbur and Zuhal Küçükyavuz, Electrical and Mechanical Properties of Polypropylene/Carbon Black Composites, *Journal of Reinforced Plastics and Composites*, Sep 2009; vol. 28: pp. 2251 - 2260

2- Yasin Kanbur, Zuhal Küçükyavuz, Surface Modification and Characterization of Multiwalled Carbon Nanotube, *Fullerenes, Nanotubes and Carbon Nanostructures*, May 2011 ,vol: **19**, pp: 497-504

3- Mihai Irimia-Vladu, Pavel A. Troshin, Melanie Reisinger, Lyuba Shmygleva, **Yasin Kanbur**, Günther Schwabegger, Marius Bodea, Reinhard Schwödiauer, Alexander Mumyatov, Jeffrey W. Fergus, Vladimir Razumov, Helmut Sitter, Niyazi Serdar Sariciftci, Siegfried Bauer, Biocompatible and Biodegradable Organic Field Effect Transistors , *Advanced Functional Materials*, December, 2010, vol. 20 ,Is :23 ,pp. 4069-4076.

4- Yasin Kanbur, Zuhal Küçükyavuz, Synthesis and characterization of Surface Modified Fullerene, *Fullerenes, Nanotubes and Carbon Nanostructures*, **Accepted**, 2010.

5- Elif Vargün, Mehmet Sankır, Ali Usanmaz, **Yasin Kanbur**, Ufuk Abacı, H. Yüksel Güney, Preparation and Characterization of Acrylonitrile-Ethyl methacrylate Copolymers and the Effect of $LiClO_4$ Salt on Electrical Properties of Copolymer Films, , *Journal of Applied Polymer Science,* **Accepted**, 2011.

6- G. Schwabegger, Mujeeb Ullah, M. Irimia-Vladu, M. Reisinger, **Y. Kanbur** , R. Ahmed, P. Stadler, S. Bauer, N. S. Sariciftci, H. Sitter, High mobility, low voltage operating C_{60} based n-type organic field effect transistors, *Synthetic Metals*, 2011, **Submitted**.

7- **Yasin Kanbur**, Zuhal Küçükyavuz, Electrical and Mechanical Properties of Polypropylene / Carbon Nanotube composites, *Journal of Reinforced Plastics and Composites*, 2011, **Submitted.**

8- **Yasin Kanbur**, Zuhal Küçükyavuz, Electrical and Mechanical Properties of Polypropylene / Fullerene composites, *Journal of Reinforced Plastics and Composites*, 2011, **Submitted.**

Publications:

Poster Presentations:

1- **Yasin Kanbur** , Zuhal Küçükyavuz, Electrical and mechanical properties of carbon black reinforced polypropylene. "232 nd American Chemical Society Meeting, San Francisco, CA; PMSEPreprints", 95, (2006), p.660.

2- Aysun Güney , **Yasin Kanbur**, Zuhal Küçükyavuz, Synthesis and Characterization of Fullerene-Maleic Anhydride Copolymer, Frontiers in Polymer Science,Mainz, Germany,2009.

3- **Yasin Kanbur**, Zuhal Küçükyavuz , Karbon siyahı ile Güçlendirilmiş Polipropilen Kompozitlerinin Elektriksel ve Mekanik Özelliklerinin İncelenmesi. XIX. Ulusal Kimya Kongresi, Kuşadası, (2005), s.728.

4- Çetin Börüban, **Yasin Kanbur**, Zuhal Küçükyavuz Polipropilen/Polipirol Kompozitlerin Elektriksel ve Mekanik Özellikleri, XXII.Ulusal Kimya Kongresi, (2008), s.234